

STREAMFLOW TIMING AND ESTIMATION OF INFILTRATION RATES IN AN
EPHEMERAL STREAM CHANNEL USING VARIABLY SATURATED HEAT AND
FLUID TRANSPORT METHODS

by



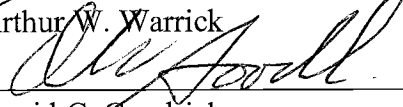
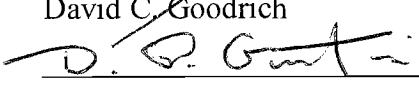

Kyle William Blasch

A Dissertation Submitted to the Faculty of the
DEPARTMENT OF HYDROLOGY AND WATER RESOURCES
In Partial Fulfillment of the Requirements
for the Degree of
DOCTOR OF PHILOSOPHY
In the Graduate College
THE UNIVERSITY OF ARIZONA

2 0 03

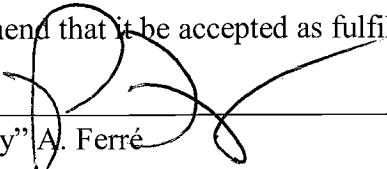
THE UNIVERSITY OF ARIZONA ®
GRADUATE COLLEGE

As members of the Final Examination Committee, we certify that we have read the dissertation prepared by Kyle William Blasch entitled “ Streamflow Timing and Estimation of Infiltration Rates in an Ephemeral Stream Channel Using Variably Saturated Heat and Fluid Transport Methods” and recommend that it be accepted as fulfilling the dissertation requirement for the degree of Doctor of Philosophy

	11-14-03
Paul “Ty” A. Ferré	Date
	11-14-03
Arthur W. Warrick	Date
	11-14-03
David C. Goodrich	Date
	11/14/03
Phillip D. Guertin	Date
	11/14/03
Stuart E. Marsh	Date

Final approval and acceptance of this dissertation is contingent upon the candidate's submission of the final copy of the dissertation to the Graduate College.

I hereby certify that I have read this dissertation prepared under my direction and recommend that it be accepted as fulfilling the dissertation requirement.

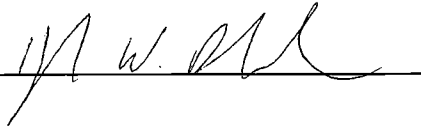
	11-14-03
Paul “Ty” A. Ferré	Date

STATEMENT BY AUTHOR

This dissertation has been submitted in partial fulfillment of requirements for an advanced degree at The University of Arizona and is deposited in the University Library to be made available to borrowers under rules of the Library.

Brief quotations from this dissertation are allowable without special permission, provided that accurate acknowledgment of source is made. Requests for permission for extended quotation from or reproduction of this manuscript in whole or in part may be granted by the head of the major department or the Dean of the Graduate College when in his or her judgment the proposed use of the material is in the interests of scholarship. In all other instances, however, permission must be obtained from the author.

SIGNED: _____

A handwritten signature in dark ink, appearing to read "J. W. Miller", is written over a horizontal line.

ACKNOWLEDGEMENTS

One of the greatest benefits I have gained from working on this dissertation is the personal contact I have had with so many wonderfully talented and generous people. At the top of this list are of course my advisor, Dr. Ty Ferré, and my supervisor at the U.S. Geological Survey, John Hoffmann. Their guidance in completion of this project as well as their friendship will not be forgotten. I would also like to extend my gratitude to my dissertation committee members Dr. Dave Goodrich, Dr. Phil Guertin, Dr. Stuart Marsh, and Dr. Art Warrick for their kind words and instruction. In addition, there are several individuals who have provided expertise to this project and taught me important hydrologic skills including Dr. James Constantz, Dr. John Fleming, Stan Leake, and Dennis Scheall. Additionally, the Arizona District of the U.S. Geological Survey, Water Resources Discipline, has provided the ideal working environment. I do not imagine that I will ever find a better group of colleagues.

Multiple organizations have been more than supportive in funding the project and my graduate studies. They include the U.S. Geological Survey (Special Initiative and Southwest Groundwater Resources Project), Arizona Department of Water Resources, NASA Space Grant, ARCS Foundation, Arizona Hydrological Society, and the National Science Foundation.

I would also like to thank my parents for instilling within me a curious nature and the desire to continually learn more about the natural world. Finally, and most importantly, I thank my best friend, Cathy, and our hounds, Cloey and Casey, for exploring Arizona from sunrise to sunset and reminding me that there is far more to life than what is contained within these chapters.

TABLE OF CONTENTS

LIST OF ILLUSTRATIONS.....	7
LIST OF TABLES.....	13
ABSTRACT	14
1. INTRODUCTION.....	16
1.0 Research Motivation.....	16
1.1 Research Objectives.....	19
1.2 Literature Review.....	20
1.3 Explanation of Dissertation Format.....	38
2. PRESENT STUDY.....	39
2.0 Statement of Candidate's Contribution to Papers.....	39
2.1 Summary of Paper #1 A statistical technique for interpreting streamflow timing using streambed sediment thermographs.....	40
2.2 Summary of Paper #2 A new field method to determine streamflow timing using electrical resistance sensors.	41
2.3 Summary of Paper #3 Transient and steady state infiltration fluxes during ephemeral streamflow	42
2.4 Summary of Paper #4 Combined use of heat and soil-water content to determine stream/ground-water exchanges, Rillito Creek, Tucson, Arizona.....	44
2.5 Summary of Paper #5 Determining temperature and thermal properties for heat-based studies of surface-water ground-water interactions.....	45
2.6 Summary of Paper #6 Processes controlling recharge beneath ephemeral streams in southern Arizona.....	46
2.7 Summary of the Dissertation.....	47
3. REFERENCES.....	51

TABLE OF CONTENTS - *Continued*

APPENDIX A: A STATISTICAL TECHNIQUE FOR INTERPRETING STREAMFLOW TIMING USING STREAMBED SEDIMENT THERMOGRAPHS...	61
APPENDIX B: A NEW FIELD METHOD TO DETERMINE STREAMFLOW TIMING USING ELECTRICAL RESISTANCE SENSORS.....	92
APPENDIX C: TRANSIENT AND STEADY STATE INFILTRATION FLUXES DURING EPHEMERAL STREAMFLOW.....	120
APPENDIX D: COMBINED USE OF HEAT AND SOIL-WATER CONTENT TO DETERMINE STREAM/GROUND-WATER EXCHANGES, RILLITO CREEK, TUCSON, ARIZONA.....	151
APPENDIX E: DETERMINING TEMPERATURE AND THERMAL PROPERTIES FOR HEAT-BASED STUDIES OF SURFACE-WATER GROUND-WATER INTERACTIONS.....	169
APPENDIX F: PROCESSES CONTROLLING RECHARGE BENEATH EPHEMERAL STREAMS IN SOUTHERN ARIZONA.....	189

LIST OF ILLUSTRATIONS

APPENDIX A

- Figure 1. Thermal responses from within a streambed divided into the case when streamflow is absent (primarily conductive heat transport through the sediments) and the case when streamflow is present (primarily advective heat transport through the sediments). Note the reduction in the amplitude of the diurnal wave at the streambed surface caused by the presence of the overlying water column and corresponding increase in thermal amplitude at depth caused by percolating water.....64
- Figure 2. (A) Advective and conductive diurnal temperature wave amplitudes as a function of depth propagating through coarse grained stream channel sediments. The radiant thermal amplitude at the surface is 1°C. The solid black line describes conductive thermal transport during no flow conditions. The no dampening case considers zero loss of heat to the water column during the presence of streamflow. The 50% dampening case considers 50% loss of heat energy to the water column during the presence of streamflow. The 50% dampening / 50% fluid flux reduction considers a 50% loss of heat to the water column and a reduction in the fluid flux from the previous two cases by 50%. (B) Difference between the advective and conductive diurnal temperature wave amplitudes as a function of depth. Intersections between the solid diurnal temperature wave amplitude segments and the dashed transition line represent depths corresponding to equivalent advective and diurnal temperature wave amplitudes during flow and no flow conditions respectively.....70
- Figure 3. Thermograph for (A) a depth above the transition depth and (B) a depth below the transition depth. The gray areas denote observed periods of streamflow....73
- Figure 4. Six-hour moving standard deviation window for temperature data measured below the transition depth. The gray areas denote observed periods of streamflow.....74
- Figure 5. Location of Rillito Creek study area and view of Rillito Creek within the Tucson Basin, Tucson, Arizona.....78
- Figure 6. Thermograph from September 16 through December 15, 2000, for (A) a depth of 0.15 meters and (B) a depth of 1.0 meters. The gray areas denote observed periods of streamflow.....81

LIST OF ILLUSTRATIONS – *Continued*

- Figure 7. A sensitivity analysis for the moving standard deviation technique considering: (A) the moving standard deviation window length, (B) the threshold multiplier times the mean standard deviation, (C) the minimum flow duration parameter and, (D) the minimum interflow duration parameter. Timing error is presented as the percentage of time over a year the method incorrectly infers the presence or absence of streamflow. Generally this error occurs at the onset and cessation of flow by either overestimating or underestimating the period of streamflow.....83
- Figure 8. (A) Thermograph from September 16, 2000, through September 15, 2001 for a depth of 0.75 meters, (B) one-hour, (C) four-hour, and (D) 12-hour moving standard deviation windows for temperature data measured at a depth of 0.75 meters. (E) Close-up of two identified events that provide an example of how moving standard deviation parameters can be selected. The gray area denotes periods of identified streamflow events.....88

APPENDIX B

- Figure 1. Schematic presentation of bulk electrical and contact resistances of a sediment medium. Dotted lines surrounding the wire leads denote the critical region for determining contact resistance. The remaining regions outside the dotted lines are important for determining the bulk electrical resistance. A measurement of electrical resistance is a combined measure of the bulk electrical resistance of the medium and contact resistance.....97
- Figure 2. Simulated infiltration of water into fine-grained sand and coarse-grained alluvium during a 2-hour streamflow event. The shaded areas in both A and B denote the period of streamflow. Measured contact resistance thresholds (dotted lines) and conductivity/saturation relations were used to calculate saturation and normalized total electrical conductivity measurements at 0.2 meter. A, shows the saturation response (light solid line) and electrical resistance sensor response (dark solid lines) within the coarse-grained alluvium to the infiltration event and redistribution. B, shows the simulated saturation and electrical resistance response for a sensor in fine-grained sand. The onset timing error is defined as the difference in time between the onset of a streamflow event and the activation of the electrical-resistance sensor. The cessation timing error is defined as the difference in time between the end of the streamflow event and the deactivation of the sensor. Both types of error are shown in A and B.....101

LIST OF ILLUSTRATIONS - *Continued*

Figure 3. Schematic diagram of a temperature sensor. A, Before modification. B, After conversion to an electrical-resistance sensor through removal of the thermistor.	104
Figure 4. Photograph and schematic diagram of the sensor locations within the laboratory column used to measure the contact-resistance threshold for the fine-grained sand and the coarse-grained alluvium.....	107
Figure 5. Sensor locations deployed in Rillito Creek, Tucson, AZ (USA)	108
Figure 6. Total electrical conductivity in relation to saturation as determined in column experiments for one of the sensors. A, Fine-grained sand. B, Coarse-grained alluvium. Note the higher contact-resistance threshold for the coarse-grained alluvium.....	110
Figure 7. A, Electrical conductivity as measured by an electrical-resistance sensor positioned 0.15 meter below the ground surface and temperature responses measured at depths of 0.05 meter and 1.0 meter. The subsurface electrical-resistance sensor was installed July 28, 2001, after the first two streamflow events. B, Electrical conductivity as measured by an electrical-resistance sensor positioned 0.15 meter below the ground surface and saturation as measured by the water content sensors. The shaded areas denote periods of streamflow as inferred using measured soil water-content data.....	113
Figure 8. Electrical conductivity as measured by an electrical-resistance sensor positioned at the surface. The shaded areas denote periods of streamflow as measured by a USGS streamflow gage.....	115

APPENDIX C

Figure 1. Transient and steady state infiltration during an ephemeral streamflow event.....	122
Figure 2. Location of Rillito Creek study area and view of Rillito Creek within the Tucson Basin, Tucson, Arizona.....	132

LIST OF ILLUSTRATIONS - *Continued*

Figure 3. Ephemeral streamflow event durations for Rillito Creek, Tucson, Arizona at study site (1990-2002).....	133
Figure 4. Photograph and schematic of the two-dimensional array of sensors within the stream-channel deposits. Each black circle represents a temperature and soil-water sensors.....	135
Figure 5. Water content data showing rapid increases at the onset of streamflow; a stabilization of water content during the event; and subsequent dewatering after streamflow is over.....	137
Figure 6. Figure 6. Representative observed and simulated thermographs for two depths, November 2000.....	138
Figure 7. Infiltration fluxes and cumulative infiltration for A) 4 November 2000 and B) 6 April 2001.....	140
Figure 8. Steady state infiltration fluxes and thermal boundary conditions for A) 4 November 2000 and B) 6 April 2001.....	143

APPENDIX D

Figure 1. Location of study area showing position of instrumentation relative to left stream bank.....	154
Figure 2. Photograph and schematic of the two-dimensional array of sensors within the stream-channel deposits. Each black circle represents a temperature and a time-domain reflectometry sensor. Refer to Figure 1 for location of array within Rillito Creek.....	156
Figure 3. Thermograph of Rillito Creek sediments at depths of 0.05, 0.5, and 1.0 meter. Solid bars above thermographs show periods of streamflow.....	157

LIST OF ILLUSTRATIONS - *Continued*

- Figure 4. Two-dimensional temperature distribution within stream-channel deposits. (A) Thermal transport through conduction before the onset of a streamflow event. (B) Thermal transport through combination of advection and conduction at the onset of a streamflow event. Multidimensional percolation through the sediments. (C) Combined advection and conduction thermal transport to the deeper sediments several hours into a flow event.....158
- Figure 5. Water-content data showing rapid infiltration at the onset of streamflow; a stabilization of water content during the streamflow event; and subsequent drainage after the streamflow is over.....159
- Figure 6. Two-dimensional water-content distribution in sediments beneath Rillito Creek. (A) Soil-water content before the onset of streamflow. (B) Soil-water content 5 minutes after the onset of streamflow. (C) One-dimensional dewatering immediately after the cessation of flow. (D) One-dimensional dewatering approximately 2 days after the cessation of streamflow.....160
- Figure 7. Measured and simulated thermographs ($^{\circ}\text{C}$) at a depth of 0.75 meter, column 3.....162
- Figure 8. Set of measured and simulated thermographs ($^{\circ}\text{C}$) for two adjacent columns.....163
- Figure 9. Simulated infiltration rates at columns 1,2,3, and 4 during a streamflow event..... 164

APPENDIX E

- Figure 1. Common electronic temperature sensors with schematic symbols, response characteristics, and advantages and disadvantages of each type (adapted from Hewlett Packard, 1983). RTD and IC are industry acronyms for resistance temperature device and integrated circuit, respectively.....172

LIST OF ILLUSTRATIONS - *Continued*

- Figure 2. (A) Self-contained temperature logger is about 3 cm in diameter. Note thermistor in mounting eyelet. (B) Dynamic response of four self-contained temperature loggers during calibration tests. Loggers, initially at room temperature, were immersed in a 0°C bath, followed by a 32°C bath. The average 95% response time of the loggers was about 5 minutes. Data sets are color coded. To avoid clutter, individual data points are shown for only one of the loggers... 175
- Figure 3. Dependence of volumetric heat capacity and thermal conduction on water-content for selected materials. Dashed lines are volumetric heat capacities calculated as described in the text, using data from Table 1A. Points are experimentally determined thermal conductivities, from DeVries (1966). Solid curves are empirical fits to the thermal-conductivity data.....176
- Figure 4. Field deployment of temperature-measuring equipment. (A,B,C) Installation of thermocouple sensors in a stream channel. (D,E) Data logger for thermocouple installation. (F) Installation of stream-bed sensor. (G) Swing-out thermocouple arm on access tube. (H) Top of access tube prior to grouting. (I) Grouting access tube with two-component foam. (J,K) Access-tube enclosure at channel surface. (L) Single-channel temperature logger on cable for suspension in access tube. Foam baffles on either side of logger prevent advection. See text for additional explanation.....186

APPENDIX F

- Figure 1. Water content data showing rapid increases at the onset of streamflow; a stabilization of water content during the event; and subsequent dewatering after streamflow is over.....201
- Figure 2. Comparison of measured streamflow losses within Rillito Creek, Tucson, Arizona, from 1933 through 1999 to computed streamflow losses using the Burkham (1970) relation with annual recharge coefficients.....204

LIST OF TABLES

APPENDIX B

Table 1. Contact resistance thresholds in fine-grained sand and coarse-grained alluvium.....	110
Table 2. Streamflow timing errors at the onset and cessation of flow using the temperature method and the electrical-resistance method. Negative values indicate the method identifies flow preceding the timing of streamflow measured using a conventional method (stream gage for surface timing and soil water content (TDR) for subsurface timing).....	112

APPENDIX C

Table 1. Evaluation of Cumulative Onset Infiltration for a Two-Layer System.....	129
Table 2. Comparison of calibrated and core-measured thermal and hydraulic properties of the channel sediments.....	136
Table 3. Description of ephemeral streamflow infiltration events.....	142

APPENDIX E

Table 1A. Thermal properties of selected material—Individual phases.....	178
Table 1B. Thermal properties of selected material—Porous media.....	178

ABSTRACT

Ephemeral streamflow infiltration through alluvial channels has been identified as an important source of aquifer replenishment in arid and semi-arid environments. In this dissertation, two field methods were developed for monitoring streamflow timing in ephemeral stream channels. The first streamflow timing method exploits differences in the advective and conductive thermal transport mechanisms during the presence and absence of streamflow. The second method of streamflow timing utilized the relationship between soil water content and electrical conductance. Electrical resistance sensors were designed to detect saturated soil conditions and thus to infer streamflow timing during periods of saturation. Both methods were field-tested in Rillito Creek, Tucson, Arizona. The electrical resistance method proved more suitable than the temperature method because it was not depth dependent and was able to more accurately infer streamflow timing with less data post processing.

Transient and steady state infiltration fluxes were simulated in a coarse-grained alluvial channel to determine the relative contribution the onset of streamflow provides to potential recharge. Water content, temperature, and pore pressure measurements were incorporated into a variably saturated heat and fluid transport model to simulate infiltration. Infiltration fluxes at the onset of streamflow were about 2-3 orders of magnitude higher than steady state fluxes and were inversely proportional to antecedent water content. The time duration from the onset of streamflow to steady-state infiltration

ranged from 1.8 to 20 hours. Two transient and steady state periods were observed indicating a lower permeable layer at depth. During steady state periods, infiltration fluxes averaged 0.33 meters per day and ranged from 0.14 to 0.45 meters per day. A long-term decline was observed in all three events. Higher frequency diurnal and episodic changes were prompted by fluctuations in atmospheric temperature and discharge. The simulated steady state values were consistent with the effective vertical conductivity values (0.22 meters per day) of an underlying less permeable layer. The average contribution from the cumulative transient infiltration for the events was approximately 18 percent. Therefore, it is apparent that potential recharge calculations for alluvial channels that do not consider infiltration during the onset transient period may underestimate the true potential for recharge.

1. INTRODUCTION

1.0 Research Motivation

Recharge to aquifers within alluvial basins of the Southwestern United States may occur through infiltration of precipitation directly through the basin floor (Gee et al., 1994), infiltration from irrigation and industrial returns, and seepage losses through stream channels. In the semiarid regions of southern Arizona, diffuse infiltration of precipitation through the basin floor is considered the smallest component of total recharge owing to limited precipitation in comparison to evapotranspiration (Scott et al., 2000). For instance, daily evaporation and precipitation rates measured in the Tucson Basin, Arizona, from 1991-2002 indicate that on average the precipitation rate exceeded the evaporation rate 25 days per year. Additionally, depth to ground water in alluvial basins can be hundreds of meters, which provides ample opportunity for storage of infiltrated water. Because of these environmental conditions, concentrated infiltration repeated over time within the same channel reaches or recharge basins is often necessary for recharge to occur. For example, repeated incidental recharge comprised of irrigation return flows from agriculture, golf courses, and green belts, and industrial return flows, such as treated effluent, can represent a significant source of basin recharge. Within the Tucson Basin, incidental recharge accounts for about 15 to 30 percent of the total recharge (Hanson and Benedict, Table 1, pages 8-9, 1994; Galyean, 1996).

Channel recharge consists of localized infiltration of streamflow along perennial, ephemeral, and intermittent streams. Where streams flow over areas with a high water table, the stream and aquifer can be connected hydraulically and continually exchange water. Perennial streams that are connected hydraulically to an underlying unconfined aquifer can control the elevation of the water table in the aquifer by acting as a drain when ground-water levels are high, and as a source when ground-water levels are low. Ground-water withdrawals from alluvial aquifers can increase the vertical hydraulic gradient below streams and increase recharge from perennial streams (Theis, 1940). In the extreme case, ground-water pumping will cause stream infiltration losses to equal discharge, and the stream will become ephemeral. Historical demands for ground water and surface water in populated basins within the Southwest, including the Tucson Basin, have transformed many perennial reaches of streams into ephemeral reaches; thus, the fraction of recharge attributed to ephemeral stream channels is increasing (Anderson et al., 1992). As this recharge component increases in significance, an improved understanding of the processes controlling recharge is needed for the effective management of surface-water and ground-water resources.

Given the erratic and variable nature of ephemeral and intermittent streamflow in arid and semiarid basins, quantifying streamflow timing, transmission losses, and recharge rates are necessary for efficient water resource management and planning. A necessary

first step is compilation of a long-term record of streamflow occurrences and timing in channels and arroyos for incorporation into rainfall/runoff relationships, for describing fluid transport through the unsaturated zone underlying ephemeral streams, and to constrain channel recharge estimation, a primary component of aquifer replenishment. Additionally, understanding streamflow timing is a necessary requirement for effective design of storm-water and flood-control networks in flood-prone environments.

The abundance of ephemeral channels within many watersheds in the Southwest limits the use of more conventional streamflow devices such as flow-rated stream gages. Consequently, low cost alternatives are required to meet the demand for highly distributed data collection. A recent investigation demonstrated the use of streambed thermographs for monitoring streamflow timing and extent however, the method relies on a set of qualitative criteria for selecting periods of streamflow limiting it to small scale applications (Constantz et al., 2002). For large-scale applications a quantitative method with a set of numerical criteria is required to detect streamflow in a time efficient and repeatable manner. In addition, streambed thermographs are not suitable for all ephemeral streams, thus a more robust method for streamflow timing is required.

Bed sediment thermographs have also been used repeatedly over the last decade to infer streamflow losses and infiltration fluxes. Using variably-saturated heat and fluid transport models it is possible to inversely solve for the fluid flux through the sediments by matching observed streambed thermographs at multiple depths to those simulated by

the model (Constantz, 1998; Ronan et al., 1998; Bailey, 2002). The application of these models has focused almost exclusively on steady state fully saturated conditions without considering the onset and cessation of streamflow. Consequently, there is a noticeable absence of data and understanding about the onset and cessation of ephemeral streamflow events.

1.1 Research Objectives

The objectives of this dissertation are organized according to the order of manuscripts presented.

- Develop a statistical method to infer the presence of streamflow in ephemeral channels using streambed thermographs
- Determine the optimal depth for temperature sensor placement to improve streamflow detection and timing
- Develop an alternative and more robust sensor for streamflow timing based on the direct measure of soil water content
- Develop a method for continuously monitoring in situ infiltration fluxes for the full duration of ephemeral streamflow events
- Estimate the variability of infiltration fluxes throughout the full cycle of an ephemeral streamflow event
- Estimate the contribution of inflow at the onset of ephemeral events compared to steady state contributions

1.2 Literature Review

Streamflow Timing

Current methods used to estimate streamflow timing include flow-rated stream gages, velocity meters, soil water-content sensors, and temperature sensors (Latkovich and Leavesly, 1993; Blasch et al., 2000; Constantz et al., 2001). These methods have met with varying success depending upon channel morphology, bed sediment characteristics, frequency and duration of streamflow, and other requirements (e.g., magnitude of temperature signal).

Stream gages and velocity meters accurately determine streamflow timing, but generally are not suitable for ephemeral channels that experience changes in channel morphology (Tadayon et al., 2001). Stream gages and velocity meters installed at the bed sediment surface can become buried or damaged by moving sediment or debris. Consequently, streamflow timing sensors deployed within the vadose zone have been shown as advantageous under these circumstances (Constantz et al., 2001).

Soil water-content methods within the near surface detect infiltration and percolation of water through the sediments, which may be used to infer timing of streamflow (Blasch et al., 2000). Placing sensors in the subsurface reduces the possibility that they will be damaged or lost during flow. Logging instrumentation, however, must be placed on or near the bank with cables extending to the buried sensors.

Temperature methods enable inference of streamflow timing on the basis of the combined transport of heat and fluid within the bed sediments (Stallman, 1963; Stallman, 1965; Jaynes, 1990). When streamflow is absent from a channel, radiant heating of the surface sediments is transported into the sediment profile primarily through conduction (Wierenga et al., 1970). The diurnal temperature forcing is often represented as a sinusoidal function propagates vertically through a homogenous sediment layer with a decreasing amplitude and increasing time lag with depth (Jaynes, 1990). When streamflow is present in the channel, the amplitude of the temperature wave at the sediment surface is often reduced because a portion of the radiant energy contacting the stream surface is absorbed as it passes through the water column. The presence of streamflow can cause percolation of water through coarse-grained streambed sediments increasing the amount of heat transported to deeper depths (Silliman et al., 1994). As a result, during periods of streamflow, heat is transported downward through the sediments by a combination of conduction and advection. Stallman (1963, 1965) developed an analytical solution for coupled heat and fluid flow assuming a constant vertical percolation rate through a single saturated layer of homogeneous sediments and a sinusoidal temperature variation at the surface.

Recent development of small ($<10\text{ cm}^3$), inexpensive, waterproof temperature sensors with integrated data storage enable measurement and storage of temperature values without the need for external connecting wires. This advantage enables in-situ temperature monitoring in ephemeral channels with unstable beds over large areas with

high spatial resolution. Currently, the most reliable method for interpretation of the temperature data is a visual method, which is both subjective and inefficient for large data sets.

Appendix A presents a statistical method for identifying periods of streamflow using streambed thermographs. The method is objective, repeatable and is an improvement in efficiency for analyzing large datasets. The method uses a moving standard deviation to discern periods of conductive heat transport associated with the absence of streamflow and advective heat transport associated with the presence of streamflow.

During this investigation it became apparent that the use of temperature for streamflow timing is a convenient tool if it is available, but may not be the most appropriate methodology for all conditions. Specifically, certain conditions are required for streamflow to produce a readily identifiable thermal signal. For example, water with the same temperature as the channel will not produce an identifiable signal. In ephemeral stream channels subject to repeated scour and deposition, changes in sediment surface elevation complicate the interpretation of the temperature data. Additional disadvantages to using temperature in a stream channel include extremely small gradients at depth, multiple sources of heat in a complex watershed, heterogeneous thermal and hydraulic properties, and multiple methods of heat transport.

Appendix B focuses on the development of electrical resistance sensors (ER sensors) to monitor water content to infer streamflow timing. The advantages of the electrical resistance approach include: functionality above or below the channel surface, functionality in all streamflow temperatures, lack of connecting wires, and minimal interpretation of data. These same attributes necessary for streamflow timing are also advantageous for monitoring sediment saturation in other similar vadose zone applications such as irrigated fields, fluctuating water tables, and post-burn environments.

Coupled Heat and Fluid Flow

While the relationship between coupled heat and fluid flow can be used to resolve streamflow timing records, it can also serve to estimate infiltration fluxes through the bed sediments. The energy transport equation for a unit volume of sediments represents the changes in energy stored within the porous media balanced by inflow and outflow through conduction, advection, dispersion, and sources within the matrix. The following equation represents the contributions from these sources in homogeneous and isotropic sediments.

$$[\theta C_w + (1 - \phi)C_s] \frac{\partial T}{\partial t} = \nabla \cdot (\kappa_T \nabla T) + \nabla \cdot (\theta C_w D_H \nabla T) - \nabla \theta C_w \nabla T + q C_w T^* \quad (1)$$

where,

t	time	t
θ	volumetric moisture content	$L^3 L^{-3}$
c_w	heat capacity (density x specific heat) of water	$M t^{-2} L^{-1} T^{-1}$

ϕ	porosity	$L^3 L^{-3}$
c_s	heat capacity of the dry solid	$M t^{-2} L^{-1} T^{-1}$
T	temperature	T
κ_T	thermal conductivity of water and solids (tensor)	$M L t^{-3} T^{-1}$
D_H	hydrodynamic dispersion (tensor)	$L^2 t^{-1}$
v	water velocity	$L t^{-1}$
q	rate of internal fluid source	$L t^{-1}$
T^*	temperature of fluid source	T

The first term on the left is the change in energy stored over time. The storage of energy is balanced by the terms on the right beginning with the energy transported by thermal conduction followed by the energy transported due to thermo-mechanical dispersion. The remaining two terms represent the advection of thermal energy and the sources or sinks of heat added to or removed from the domain.

Stallman (1960) developed a general differential equation to describe nonsteady heat and fluid flow through a fully saturated, isotropic, homogeneous medium assuming no fluid or thermal sources within the medium.

$$\frac{\partial^2 T}{\partial x^2} + \frac{\partial^2 T}{\partial y^2} + \frac{\partial^2 T}{\partial z^2} - \frac{c_w \rho_w}{\kappa} \left[\frac{\partial(v_x T)}{\partial x} + \frac{\partial(v_y T)}{\partial y} + \frac{\partial(v_z T)}{\partial z} \right] = \frac{c_m \rho_m}{\kappa} \frac{\partial T}{\partial t} \quad (2)$$

where,

ρ_w is the density of the fluid, c_w is the specific heat of the fluid, ρ_m is the density of the combined solid-fluid media, c_m is the specific heat of the combined solid-fluid media.

This simplification does not consider hydrodynamic dispersion. This is reasonable if the depth of observation is small. In addition, temperature variations from biological and chemical activity are considered negligible. Finally, the thermal and hydraulic properties of the sediments and fluid are assumed constant over space and time.

Several methods have been developed to solve the coupled heat and water transport equations for the case of one-dimensional steady vertical flow in saturated sediments.

$$\frac{\partial^2 T}{\partial z^2} - \frac{c_w \rho_w v_z}{\kappa} \left(\frac{\partial T}{\partial z} \right) = 0 \quad (3)$$

The methods include a type-curve method (Bredehoft and Papadopoulos, 1965) and the heat balance method (Wierenga et al., 1970).

The type-curve method has been used (Cartwright, 1970; Sakura, 1978; Cartwright, 1979) for determining groundwater velocities as it requires minimal data collection and is easy to calculate using the solution and type curve provided by Bredehoft and Papadopoulos (1965). The authors predict that they could measure groundwater Darcian fluxes as low as 1×10^{-6} cm/s.

The heat balance method presented by Wierenga et al. (1970) was developed to simulate change in irrigated soil temperatures. During periods of active infiltration and immediately afterwards the authors use an arithmetic method to balance the heat advected into each of layers by adjusting the volume of water entering the profile. Following active infiltration the authors modeled heat flow using an explicit finite difference form of the one-dimensional heat equation. This method considers heat transport exclusively through conduction. However, the authors did not present guidance on when to transition from the heat balance method to the solution to the heat flow equation. Taniguchi and Sharma (1993) evaluated the heat balance method. They found it advantageous because of its ease of calculation; however its application was limited to the near surface (< 2 m) because changes in temperature below this depth could not be resolved sufficiently for use in the method. Boyle and Saleem (1979) compared the heat balance method to the type-curve methods during their subsurface water investigation.

Suzuki (1960) proposed the use of temperature as an indirect measure of infiltration rates beneath flooded rice fields assuming saturated, one-dimensional, steady state flow into a homogeneous isotropic, porous medium with a sinusoidal surface temperature variation.

$$\kappa \frac{\partial^2 T}{\partial z^2} - c_w \rho_w v_z \left(\frac{\partial T}{\partial z} \right) = c_s \rho_s \left(\frac{\partial T}{\partial t} \right) \quad (4)$$

Suzuki introduced an algebraic solution to the one-dimensional flow equation. Stallman (1965) developed an exact solution for these conditions assuming a harmonically varying temperature forcing at the stream channel surface and a subsurface groundwater temperature that is equal to the mean amplitude of the upper boundary condition. The boundary conditions are suitable for diurnal and seasonally varying temperatures conditions assuming vertical flow and fully saturated conditions. Stallman estimated that the method could detect percolation rates of 0.1 cm/day using annual temperature fluctuations and 2 cm/day for diurnal temperature fluctuations. Taniguchi and Sharma (1993) employed Stallman's (1965) one-dimensional solution to determine recharge beneath two forest sites near Perth, Australia. Their investigation demonstrated that the method was successful for the case when recharge rates are low and sensor depths are shallow.

Wankiewicz (1984) studied thermal profiles beneath streams in the Northwest Territories and determined thermal transport beneath one stream was almost exclusively from conduction and the other through advection. Lapham (1987) was one of the first to describe coupled fluid and heat flow below a stream channel using an explicit finite difference approximation. This approximation has the flexibility of being able to use a nonsinusoidal temperature forcing and a ground-water temperature that is not equal to the mean forcing value. Lapham monitored temperature profiles beneath streams in order to determine the magnitude and direction of percolating waters between streams and their

underlying aquifers. He estimated hydraulic conductivities of the sediments using annual temperature profiles with depths down to 10 m.

Jaynes (1990) incorporated the temperature dependence of the hydraulic conductivity into the one-dimensional heat transfer equation to account for observed diurnal fluctuations in infiltration. Simulating changes in the hydraulic conductivity of surface layers was able to produce infiltration estimates similar to those observed. Constantz et al. (1994) measured variations in stream channel infiltration for two streams in New Mexico and compared those to estimated fluctuations in seepage losses based on the temperature relationship with hydraulic conductivity. The authors concluded that fluctuations in streambed temperature could account for almost all the variation in seepage losses.

Silliman (1995) expands upon earlier heat and fluid transport investigations to estimate stream flow loss to the bed sediments under fully saturated conditions using thermal measurements at the base of the water column and at 25 cm depth in the sediments.

Silliman (1995) incorporates a series of solutions to the linear differential equation in order to provide the flexibility of using a measured surface temperature. For fully saturated steady state one-dimensional flow at velocities sufficient to neglect conduction, Taniguchi and Sharma (1990) evaluated a purely advective solution that produced comparable flux estimates to a method using bromide tracers in a laboratory experiment. They calculated the Darcy flux from temperature peaks throughout the profile

$$v = V_T \left(\frac{\rho_s c_s}{\rho_w c_w} \right) \quad (5)$$

where V_T is the vertical velocity of the temperature peaks. Constantz and Thomas (1996) utilized this relation in highly permeable sediments beneath an ephemeral arroyo. They compared infiltration rates using purely advective heat transport with infiltration rates from seepage measurements of streamflow loss. Estimates using temperature peaks were within a factor of 2 of streamflow loss estimates.

Recent development of digital computers has advanced the use of numerical models for solving coupled heat and mass transport equations in variably saturated media. Examples of software for these purposes include VS2DH (Healy & Ronan, 1996), SUTRA (Voss, 1984), and HYDRUS (Simunek et al., 1998). Generally, these models solve coupled relationships between Richards' equations and a form of the advection-diffusion equation using either finite difference or finite element methods in an iterative fashion.

Constantz et al. (1997), Constantz et al. (1998), Ronan et al. (1998), Bartolino and Niswonger (1999), Constantz et al. (2001), and Constantz et al. (2003) used coupled fluid and heat transport models for various purposes including estimating seepage losses beneath alluvial stream channels, identifying the occurrence and duration of ephemeral flow events and estimating the hydraulic parameters of the soil sediments beneath stream channels. With the exception of Ronan et al. (1998) the investigations have concentrated on fully saturated streamflow during steady state periods of streamflow. Ronan et al.

(1998) modeled the onset of an ephemeral streamflow event however they were not able to verify the results. Appendix C describes the use a variably saturated heat and fluid model along with water content and pore pressure measurements to simulate streamflow infiltration. The variabilities in streamflow infiltration during the event are analyzed and use of steady state infiltration factors are evaluated.

Recharge within Rillito Creek

Rillito Creek was selected as the experimental field site for the investigations described in this dissertation. A brief description of Rillito Creek and the field site follows along with a description of previous recharge studies.

Rillito Description

Rillito Creek is an ephemeral stream channel at the north end of an intermontane trough referred to as the Tucson Basin. The Rillito Creek watershed has a drainage area of 2,256 square kilometers (km^2) with two major tributaries, Tanque Verde Wash and Pantano Wash. Tanque Verde Wash drains 702 km^2 from the Santa Catalina and Rincon Mountains; Pantano Wash drains $1,554 \text{ km}^2$ between the Rincon, Santa Rita, and Whetstone Mountains. Precipitation runoff and snowmelt from the Santa Catalina, Whetstone, and Rincon Mountains as well as urban runoff from the northeastern suburbs of Tucson contribute most of the flow to Rillito Creek. Surface flow and subflow of Rillito Creek empty into the Santa Cruz River at the northerly end of the basin.

Significant changes have occurred to Rillito Creek since the population of the Rillito Creek watershed. Anecdotal accounts of Rillito creek in the 19th century describe perennial flow near the reaches of the new Ft. Lowell (circa 1873). The new Fort Lowell obtained water directly from the creek for livestock and irrigation of the Fort's fields. Water from Rillito creek was not used for drinking, but was instead obtained from wells that were approximately 25 to 35 feet in depth. During this period, the creek meandered unrestricted through mesquite bosques, and groves of cottonwood, ash, walnut and willow trees. The Creek did not have a definite path until about the mid 1870's to 1890's. After this time the Rillito Creek became entrenched in a fifteen-foot deep channel similar to the path it takes today. The earliest documented evidence of this channel cutting is August 5, 1890, (Rillito Creek Hydrologic Research Committee, 1959).

The second series of changes to Rillito Creek occurred in response to the El Nino flooding of 1983. During this period of time Rillito Creek experienced the largest flows in recorded history accompanied by significant damage to instream bridges and roadways as well as damage to nearby businesses and residences. In response to the damage Pima County flood control deepened the channel and lined the north and south banks with soil cement to improve bank stabilization and prevent undercutting and erosion.

The study site at Dodge Boulevard is underlain by recent stream-channel deposits and basin-fill deposits that are Pleistocene in age or older (Davidson, 1973). The recent

stream-channel deposits, consisting of fine- to coarse-grained alluvium, are about 10 m thick and derived from the surrounding mountain ranges. The alluvium predominantly consists of sand and gravel and contains less than 10 percent clay and silt. The underlying basin-fill deposits comprise the Fort Lowell Formation and extend to depths of several hundreds of meters (Davidson, 1973). The weakly consolidated to unconsolidated sediments are finer-grained than the stream-channel deposits.

Groundwater levels fluctuate within the basin-fill deposits. Underlying the basin fill deposits are the Tinaja beds and Pantano formation of Tertiary age. The upper part of the Tinaja beds together with the basin fill deposits comprise the primary aquifer underlying the Tucson Basin.

Hoffman et al. (2002) measured the vertical hydraulic conductivity from cores excavated every 0.3m from the stream channel surface to a depth of approximately 42 m. The vertical hydraulic conductivity of the stream-channel deposits range from 0.3 to 2.5 m/d, whereas the basin-fill deposits tend to have a hydraulic conductivity less than about 0.61 m/d and in places as low as 0.012 m/d. For heterogeneous media such as the deposits beneath Rillito Creek, the equivalent vertical hydraulic conductivity is calculated as the harmonic mean of the K_{sat} for each layer within the deposits and is always less than the arithmetic mean. The equivalent hydraulic conductivity of the stream-channel deposits is 2.2 m/d; the equivalent hydraulic conductivity of the basin-fill deposits is 0.22 m/d; and the equivalent hydraulic conductivity of the combined sediments (stream-channel and basin-fill deposits) is 0.23 m/d. Assuming a unit gradient, these equivalent vertical

hydraulic conductivity values provide an estimate of potential recharge rates under saturated conditions. Saturated conditions will exist only after sustained periods of streamflow infiltration at a rate that enables water to fully saturate the underlying sediments. Once saturated hydraulic connection is achieved between the stream and water table, the system behaves as though the stream were perennial. Prior to full saturation, unsaturated hydraulic conductivity values need to be considered when estimating potential recharge rates. Unsaturated hydraulic conductivity of the deposits beneath Rillito Creek varies by several orders of magnitude as a function of water content. For moisture conditions at the time of core collection, the unsaturated hydraulic conductivity was generally at least two orders of magnitude less than the saturated hydraulic conductivity (Hoffmann et al., 2002).

The study site was selected on the basis of its proximity to supporting field instrumentation, its lack of vegetation, and its position about 200 m downstream and 100 m upstream from curvatures in the creek channel. A piezometer nest equipped with a pressure transducer to monitor depth to water is about 25 m upstream from the instrumented site. Depth to the regional water table is about 42 m at the site. Cores collected during the drilling of the piezometer-nest borehole were analyzed for physical, hydraulic, and thermal properties (Hoffmann et al., 2002). A U. S. Geological Survey (USGS) streamflow-gaging station, 09485700 (Tadayon et al, 2000), is 45 m downstream from the site. An Arizona Meteorological Network weather station that measures air

temperature and precipitation is 2 km downstream from the instrumented site at the University of Arizona Campus Agricultural Center.

Rillito Creek is an ephemeral stream with three active seasons, summer North American Monsoon (July- September), fall (October – November), and winter (December-March). Characteristic summer flows result from localized, short-duration convective storms, whereas longer-duration frontal storms and snowmelt produce winter flows. Fall storms and resulting flows are caused by either tropical storms or changes in weather patterns caused by periodic climate fluctuations. Typical flows measured at the Dodge Boulevard study site are less than 28 cubic meters per second (m^3/s); a maximum discharge of about $680 \text{ m}^3/\text{s}$ occurred during the 1993 El Niño season (Tadayon et al., 2000). The average annual flow is about 33,300,000 cubic meters (m^3). From 1990-2000 the average number of annual streamflow events was 14, and the typical duration of the events was less than a week.

Previous Infiltration Studies on Rillito Creek

Since the middle of the 19th century Rillito Creek has been a source of water for the residents of the Tucson basin. The first stream gage was installed in 1908 by the Agricultural Engineering Department, University of Arizona. Operation of the gage was transferred to the U.S. Geological Survey in January of 1926. Smith (1910) was probably the first investigator to examine recharge along Rillito Creek. He concluded there was a difference in infiltration rates between the flashy, silt-laden summer flows, and the

steady, long duration flows of the winter snowmelt runoff. This conclusion was based partly on seasonal well hydrographs and ground-water temperature data.

Others to follow, measured stream channel infiltration employing a variety of methods including stream gaging, flumes, water balances, and infiltrometer method (Turner, 1943; Matlock, 1965; Burkham, 1970; Katz, 1987; Pool, In Review; Hoffman, In Review). Streamflow infiltration values from these studies range from about 0.3 to 3.35 m/d. Using seepage runs, Turner (1943) measured infiltration rates in for a snowmelt event. He estimated infiltration rates ranging from 0.34 to 1.13 m/d. The lower rate coincided with a shallow water table and likely surface/ground water connection that impeded infiltration.

Matlock (1965) presents infiltration estimates using a variety of methods. Using seepage runs for an almost completely continuous four month long snowmelt event in the Spring of 1962 he estimated the average infiltration rate of 1.1 m/d. He surmised that the low flow and reduced sediment loading from monsoon flows was responsible for the higher numbers. Using infiltrometer experiments in the streamflow he concluded that a silt layer ranging from 0.16 to 0.32 cm was sufficient to reduce infiltration and a layer 7-11 cm thick all but stopped infiltration. Based on a water budget conducted by Schwalen in 1960 and 1962 (reported by Matlock, 1965) estimated cold season infiltration as 0.85 m/day and predicted higher rates for summer events.

Burkham (1970) developed a nonlinear regression equation relating streamflow loss to discharge for Rillito Creek, Arizona. However, comparison of streamflow losses between two stream gages over a 60-year period indicate that Burkham's relation underestimates measured streamflow losses (Pool, In review). This increase emphasizes that stream channel infiltration within dynamic systems cannot be considered stationary, whether the increase in recharge is due to changes in basin runoff characteristics or changes in stream channel infiltration efficiency.

Katz (1987) investigated steady state recharge values within Rillito Creek by measuring streamflow and wetted perimeter during a 119-day event from December 1984 through April 1985. Katz used stream gages to estimate streamflow loss and video footage to ascertain wetted perimeter. Katz estimated streamflow loss values of 0.5 m/d.

In lieu of directly measuring recharge rates other investigators have focused on subsurface flow. Schwalen et al. (1960) used water level measurements from March 10, 1959, through March 20, 1960 to estimate annual recharge. The authors estimated approximately 23,700 acre-feet of recharge, which was 4450 acre-feet less than recharge predicted using streamflow loss methods. This could be attributed to higher infiltration rates not accounted for by steady-state values.

Bailey (2002) was the first to use temperature monitoring and inverse simulation of heat and water transport through stream sediments to estimate infiltration rates during

streamflow at three locations along Rillito Creek. Through a numerical sensitivity analysis, he showed that vertical heat transport during stream flow is more sensitive to the hydraulic conductivity of the streambed than to stage. Using a hierarchical simulation approach, he first examined the use of the hydraulic conductivity measured in cores to predict infiltration rates during streamflow. Numerical models using the core-measured hydraulic conductivity were not able to reproduce the observed temperature time series at depth. Improved agreement with the observed temperature signal generally required a reduction of the subsurface hydraulic conductivity from the core values (Hoffmann et al, 2002) and often required the addition of a thin surface layer (< 5 cm) having a variable hydraulic conductivity to represent sediments that may have been redistributed during flow.

Modeling performed by Bailey (2002) showed that, for two sequential flow events, the hydraulic conductivity of this surface layer changed by four orders of magnitude. Another simulation by Bailey (2002) required a change in the hydraulic conductivity of the surface layer during the flow event to reproduce the observed subsurface temperature series. Equivalent saturated hydraulic conductivity values for the stream channel sediments ranged from 0.316 m/d to 4.78 m/d.

Hoffmann et al. (in review) conducted a series of seepage runs during an event in October, 2000. Results for seepage measurements averaged 0.9 m/d. Additionally, the authors analyzed chemical tracers from cores underlying Rillito Creek at Dodge

Boulevard. In situ percolation rates were estimated as 0.049 m/d using $\delta^{18}\text{O}$ and δD and 0.055 m/d for chloride. The percolation rates estimated using chemical tracers represent the combined saturated and unsaturated transport through the vadose zone and consequently are significantly lower than infiltration rates measured at the streambed surface.

1.3 Explanation of Dissertation Format

The organization of this dissertation highlights six manuscripts presented as appendices. The introductory chapter presents a brief description of the research topic and a review of the supporting literature. The second chapter summarizes the important findings of this doctoral investigation and the contributions of each of the manuscripts. The first manuscript was accepted for publication in the Vadose Zone Journal December 2003. The second manuscript was published in Vadose Zone Journal, Vol. 1, pages 289-299, November 2002. The third manuscript was submitted to the U.S. Geological Society (USGS) for review in November 2003. The fourth and fifth manuscripts were accepted for publication in a USGS Circular in September 2003. The final manuscript was accepted for publication in an American Geophysical Union Manuscript in June 2003.

2. PRESENT STUDY

2.0 Statement of Candidate's Contribution to Papers

The first three research manuscripts described in Appendices A-C and sections 2.1-2.3 are almost exclusively the work of the candidate. The candidate was primarily responsible for project design, construction of laboratory and field monitoring systems, collection of measurement data, mathematical and statistical analysis of data, implementation of numerical models and drafting of text and figures for the manuscripts. The coauthors are recognized for their field labor, scientific guidance, and editorial review. Overall the candidate contributed 95% to the manuscripts described in Appendices A-C. The author contributed about 50% of the content to Appendices D and E (sections 2.4 - 2.5) but only contributed about 25% to the construction of the manuscripts and graphics. The final research manuscript presented in Appendix F (section 2.6) was a review of recent recharge investigations within Southern Arizona. A majority (90%) of design and drafting of the manuscript was once again contributed by the candidate but only a small component of the investigations described are those of the candidate. The coauthors contributed editorial review and a portion of Rillito Creek recharge data presented in the investigation.

2.1 Summary of Paper #1 A statistical technique for interpreting streamflow timing using streambed sediment thermographs

Accepted by *Vadose Zone Journal*, 2003

The objective of this paper was to improve upon the use of streambed thermographs for streamflow timing. This was accomplished through 1) providing a detailed process for selection of optimal temperature monitoring depth and 2) developing a statistical method capable of inferring streamflow timing from a streambed thermograph. Optimal measurement depths for inferring streamflow were defined as depths where streamflow induced percolation causes the greatest measurable changes in diurnal temperature wave amplitudes compared to no flow conditions.

The primary conclusions of this study follow:

- The successful execution of streamflow timing using streambed thermographs is primarily dependent on the correct selection of temperature monitoring depth. Thermal and hydraulic parameters of the soil can be used to estimate the correct depths.
- The standard deviation method provides an improvement over visual identification methods primarily because the statistical method is objective, reproducible, and efficient for large data sets.
- The standard deviation window length and threshold are the most sensitive parameters in the model for identifying streamflow timing. Standard deviation window lengths from 1 hour to 6 hours were more accurate than longer windows. The magnitude

of the threshold parameter was approximately equal to the 1.5 times the mean of the moving standard deviation.

- Errors for Rillito Creek at a depth of 1.0m ranged from 77 minutes at the onset of flow and 257 minutes at the cessation of streamflow.
- The standard deviation method is more accurate when calibrated using an alternative flow device however, it is still appropriate if the parameters are optimized using streamflow and climate data. Inspection of multiple standard deviation plots using a range of standard deviation window lengths is a necessary step in identifying streamflow events.

2.2 Summary of Paper #2 A new field method to determine streamflow timing using electrical resistance sensors

Published in *Vadose Zone Journal*, 1: 289-299 (2002)

For this investigation, we converted commercially available temperature sensors into electrical resistance sensors (ER sensors) to monitor water content and tested their utility for streamflow detection. More specifically, electrical resistance sensors were constructed to act as a switch recording zero values during the absence of streamflow and nonzero values during the presence of streamflow.

The primary conclusions of this study follow:

- Electronic resistance sensors are more accurate than temperature methods for stream flow timing and are comparable in accuracy to soil water content (time domain reflectometry) and stream gaging methods.
- Electronic resistance sensors functioned both at the streambed surface and in the subsurface. The sensors are depth independent providing a distinct advantage over temperature methods.
- Electronic resistance sensors required less data analysis than thermal methods to infer streamflow timing. The advantage is pronounced for short duration events.
- Use of electronic resistance sensors required less knowledge of the streambed thermal and hydrologic properties than temperature methods.
- The electronic resistance sensors can be used as a surrogate to monitor soil water content. Saturation and dewatering of fine-grained streambed sediments was observed repeatedly in the stream channel providing both a record of streamflow timing and evidence of changing streambed hydrologic characteristics.

2.3 Summary of Paper #3 Transient and steady state infiltration fluxes during ephemeral streamflow

Submitted to the U.S. Geological Society, 2003

The objectives of this investigation were to improve our understanding of the transient and steady state recharge contributions during streamflow and to develop a field method to measure the transient and steady state infiltration fluxes throughout the duration of an ephemeral streamflow event.

The primary conclusions of this study follow:

- Infiltration rates at the onset of the events were on average about 2-3 orders of magnitude larger than steady state infiltration rates. Transient periods were 3 to 20 hours in duration.
- Use of steady state infiltration rates to estimate total infiltration underestimated simulated values by nearly 18% indicating the need to consider transient infiltration for large coarse-grained stream channels in aquifer recharge investigations.
- A two-layer system can produce multiple steady state infiltration hydrographs depending on the antecedent moisture content, depth of the overlying layer, and duration of the event.
- Simulated steady state infiltration fluxes varied throughout the event by a factor of 2.5.
- The average simulated steady state value was approximately equal to the effective vertical hydraulic conductivity of cores sampled from the less permeable underlying sediment layer.

- A one-dimensional linear solution for infiltration into a single layer of homogeneous sediments provided a limited description of the simulated infiltration rates and was most accurate at predicting transient recharge rates at high antecedent water contents.

2.4 Summary of Paper #4 Combined use of heat and soil-water content to determine stream/ground-water exchanges, Rillito Creek, Tucson, Arizona

Published by the U.S. Geological Survey as a Circular Chapter

The City of Tucson and surrounding area receives virtually all of its municipal, agricultural, and industrial water from ground water that is pumped from thick alluvial basins. Ground water in these aquifers is recharged mostly by water that percolates through ephemeral stream-channel deposits (Davidson, 1973; Matlock and Davis, 1972; Hanson and Benedict, 1994). An increase in ground-water use to support a growing population has resulted in water-level declines of more than 60 meters in the past 50 years. To help mitigate water-level declines, an in-stream recharge facility has been proposed for Rillito Creek, an ephemeral stream on the north side of Tucson. This chapter describes one component of an investigation designed to improve the understanding the infiltration processes beneath Rillito Creek.

The primary conclusions of this study follow:

- Water content measurements and temperature measurements can be used to evaluate the potential suitability of in-stream recharge facilities and to provide guidance on siting such facilities.
- Flow was primarily one-dimensional at the near surface after the sediments were saturated.
- One-dimensional analyses of temperature measurements collected during a streamflow period in April 2001 show that infiltration rates through the Rillito Creek stream deposits were sustained at approximately 0.37 meters per day.
- During events there was a general decline in infiltration rate over time during a streamflow event.

2.5 Summary of Paper #5 Determining temperature and thermal properties for heat-based studies of surface-water ground-water interactions
Published by the U.S. Geological Survey as a Circular Chapter

Advances in electronics leading to improved sensor technologies, large-scale circuit integration, and attendant miniaturization have created new opportunities to use heat as a tracer of subsurface flow. Because nature provides abundant thermal signals at the land surface, heat is particularly useful in studying stream-groundwater interactions. This appendix describes methods for obtaining the thermal data needed in heat-based investigations of shallow subsurface flow.

The primary conclusions of this study follow:

- Temperature sensors need to be located within the thermally active zone for studies of surface water-ground water exchanges.
- A variety of existing and emerging instrumentation technologies are available for monitoring surface-water and ground-water temperatures and for determining thermal parameters of sediments.

2.6 Summary of Paper #6 Processes controlling recharge beneath ephemeral streams in southern Arizona

Accepted for publication by the *American Geophysical Union Monograph Series*
Recharge and Vadose-Zone Processes: Alluvial Basins of the Southwestern United States

The objective of the final paper was to review recent recharge investigations focused on large ephemeral channels in Southern Arizona. The paper briefly discusses the combined hydrological, geophysical, and isotopic methods used to monitor the transport of water within ephemeral streams and through their underlying sediments. Previous studies were reviewed to assess processes controlling infiltration into the near sediments, redistribution through the unsaturated zone, and finally recharge to the underlying aquifer. The review ends with a summary of investigations focused on temporal influences on stream channel recharge.

The primary conclusions of this study follow:

- Investigations have demonstrated the utility of new monitoring techniques, such as the use of temperature, and stable isotopes to monitor temporally induced variations in recharge rates and to explore the pathways of infiltrating water.
- Transformation of the near surface bed sediments through deposition and scour, microbial flora growth, and colloidal swelling will cause fluctuations in the surface permeability and recharge rates.
- Seasonal fluctuations in channel losses indicated that annual recharge rates and empirical equations based on uniform coefficients may not be suitable for computing long-term recharge.
- Representative recharge values for ephemeral channels will require collection and analysis of long-term hydrologic data because of periodic climate oscillations with decadal or longer frequencies
- Future deliberations on recharge will be most effective when each aspect of the process is considered from infiltration at the channel surface through percolation across the water table.

2.7 Summary of the Dissertation

Ephemeral streamflow infiltration through alluvial channels has been identified as an important source of aquifer replenishment in arid and semi-arid environments (Anderson

et al., 1992). The use of steady state infiltration factors for basin wide estimates of channel infiltration necessitates low cost streamflow timing techniques suitable for installation in various channel settings. In this dissertation, two field methods were developed for monitoring streamflow timing in ephemeral stream channels. The first streamflow timing method exploits differences in the advective and conductive thermal transport mechanisms during the presence and absence of streamflow. When streamflow is present, heat is transported through the sediments primarily through advection. In the absence of streamflow conduction is dominant. A statistical method was developed to analyze bed sediment thermographs to identify the different thermal transport mechanisms and thus to infer streamflow timing. The technique requires the definition of five analysis parameters. The accuracy of streamflow identification is most sensitive to the standard deviation window length and a threshold parameter. Once the analysis parameters are established, either through calibration with independent flow timing measurements or through supporting climate information, identification of the presence or absence of flow is repeatable, objective, and easily automated to process large data sets. Furthermore, the thermal method and analysis technique allows for the use of deeper temperature measurements, which may be advantageous under some field conditions that prohibit near surface thermal monitoring.

The second method of streamflow timing utilized the relationship between soil water content and electrical resistance. Electrical resistance sensors were designed to detect saturated soil conditions and thus to infer streamflow timing during periods of saturation.

Temperature sensors and electrical resistance sensors were field-tested in Rillito Creek, Tucson, Arizona. Estimates of streamflow timing were more accurate when made using the electrical resistance sensors than the temperature sensors and were comparable in accuracy to stream-gage and soil water-content methods. Advantages of electrical resistance sensors include depth independence and reduced analysis requirements. The low cost, ease of implementation, and absence of datalogger connecting wires from the sensor to the stream bank provide a distinct advantage over conventional streamflow timing methods.

Infiltration fluxes were measured throughout the duration of three ephemeral streamflow events to evaluate the use of steady state infiltration rates for estimating cumulative infiltration for a large alluvial stream. Temperature and water content measurements were used to calculate infiltration fluxes for streamflow events in a large stream channel with a higher conductivity alluvial layer overlying a lower conductivity alluvial material. The steady-state infiltration rate was related to the effective hydraulic conductivity of the lower alluvial material. Average infiltration rates at the onset of the events were 2-3 orders of magnitude larger than steady state infiltration rates. Transient periods were 1.8 to 20 hours in duration, in inverse proportion to the antecedent moisture content. Use of steady state infiltration rates to estimate total infiltration underestimated cumulative infiltration by 18%, demonstrating the need to consider transient infiltration to improve streambed infiltration estimates for aquifer recharge investigations.

As indicated by these studies, an increasing variety of techniques are becoming available for measuring temperature, infiltration fluxes, and soil saturation in field settings. As sensors and data-acquisition systems continue to develop, instrumentation costs should continue to decrease and the number and quality of measurement options improves. Thermal and water content techniques are providing increasingly useful information about surface water-ground water interactions enabling hydrologists to improve measurement of infiltration in ephemeral stream channels.

3. REFERENCES

- Anderson, T. W., G. W. Freethey, and P. Tucci, *Geohydrology and Water Resources of Alluvial Basins in South-Central Arizona and Parts of Adjacent States*. U.S. Geological Survey Professional Paper 1406-B, 67 pp., 1992.
- Archie, G. E. 1942. The electrical resistivity log as an aid in determining some reservoir characteristics, Trans. AIME, 146, 146, 54-62.
- Bailey, M. A., *Analysis Of One-Dimensional Vertical Infiltration Using Heat As A Tracer In Rillito Creek*, Tucson, The University of Arizona, master's thesis, 152 pp., 2002.
- Blasch, K.W., J.B. Fleming, J.P Hoffmann, and P.A. "Ty" Ferré, "Temperature and Moisture Content Profiling of an Ephemeral Stream Channel In a Semiarid Watershed: Comparison of vertical infiltration velocities at the onset and cessation of flow", EOS Transactions American Geophysical Union, v.81 no.48, December 2000, p. F502.
- Boyle, J.M. and Z.A. Saleem 1979. "Determination of recharge rates using temperature depth profiles in wells", *Water Resources Research*, vol. 15, pp. 1616-1622.

Bredehoeft, J.D. and I.S. Papadopoulos 1965. "Rates of vertical groundwater movement estimated from the Earth's thermal profile", *Water Resources Research*, vol. 1, no. 2, pp.325-328.

Burkham, D.E., Depletion of streamflow by infiltration in the main channels of the Tucson Basin, Southwestern Arizona: U.S. Geological Survey Water-Supply Paper 1939-B, Government Printing Office, Washington D.C., 36, 1970.

Cartwright, Keros 1970. "Groundwater discharge in the Illinois Basin as suggested by temperature anomalies", *Water Resources Research*, vol. 6, no. 3, pp.912-918.

Cartwright, Keros 1979. "Measurement of fluid velocity using temperature profiles: experimental verification", *Journal of Hydrology*, vol. 43, pp. 185-194.

Constantz, J., C. L. Thomas, and G. Zellweger, Influence of diurnal variations in stream temperature on streamflow loss and groundwater recharge, *Water Resources Research*, 30(12), 3253-3264, 1994.

Constantz, J. and C.L. Thomas, The use of streambed temperature profiles to estimate depth, duration, and rate of percolation beneath arroyos, *Water Resour. Res.*, 32(12), 3597-3602, 1996.

Constantz, J. and C.L. Thomas, Streambed temperature profiles as indicators of percolation characteristics beneath arroyos in the Middle Rio Grande Basin, USA, *Hydrol. Process.*, 11, 1621-1634, 1997.

Constantz, J., Interaction between stream temperature, streamflow, and groundwater exchanges in alpine streams, *Water Resources Research*, 34(7), 1609-1615, 1998.

Constantz, J., D. Stonestrom, A.E. Stewart, R. Niswonger, and T.R. Smith, "Analysis of streambed temperature in ephemeral stream channels to determine streamflow frequency and duration," *Water Resources Research*, 37(2), 317-328, 2001.

Constantz, J., A. E. Stewart, R. Niswonger, and L. Sarma, Analysis of temperature profiles for investigating stream losses beneath ephemeral channels, *Water Resources Research*, 38(12), 1316, doi:10.1029/2001WR001221, 2002.

Constantz, J., S.W. Tyler, and E. Kwicklis, Temperature-Profile Methods for Estimating Percolation Rates in Arid Environments, *Vadose Zone Journal*, 2, 12-24, 2003.

Davidson, E.S., Geohydrology and Water Resources of the Tucson Basin, Arizona: U.S. Geological Survey Water-Supply Paper 1939-E, U.S. Government Printing Office, Washington, E1-E78, 1973.

Galyean, K., Infiltration of Wastewater Effluent in the Santa Cruz River Channel, Pima County, Arizona, U.S. Geological Survey Water-Resources Investigations Report 96-4021, 82 pp., 1996.

Gee, G. W., P. J. Wierenga, B. J. Andraski, M. H. Young, M. J. Fayer, and M. L. Rockhold, Variations in Water Balance and Recharge Potential at Three Western Desert Sites, *Soil Sci. Soc. Am. J.*, 58, 63-72, 1994.

Hanson, R. T. and J. T. Benedict, *Simulation of ground-water flow and potential land subsidence, Upper Santa Cruz Basin, Arizona*, U.S. Geological Survey Water-Resources Investigations Report, 93-4196, 47 pp., 1994.

Healy, R.W. and A.D. Ronan, Documentation of computer program VS2DH for simulation of energy transport in variably saturated porous media: Modification of the U.S. Geological Survey computer program VS2DT, U.S. Geol. Surv. Water Resour. Invest. Rep., 96-4230, 1996.

Hoffman, J.P., M.A., Ripich and K.E., Ellett, 2002, Characteristics of shallow deposits beneath Rillito Creek, Pima County, Arizona, U.S. Geological Survey Water-Resources Investigations Report 01-4257, 51 pp.

Hoffman, J.P., K.W. Blasch, D.R. Pool, and M.A. Bailey, In Review, Estimated infiltration, percolation, and recharge rates at the Rillito Creek focused recharge investigation site, Tucson, Arizona, U.S. Geological Survey Professional Paper.

Jaynes, D.B. 1990. Temperature variation effects on field measured infiltration, *Soil Sci. Soc. Amer. J.* , vol.54, no. 2, pp. 305-312.

Kalin, R.M., 1994, The hydrogeochemical evolution of the groundwater of the Tucson basin with application to 3 dimensional groundwater flow modeling: PhD dissertation, University of Arizona, Department of Geosciences, 510 p.

Katz, L.T., 1987, Steady State Infiltration Processes Along the Santa Cruz and Rillito Rivers, Ph.D. Dissertation, University of Arizona, Tucson.

Lapham, W.W. 1987 Use of temperature profiles beneath streams to determine rates of vertical ground-water flow and vertical hydraulic conductivity, US Geological Survey Water Supply Paper No. 2337, Government Printing Office, Washington D.C. p1-35.

Latkovich, V.J. and G.H. Leavesly. 1993. "Automated Data Acquisition and Transmission" in Handbook of Hydrology, D.R. Maidment, McGraw-Hill, New York, p.25.1-25.21.

Matlock, W.G., 1965, The effect of silt-laden water on infiltration in alluvial channels, Ph.D. Dissertation, University of Arizona, Tucson.

Matlock, W.G. and P.R. Davis, 1972. Groundwater in the Santa Cruz Valley, Arizona: Tucson, Az., Technical Bulletin 194, University of Arizona Agricultural Experiment Station, 37 p.

Maurer, D. K. and J. M. Fischer, *Recharge to the Eagle Valley Ground-Water Basin by Streamflow in Vicee Canyon, West-Central Nevada*. U.S. Geological Survey Water-Resources Investigations Report 88-4158, 66 pp., 1988.

McNeil, J.D., 1980, Electromagnetic terrain conductivity measurements at low induction numbers: Mississauga, Ontario, Canada, Geonics Ltd. Technical Note TN-6, 15 pp.

Pool, D.R., In Review. Variations in Climate and Natural Recharge in Southeast Arizona, U.S. Geological Survey Report.

Ronan, A. D., D. E. Prudic, C. E. Thodal, and J. Constantz, Field study and simulation of diurnal temperature effects on infiltration and variably saturated flow beneath an ephemeral stream, *Water Resources Research*, 34(9), 2137-2153, 1998.

Sakura, Y. 1978. Study on groundwater cycle by water temperature. In: M. Ichikawa and I. Kayane (Editors), *Water Balance in Japan*. Kokon-shoin, pp. 211-303.

Scott, R. L., W. J. Shuttleworth, T. O. Keefer, and A. W. Warrick, Modeling multiyear observations of soil moisture recharge in the semiarid American Southwest, *Water Resources Research*, 36(8), 2233-2247, 2000.

Silliman, S.E., J. Ramirez, and R.L. McCabe, Quantifying downflow through creek sediments using temperature time series: one-dimensional solution incorporating measured surface temperature, *Journal of Hydrology*, 167, 99-119, 1995.

Simunek, J., M. Sejna, and M. Th. van Genuchten. 1998. The Hydrus-1D software package for simulating the one-dimensional movement of water, heat, and multiple solutes in variably-saturated media – version 2.0, U.S. Salinity Laboratory, Agricultural Research Service, U. S. Department of Agriculture, Riverside, California.

Smith, G. E. P., Groundwater supply and irrigation in the Rillito Valley: Tucson, AZ, Bulletin No. 64, University of Arizona Agricultural Experiment Station, 81-243, 1910.

Stallman, R.W. 1960& 1963. Computation of ground-water velocity from temperature data, in Bentall, Ray, comp., Methods of collecting and interpreting ground-water data: U.S. Geological Survey Water-Supply Paper 1544-H, p. 36-46 (also in Notes on the use of temperature data for computing ground-water velocity: Societe Hydrotechnique de France (Nancy), 6th Assem. Hydraul., Rapp. 3, question1, pp. 1-7 1960).

Stallman, R.W., 1965. Steady one-dimensional fluid flow in a semi-infinite porous medium with sinusoidal surface temperature, *J. Geophys. Res.*, vol. 70, no. 12, pp. 2821-2827.

Supko, D. J., *Subsurface Heat Flow as a Means for Determining Aquifer Characteristics in the Tucson Basin, Pima County, Arizona*, Tucson, University of Arizona, Ph.D. dissertation, 184 pp., 1970.

Suzuki, S., Percolation measurements based on heat flow through soil with special reference to paddy fields, *J. Geophys. Res.*, 65(9), 2883-2885, 1960.

Tadayon, S., N.R. Duet, G.G. Fisk, H.F. McCormack, C.K. Partin, G.L. Pope, and P.D. Rigas. 2000. Water Resources Data for Arizona, water year 2000, U.S. Geological Survey Water-Data Report AZ-00-1, p. 9-210.

Taniguchi, M. and M.L. Sharma 1993. "Determination of groundwater recharge using the change in soil temperature", *Journal of Hydrology*, vol. 148, pp. 219-229.

Theis, C. V., The source of water derived from wells—essential factors controlling the response of an aquifer to development, *Civil Engineering Magazine*, 277-280, 1940.

Turner, S.F., and others, 1943, Ground-water resources of the Santa Cruz basin, U.S. Geological Open File Report.

Voss, C.I., A finite-element simulation model for saturated-unsaturated, fluid-density dependent groundwater flow with energy transport or chemically-reactive single-species solute transport, U.S. Geol. Surv. Water Resour. Invest. Rep., 84-4369, 409 pp., 1984.

Walvoord, M. A. and B. R. Scanlon, Hydrologic Processes in Deep Vadose Zones in Interdrainage Arid Environments , in F. M. Phillips, J. Hogan, and B. R. Scanlon, editors. Recharge and Vadose Zone Processes in Alluvial Basins in the Southwestern United States. AGU. 2003.

Wankiewicz, A. (1984) Hydrothermal processes beneath arctic river channels: *Water Resources Research*, 20(10), 1417-1426, 1984.

Wierenga, P.J., R.M. Hagan, and D.R. Nielsen 1970. "Soil temperature profiles during infiltration and redistribution of cool and warm irrigation water", *Water Resources Research*, vol. 6, no. 1, pp. 230-238.

Wilson, L.G., K.J. DeCook, and S.P. Neuman, 1980. Regional Recharge Research for Southwest Alluvial Basins, Water Resources Research Center, University of Arizona, Tucson.

APPENDIX A: A STATISTICAL TECHNIQUE FOR INTERPRETING STREAMFLOW TIMING USING STREAMBED SEDIMENT THERMOGRAPHS

Kyle W. Blasch, Ty P.A. Ferré, and John P. Hoffmann

Accepted by *Vadose Zone Journal*, 2003

Abstract

A moving standard deviation technique was developed to infer the onset and cessation of ephemeral streamflow using temperature data from the upper 2.25 meters of streambed sediments. During periods of streamflow, heat loss to the water column and shifting of the predominant thermal-transport mechanism within the sediments from conduction to advection produced changes in the amplitude of the vertically propagating diurnal temperature waves. Analytical expressions describing propagation of conductive and advective diurnal temperature waves through streambed sediments were presented for identifying depths with the largest changes in the diurnal temperature wave amplitude between periods of flow and no flow. A moving standard deviation statistical technique was developed to identify the thermal amplitude changes from bed sediment thermographs and to infer streamflow timing. The accuracy of the moving standard deviation technique was quantified by calibrating the statistical method using streamflow measurements made with alternative flow detection devices. Accuracy of the technique was most sensitive to the standard deviation window length and the threshold parameter

separating periods of conductive and advective thermal transport. An alternative calibration procedure was developed that does not require alternative flow detection devices. The average error for streamflow timing was approximately 400 minutes for each event. The results show that temperature sensors may be deployed at a range of sediment depths depending on streamflow stage and soil thermal and hydraulic properties and that an automated statistical procedure can provide an objective and repeatable means to quantify streamflow timing.

1. Introduction

Recording the continual presence and absence of streamflow within ephemeral channels in large semi-arid and arid basins for use in water balance and hydrologic models requires an inexpensive and reliable method for broad distribution. The difficulties of monitoring streamflow timing and extent within ephemeral channels using traditional stream gaging techniques arise because of the flashy nature of streamflow events and shifting elevations of the channel surface (Constantz and Thomas, 1997; Blasch, 2003). Consequently, measurement of streamflow presence using subsurface methods has been proposed (Constantz and Thomas, 1997). Because streambed temperature measurements are inexpensive and easy to obtain relative to other subsurface measurements, streambed thermographs have been introduced as a means to infer streamflow timing and extent in ephemeral streams (Constantz et al., 2001).

Constantz et al. (2001) placed thermal sensors at shallow depths (15 cm) to identify reductions in thermal amplitudes caused by absorption of radiant energy in the water column (Figure 1). They visually identified changes in streambed temperature wave amplitudes to determine the start and end of streamflow events. Although this visual inspection technique has been successfully demonstrated in ephemeral streamflow settings for multiple day events, the technique is both subjective and time consuming when analyzing large data sets. The technique can also be ineffective for identifying stream flow events that are less than 24 hours in duration, which is typical of ephemeral streams in southern Arizona, for example. Finally, this method of analysis requires relatively shallow measurement depths to take advantage of reductions in the diurnal temperature wave amplitude that occur as heat is lost to the standing water above the sediments. Such shallow installed instruments are especially susceptible to removal by scour of the channel sediments.

The first objective of this investigation was to present a description of thermal transport that considers the effects of both conductive and advective temperature transport. This description will expand the relevance of this method to a greater number of ephemeral streams by allowing for monitoring of temperature at deeper depths where shallow temperature measurements are impractical, such as reaches that experience significant scour (Constantz et al., 2003). The second objective was to introduce an automated technique for identifying the onset and cessation of ephemeral streamflow based on a statistical analysis of streambed thermographs.

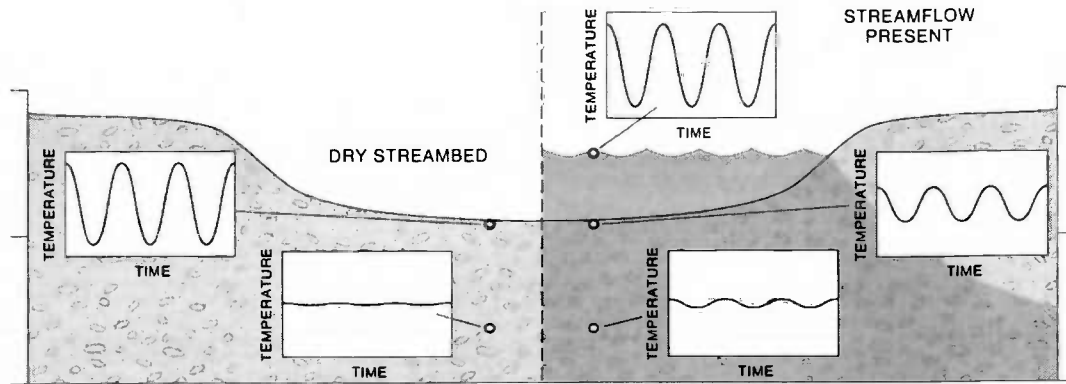


Figure 1. Thermal responses from within a streambed divided into the case when streamflow is absent (primarily conductive heat transport through the sediments) and the case when streamflow is present (primarily advective heat transport through the sediments). Note the reduction in the thermal amplitude at the streambed surface caused by heat loss to the overlying water column and corresponding increase in thermal amplitude at depth caused by percolating water.

The following section presents two analytical expressions describing conductive and advective thermal transport as well as the hydrological conditions necessary to use bed sediment thermographs for streamflow timing. The discussion continues by introducing the moving standard deviation technique for analyzing bed sediment thermographs. Finally, bed sediment thermographs collected from an array of temperature sensors within an ephemeral stream are used to evaluate the utility of the moving standard deviation technique.

2. Optimal depth selection for placement of temperature sensors

When streamflow is absent from a channel, radiant heating of the surface sediments is transported into the sediment profile primarily through conduction (Figure 1). The diurnal temperature, often represented as a sinusoidal function, propagates through the sediments with a decreasing amplitude and increasing time lag with depth (Van Wijk and

De Vries, 1963). The magnitude of the one-dimensional diurnal temperature wave as a function of depth for a homogenous single layer is described by (Van Wijk and De Vries, 1963):

$$T_{cond}(z) = T_o e^{-\frac{z}{D}}, \quad (1)$$

T_{cond} is the amplitude of the sediment temperature variation ($^{\circ}\text{C}$) at depth z (cm) below the land surface, T_o is the amplitude of the diurnal temperature wave ($^{\circ}\text{C}$) at the sediment surface, and D is the damping depth (cm) of the diurnal temperature waves represented as,

$$D = \left(\frac{P\alpha_s}{\pi} \right)^{0.5}, \quad (2)$$

where, α_s is the thermal diffusivity ($\text{cm}^2 \text{s}^{-1}$) and P is the period (s) of temperature oscillation at the sediment surface. At a depth D the relative temperature amplitude of the wave declines to e^{-1} (0.37) and at a depth $D\pi$ the wave is 180° out of phase with the wave at the surface. Typical damping depth values for sandy soils are about 15 cm and for clay soils are about 12 cm (Van Wijk and De Vries, 1963).

The presence of streamflow within a channel can cause infiltration and percolation of water through streambed sediments, increasing the amount of heat transported to deeper depths through a combination of advection and conduction. As a result, thermographs at deeper depths will show an increase in the diurnal temperature amplitude (Figure 1).

Stallman (1963, 1965) developed an analytical solution to the one-dimensional coupled

heat and water transport equations assuming one-dimensional steady vertical flow in a single saturated layer and a sinusoidal temperature variation at the surface. The diurnal temperature wave amplitude for the combined advection and conduction equation using the Stallman solution is:

$$T_{adv}(z) = T_s e^{-az}, \quad (3)$$

where T_{adv} is the amplitude of the sediment temperature variation ($^{\circ}\text{C}$) at depth z (m) below the land surface, T_s is the amplitude of the temperature wave ($^{\circ}\text{C}$) at the sediment surface, and a (m) is a coefficient based on the fluid flow and thermal properties of the sediment

$$a = \left[\left(K^2 + \frac{V^4}{4} \right)^{\frac{1}{2}} + \frac{V^2}{2} \right]^{\frac{1}{2}} - V, \quad (4)$$

with

$$K = \frac{\pi c \rho}{\kappa P}, \quad (5)$$

and

$$V = \frac{v c_o \rho_o}{2\kappa}. \quad (6)$$

The variable c is the specific heat of the fluid and sediment in combination ($\text{cal g}^{-1} ^{\circ}\text{C}^{-1}$), ρ is the density of the fluid and sediment in combination (g m^{-3}), κ is the thermal conductivity of the fluid and sediment in combination ($\text{cal s}^{-1} \text{m}^{-1} ^{\circ}\text{C}^{-1}$), v is the fluid flux (m s^{-1}), c_o is the specific heat of the fluid ($\text{cal g}^{-1} ^{\circ}\text{C}^{-1}$), and ρ_o is the density of the fluid (g m^{-3}). If v is zero then equation 3 reduces to the conduction equation, but as v increases the transport of heat due to advection increases. The predominant heat transport

mechanism within the sediments will depend upon the infiltration rate, thermal parameters, and of course the depth of interest. For simplicity we will refer to the transport of heat during the presence of streamflow as advection even though conduction also contributes to the transport of heat.

Comparison of shallow and deeper thermographs with and without the presence of streamflow (Figure 1) show two clear characteristics. First, as shown by Constantz et al (2001), during streamflow there is a reduction in the conductive heat transport due to the loss of radiant heat to the water column. Second, due to increased advective transport, the temperature amplitudes at deeper depths are higher during periods of streamflow than during the absence of streamflow.

Constantz et al (2001) monitored temperature at the near surface (15 cm) to successfully infer the presence of streamflow. The method was appropriate for the streams the authors studied because two critical conditions for the success of this method were achieved. First, the diurnal temperature amplitude at the surface was sufficiently large so that minor temperature fluctuations such as those caused by clouds did not obscure the diurnal signal. Second, during the presence of streamflow the overlying water column produced a measurable reduction of the amplitude of the diurnal temperature wave at the streambed surface compared to the magnitude of the diurnal temperature wave at the streambed surface during the absence of streamflow (Figure 1). If, however, either of these conditions had not been satisfied then changes in the near surface diurnal temperature

wave amplitude during streamflow would have been insufficient to infer the presence of streamflow.

Other circumstances noted by Constantz et al. (2001) that can preclude the use of streambed temperature for monitoring streamflow include precipitation, sudden changes in air temperature, and scour. Precipitation and sudden changes in air temperature associated with weather fronts can cause fluctuations in the sediment temperatures similar to those caused by the presence of streamflow. In general, precipitation induced fluid fluxes and abrupt air temperature changes do not penetrate as deeply below the sediment surface as streamflow events and will have a greater influence on sensors near the surface. For these circumstances thermographs at deeper depths can be more suitable.

As an example of conductive (no flow) and advective (flow) thermal transport, hydraulic and thermal parameters for coarse-grained sediments typically found in ephemeral streambeds were incorporated into equations 1-6. The conductive and advective diurnal temperature waves were plotted as a function of depth for three different streamflow cases (Figure 2). The no dampening case assumes there is no heat loss to the overhead water column and the 50% reduction case assumes the radiant thermal amplitude is reduced by 50% as it travels through the water column. The fluid flux was reduced for the third case to demonstrate the dependence of the advective thermal amplitude on this variable. Comparison of the conductive (no flow) and advective (flow present) diurnal temperature waves as a function of depth shows that near the surface the conductive

thermal amplitude is larger than the advective thermal amplitude because heat is lost to the overhead water column during streamflow (Figure 2). It is also apparent that percolating water transports more heat to deeper depths compared to conduction alone during the absence of streamflow. Consequently, an important prerequisite for using thermographs at deeper depths to infer streamflow is that the hydrologic flux is sufficiently large to cause measurable changes in the amplitude of the diurnal temperature wave during the presence of streamflow compared to the absence of streamflow.

The conductive diurnal temperature wave amplitude at each depth was subtracted from the advective diurnal temperature wave amplitude to quantify the difference in thermal transport as a function of depth (Figure 2). If there is no heat loss to the water column, then at the surface (0.0 m) the difference in conductive and advective amplitudes is zero. However, at depth there is still a difference in amplitude. Greater losses of heat to the water column result in larger amplitude differences at the surface but only a slight reduction in the amplitude reductions at depth. Thus temperature monitoring at depth may be more dependable and informative than the near surface for inferring flow in stream channels experiencing a range of stages.

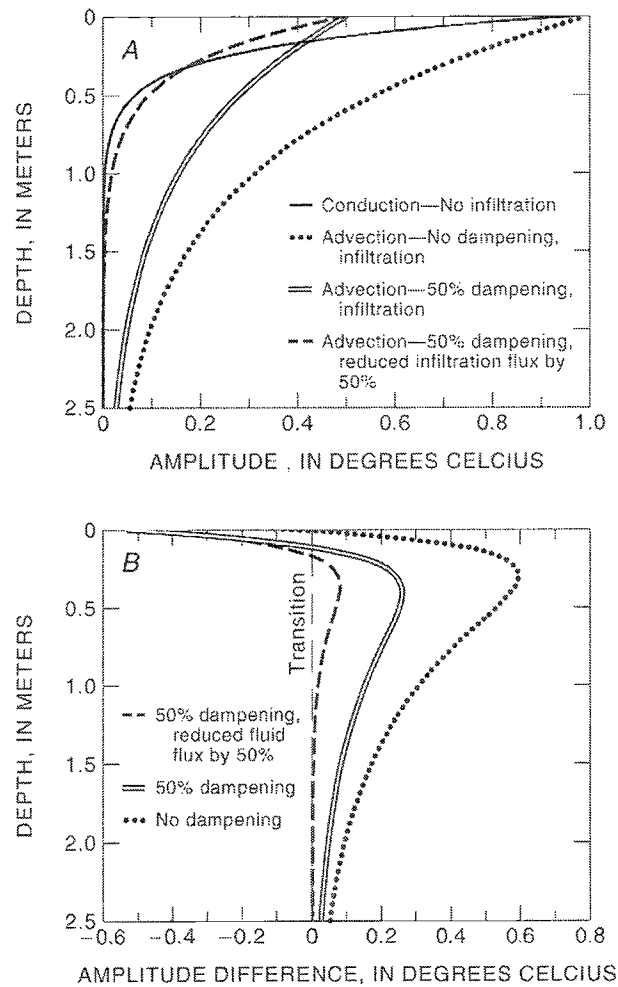


Figure 2. (A) Advective and conductive diurnal temperature wave amplitudes as a function of depth propagating through coarse-grained stream channel sediments. The radiant thermal amplitude at the surface is 1°C . The solid black line describes conductive thermal transport during no flow conditions. The no dampening case considers zero loss of heat to the water column during the presence of streamflow. The 50% dampening case considers 50% loss of heat energy to the water column during the presence of streamflow. The 50% dampening / 50% fluid flux reduction considers a 50% loss of heat to the water column and a reduction in the fluid flux from the previous two cases by 50%. (B) Difference between the advective and conductive diurnal temperature wave amplitudes as a function of depth. Intersections between the solid diurnal temperature wave amplitude segments and the dashed transition line represent depths corresponding to equivalent advective and diurnal temperature wave amplitudes during flow and no flow conditions respectively.

Optimal measurement depths for inferring streamflow can be defined as depths where streamflow induced infiltration causes the greatest measurable changes in diurnal temperature wave amplitudes compared to no flow conditions. Equations 1-6 can be used with knowledge of the sediment profile and streamflow stage to estimate the optimal depths. The least optimal depths are those where the thermal amplitude does not change due to the presence of streamflow. One depth that is not suitable is called the transition depth, z_t , where the conduction and advection diurnal temperature wave amplitudes are equivalent during the presence and absence of streamflow. The transition depth also represents the point where the magnitude of the diurnal temperature wave amplitude during the presence of streamflow becomes larger than the diurnal temperature wave during the absence of streamflow. The transition depth is represented in Figure 2 for the three different streamflow cases. The transition depth for each case is located where the lines representing the difference in thermal transport intersect the vertical dashed line. For the no dampening case the combination of advection and conduction will transport more heat throughout the entire profile so the transition depth does not occur. As dampening increases the transition depth increases. For the 50% dampening case the transition depth occurs at approximately 0.11 m and for the 50% dampening and fluid flux reduction case the transition depth is approximately 0.17 m. Thus the transition depth is also dependent on the magnitude of the infiltration flux. Additionally, depths closer to the surface are less suitable if they are not below the zone of scour or are influenced by temperature fluctuations induced by precipitation and weather fronts as discussed earlier.

3. Standard deviation technique for detecting periods of streamflow

Analysis of a streambed thermograph to infer streamflow timing is based on identification of the aforementioned temporal changes in the streambed thermograph (Figure 1). As an example, two thermographs measured in a coarse-grained alluvial stream at depths above and below the transition depth are presented in Figure 3. When streamflow is present (indicated by the gray areas) as indicated by a stream gage the diurnal temperature wave amplitudes in the thermograph above the transition depth decline whereas the opposite is true of the thermograph below the transition depth. Streamflow timing can be inferred from the thermographs by identifying these changes in thermal amplitude either above or below the transition depth. This analysis can be conducted visually (Constantz et al., 2001), or using statistical tools (Stewart and Constantz, 1999; Stewart, 2003). Moving window averaging is a standard data smoothing technique. We apply a similar approach wherein the standard deviation of temperatures is determined within a defined time window (Figure 4). For each window of time, τ , the number of measurements, n , is determined by the temperature sampling interval, i ,

$$n = \frac{\tau}{i} . \quad (7)$$

The moving standard deviation, s , can be expressed as

$$s(t) = \sqrt{\frac{1}{n-1} \sum_{i=t}^{n+t-1} (x_i - \bar{x}(t))^2} , \quad \text{for } t = 1, \dots, T \quad (8)$$

where,

$$\bar{x}(t) = \frac{1}{n} \sum_{i=t}^{n+t-1} x_i, \quad \text{for } t = 1, \dots, T \quad (9)$$

is the moving average and T is the total number of measurements. The analysis window is advanced in time, yielding a moving window of standard deviation over the entire thermograph. Identification of streamflow is then based on measurable differences in the moving standard deviation during flow and no flow periods. The advantage of using the moving standard deviation is that variations in the thermal record caused by streamflow infiltration are magnified in the standard deviation plots, increasing the ability to discern event timing. Additionally, the moving standard deviation removes longer time-scale fluctuations in the thermograph, which can obscure short-term variations.

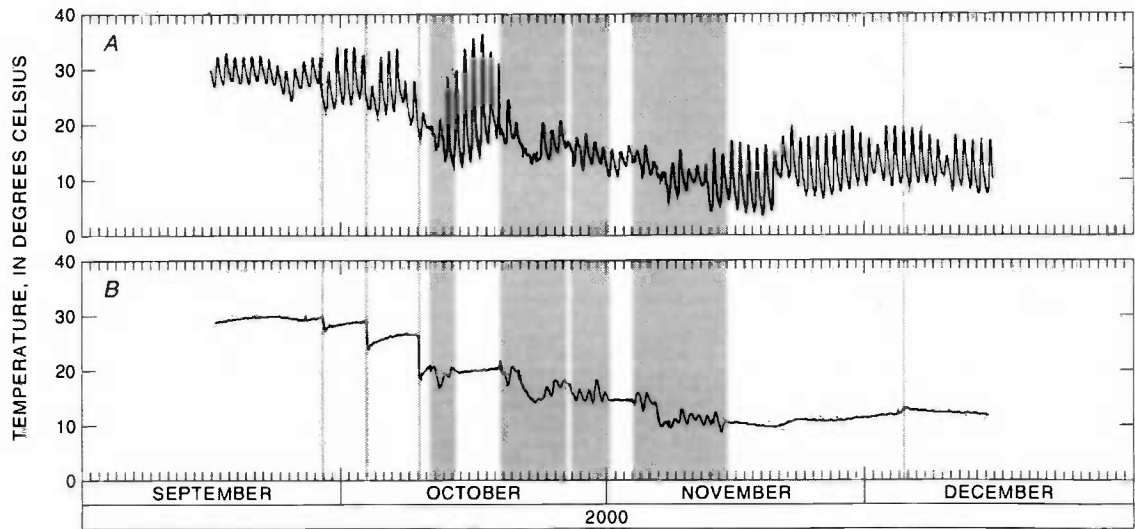


Figure 3. Thermograph for (A) a depth above the transition depth and (B) a depth below the transition depth. The gray areas denote observed periods of streamflow.

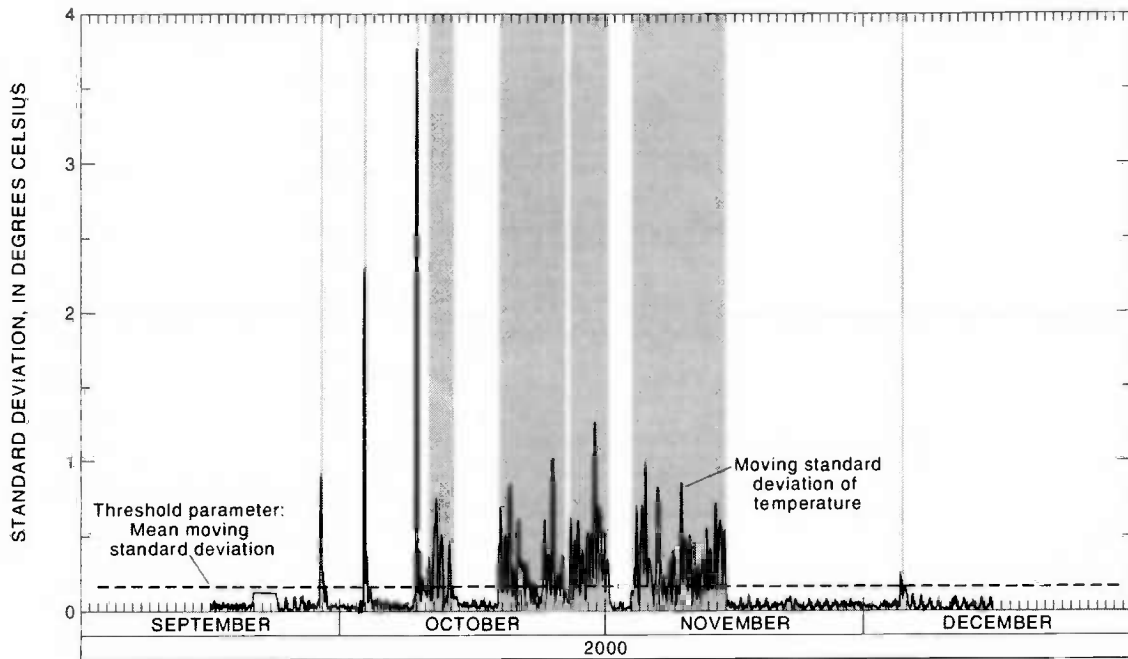


Figure 4. Six-hour moving standard deviation window for temperature data measured below the transition depth. The gray areas denote observed periods of streamflow.

Five parameters are required to design the moving standard deviation filter: the standard deviation window length, the reference time within the window, the flow / no flow threshold, and two flow duration parameters. The window length, τ , is the time interval over which the standard deviation is calculated. The reference time can be centered on the current time step, t , so that the interval spans either from $(t - 0.5\tau)$ to $(t + 0.5\tau)$, set to the beginning of the window so that the window spans from (t) to $(t + \tau)$, or alternatively is set to the end of the window so that the window spans from $(t - \tau)$ to (t) . The threshold parameter (s_m), measured in $^{\circ}\text{C}$, is interpreted as the magnitude of the standard deviation (i.e., temperature variability in the thermograph) separating advection-dominated from conduction-dominated thermal conditions. Periods of streamflow will appear either

above or below the threshold standard deviation depending on the location of the monitoring depth relative to the transition depth.

$$\begin{aligned} & \left\{ \begin{array}{l} \text{streamflow absent } s(t) < s_m \\ \text{streamflow present } s(t) > s_m \end{array} \right\} \text{ for } z > z_t \\ & \left\{ \begin{array}{l} \text{streamflow absent } s(t) > s_m \\ \text{streamflow present } s(t) < s_m \end{array} \right\} \text{ for } z < z_t \end{aligned} \quad (10)$$

The duration parameters, measured in minutes, are used as filters to remove false interruptions in the prevailing flow conditions. A minimum flow duration parameter, t_{\min} , is defined as the shortest duration of a streamflow event likely to occur at a given location. This filter removes false positive streamflow identifications due to rapid air temperature changes that are associated with fluctuating weather conditions. These atmospheric events mimic the onset of streamflow, but are typically of shorter duration than streamflow events. Secondly, a minimum interflow duration parameter, t_{int} , is defined as the shortest interval likely to separate two consecutive streamflow events. This parameter is used to eliminate false negative flow identifications during streamflow. For example, during streamflow events surface heating may be reduced due to the presence of clouds, resulting in smaller diurnal temperature wave amplitudes at the streambed surface. For thermal monitoring below the transition depth this drop in diurnal heating can cause the standard deviation to drop below the threshold for short periods of time even though water is still percolating through the sediments.

4. Field Methods

A field experiment was designed to determine the suitability of equations 1-6 for selection of optimal measurement depths and to determine the accuracy of the moving standard deviation technique. The study site (within Rillito Creek in Southern Arizona) is located 40 m upstream of the U.S. Geological Survey streamflow-gaging station 09485700 and experiences approximately 15 ephemeral streamflow events each year (Figure 5). The channel reach is approximately 60 m wide and the elevation of the stream channel over the cross section varies by less than 0.8 m. The study site is underlain by recent stream-channel deposits, which are underlain by basin-fill deposits. The recent deposits, consisting of over 90% fine- to coarse-grained alluvium, are about 10 m thick. The underlying basin-fill deposits generally are finer grained and extend to depths of several hundreds of meters. Depth from the channel surface to the water table is about 40 meters.

Rillito Creek is an ephemeral stream with three active seasons, summer North American Monsoon (July- September), fall (October – November) and winter (December-March). Characteristic summer flows result from localized, short-duration convective storms, whereas longer-duration frontal storms and snowmelt produce winter flows. Flow events during all three seasons generally range in duration from several hours to less than 15 days at the study site.

A vertical array of thermocouple sensors was buried beneath the lowest part of the channel cross-section. A 2.5-m deep profile was excavated and seven thermocouple temperature sensors were inserted into the side of the profile at depths of approximately 0.50, 0.75, 1.0, 1.25, 1.50, 2.0, and 2.5 m below the stream channel surface. A thermistor was placed at a depth of 0.15 m below the surface. The sediments were then returned to the profile. A second thermistor was placed on the south bank to record air temperature. All installed temperature sensors were programmed to measure temperature every 5 seconds and to record a time-averaged temperature at 5-minute intervals with a precision of 0.1 °C.

After each streamflow event the channel cross section was surveyed to record the level of deposition and scour. Immediately after installation, a series of flow events scoured approximately 0.25 m of sediment from the site. During the succeeding 24 events sediment scour and deposition varied by less than 0.10 m and on average did not change. These 24 events were selected for analysis.

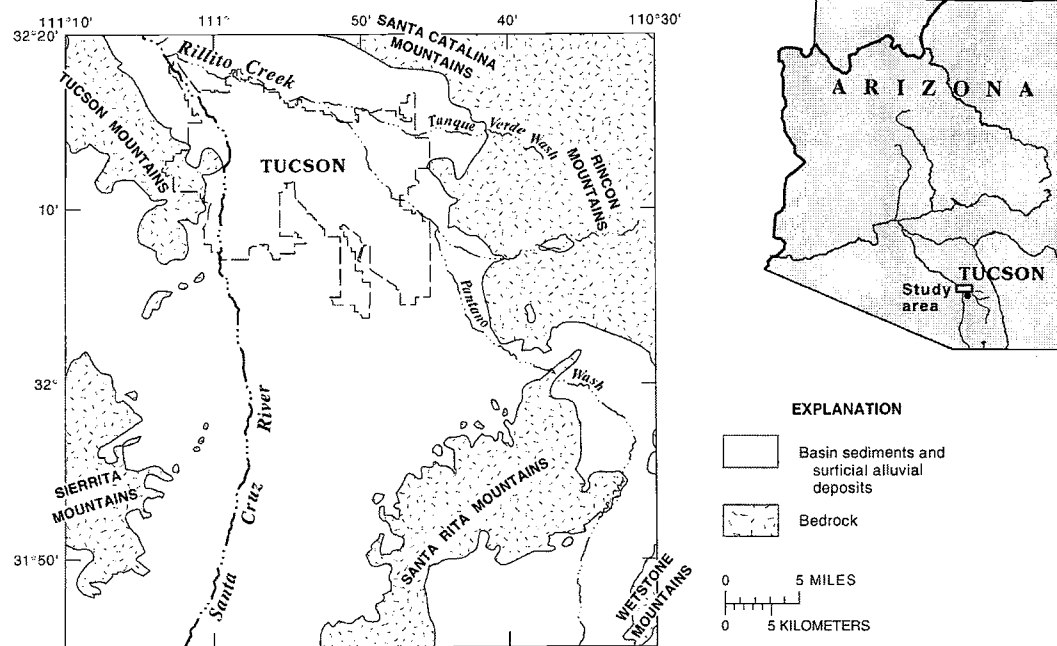
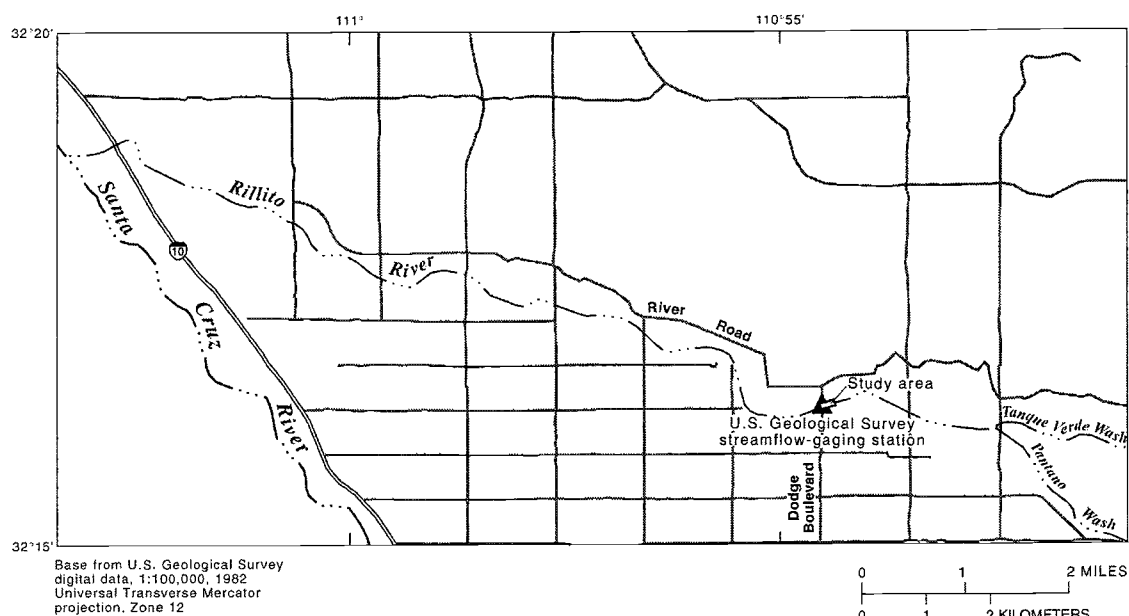


Figure 5. Location of Rillito Creek study area and view of Rillito Creek within the Tucson Basin, Tucson, Arizona.

Time domain reflectometry (TDR) probes were installed adjacent to each thermocouple to provide independent measurements of the onset and cessation of streamflow. The TDR probes measured and recorded volumetric water content at 2-minute intervals with a precision of approximately $0.03 \text{ cm}^3 \text{ cm}^{-3}$. A Campbell Scientific (Logan, UT) TDR100 time domain reflectometer was used in conjunction with a Campbell Scientific CR10X datalogger to transmit, receive, and convert waveforms into water content. TDR probes were comprised of two stainless steel prongs 0.20 m in length, spaced 0.03 m apart. Probes were constructed and calibrated in-house.

The onset and duration of stream flow was identified by elevated volumetric water contents above $0.3 \text{ m}^3/\text{m}^3$. At the onset of streamflow this TDR-based measurement will lag behind the onset of flow at the surface, because of the time required for water to infiltrate to the instrument depth, however it represents the closest measurement of onset and cessation times because the TDR and temperature probes are collocated. Furthermore, saturation of the sediment profile, measured using TDR, was achieved in less than 10 minutes at the onset of the streamflow events as determined by the stream gage. Similarly the cessation of streamflow inferred by the water content sensors lags behind the cessation at the surface.

Measurements were collected over a 365-day record (September 16, 2000 – September 15, 2001), which included 24 streamflow events. Thermographs for the entire measurement period are shown in Figure 6 with streamflow events denoted by the shaded

areas. The ranges of diurnal temperature amplitudes measured at a depth of 0.25 m were, on average, 14.4 °C in the winter and 16.2 °C in the summer. The variability in streamflow duration ranged from a few hours to several days, which was considered ideal for evaluation of the moving standard deviation technique. In addition to the variability in event duration, the interflow period between events was also highly variable. The interflow period range from approximately 6 hours to 64 days. The onset of streamflow for five streamflow events occurred less than 16 hours from the cessation of the previous event.

Thermographs for depths of 0.15m and 1.0m exhibit thermal amplitude responses for temperature sensors above and below the transition depth, respectively (Figure 6). When streamflow is present, the thermal amplitude at a depth of 0.15m is reduced while the thermal amplitude at a depth of 1.0m increases. The shaded areas denote periods of streamflow as determined by the water content sensors.

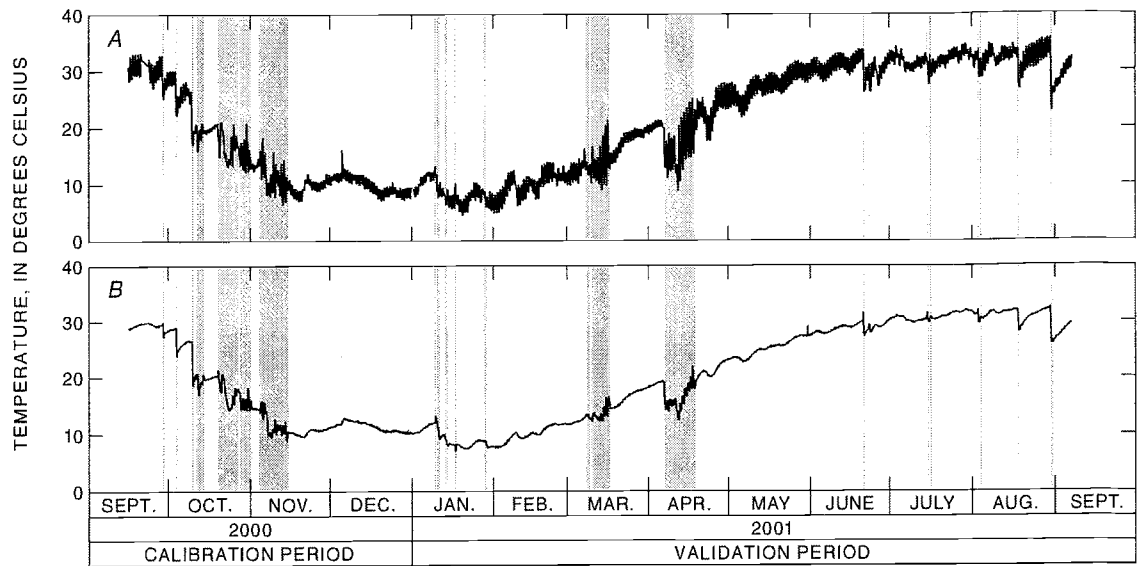


Figure 6. Thermograph from September 16 through December 15, 2000, for (A) a depth of 0.15 meters and (B) a depth of 1.0 meters. The gray areas denote observed periods of streamflow.

5. Results

Initially, the sensitivity of streamflow timing accuracy to each of the five analysis parameters was examined using a continuous record of thermal measurements collected in Rillito Creek in Tucson, AZ, from September 16, 2000 - September 15, 2001. The record was divided into approximately 105,000 five-minute intervals and each interval was identified as either a no-flow or flow period using the water content measurements to identify the presence of streamflow. A sequential parameter sensitivity analysis was performed using a range of likely parameter values.

The standard deviation window length and the threshold were the most sensitive of the five parameters (Figure 7). In general, shorter standard deviation windows are influenced by atmospheric temperature shifts, resulting in more frequent false identifications of

streamflow. Longer windows reduce the number of false identifications of streamflow periods, but underestimated the duration of streamflow. The standard deviation window length was optimal at 1 hour using 5-minute data ($n = 12$) and from 1 to 6 hours for 15-, 30-, and 60-minute data ($n = 4, 2, 1$ respectively). The threshold parameter is most sensitive at values below the mean moving standard deviation value and is comparatively insensitive between 1.25 and 1.75 times the mean moving standard deviation value for standard deviation window lengths from 1 hour to 12 hours.

Location of the reference time within the standard deviation window is more important for the longer standard deviation window lengths. Otherwise, the error associated with this technique is relatively insensitive to the reference time location within the window. Centered locations produced the lowest timing error overall.

Selection of the minimum flow duration parameter is dependent on the influence of atmospheric temperature fluctuations. False indications of flow periods due to atmospheric temperature variations were more prevalent for temperature sensors near the surface. The lengths of false events caused by weather changes are usually less than 4 hours and this is exhibited in the sensitivity analysis with an increase in error for event durations less than about 240 minutes (Figure 7). However, the timing error increased when the minimum duration of a flow event exceeded 240 minutes. It is important to note that the minimum flow duration parameter differentiates between short duration flow events and abrupt atmospheric temperature shifts. The parameter will be less

important for streams that experience longer duration events than those recorded at Rillito Creek.

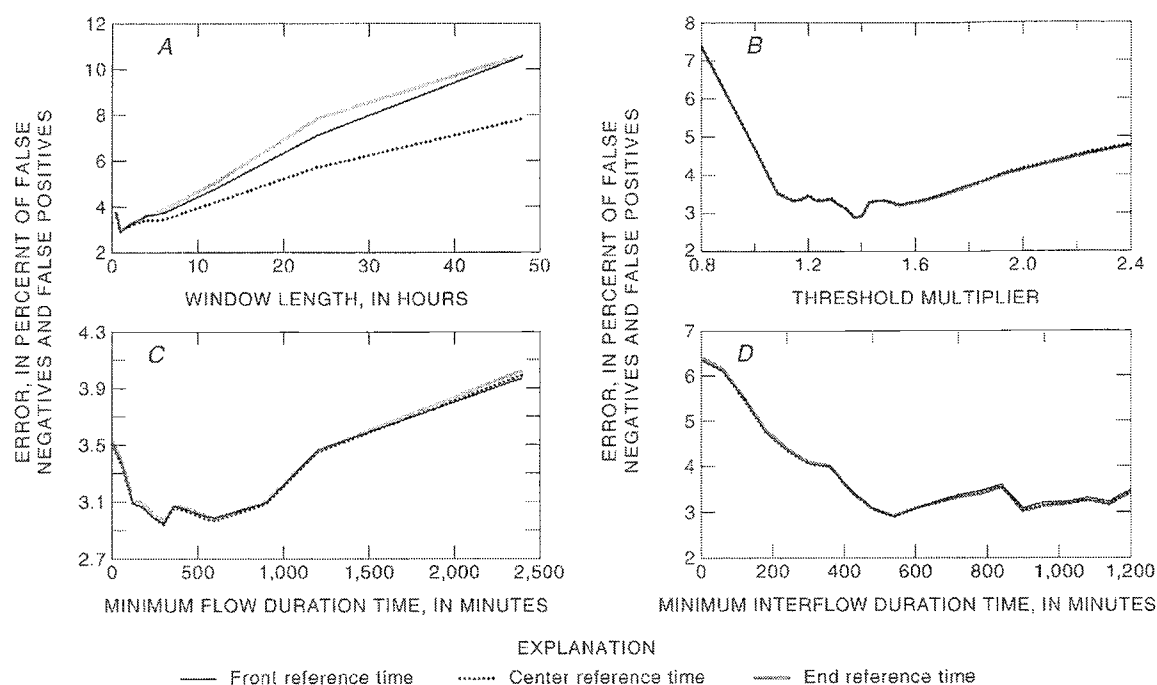


Figure 3-7. A sensitivity analysis for the moving standard deviation technique considering: (A) the moving standard deviation window length, (B) the threshold multiplier times the mean standard deviation, (C) the minimum flow duration parameter and, (D) the minimum interflow duration parameter. Timing error is presented as the percentage of time over a year the method incorrectly infers the presence or absence of streamflow. Generally this error occurs at the onset and cessation of flow by either overestimating or underestimating the period of streamflow.

The minimum interflow duration parameter is a balance between the length of flow interruptions caused by reduced surface heating and the separation of consecutive streamflow events (Figure 7). Five streamflow events in Rillito Creek were separated by less than 16 hours. Optimized values for the flow duration parameter ranged from 6 to 12

hours. Once again this parameter is not as important for streams experiencing fewer, longer duration events than Rillito Creek.

Following the sensitivity analysis, the standard deviation model was calibrated for each depth using the TDR data over a 76-day record (September 16, 2000 – December 15, 2000), which included eight events. The optimal parameters were evaluated over a succeeding 250-day record (January 1, 2001 – September 15, 2001), which included 16 events. The optimization was conducted by holding four of the parameters constant while a single parameter was varied. The parameter value producing the least error in streamflow timing (defined as the sum of the number of false indications of flow and false indications of no flow) was selected. Successive parameters were varied in the same manner. This process was repeated for all five parameters. The cycle of optimization was repeated until improvement in streamflow timing accuracy was less than 0.1%.

Results from the field experiment and standard deviation model indicate that the temperature sensor located at 0.75-m depth was optimal for identifying streamflow timing. The optimal depth was about 0.3 m deeper than predicted by using the analytical expressions. This discrepancy is likely due to inaccurate estimates of the thermal and hydraulic parameters for the site. Specifically, the thermal transport equations 1 through 6 assume steady state infiltration. Transient infiltration fluxes at the onset of streamflow are typically higher than steady-state infiltration fluxes used in the analysis. Use of a

higher infiltration flux that was an average of the transient and steady state infiltration fluxes would have reduced the discrepancy between the predicted and observed optimal depth. Identification of streamflow at shallower depths was less accurate than at 0.75 m because the amplitudes of the conductive and advective diurnal temperature waves were more similar than had been estimated by equations 1-6. While there were no false identifications of streamflow events attributed to precipitation, changes in temperature caused by weather fronts were identified as deep as 1.5m. This effect was more pronounced near the surface. Thermographs from deeper depths were less accurate than the thermograph at a depth of 0.75m because the ranges in amplitude of the diurnal temperature waves declined and at depths below 2.0 m were smaller than the precision of the temperature sensors.

Precipitation over the channel did not produce an increase in water content between 0.25 and 2.25 meters. Thus rainfall did not produce sufficient percolation to advect heat to these depths as would a streamflow event. This is one of the advantages of monitoring temperature at deeper depths.

The optimized analysis parameters were a 1-hour standard deviation window, a threshold approximately 1.5 times the mean standard deviation, a 300-minute minimum flow duration parameter, and a 900-minute minimum interflow duration parameter. Using these analysis parameters, all of the events were identified and no false events were identified. Timing errors arose primarily at the onset and cessation of streamflow. The

standard deviation technique inferred streamflow on average 77 minutes before it was observed by TDR at the same depth. That is, temperature fluctuations were observed before the TDR probes indicated a change in soil water content. This onset timing error was primarily due to fluctuations in air temperature preceding 2 of 14 streamflow events. Excluding these two events, the standard deviation technique inferred flow on average 8 minutes before the onset of streamflow as identified by TDR.

The cessation of flow is more difficult to identify than onset because of the gradual shift in the dominant mechanism of heat transport from advection to conduction at the termination of flow. On average the optimized standard deviation technique inferred the cessation of flow 257 minutes after the observed cessation of streamflow as determined by TDR. This error was fairly consistent so that in practice cessation times could be reduced to account for this overestimation.

6. Stand-Alone Field Application

For most field applications, additional flow-monitoring devices will not be available on site to calibrate temperature-based methods for inferring streamflow timing.

Consequently, the standard deviation method must exhibit a level of effectiveness suitable in a stand-alone fashion. To test the accuracy of the standard deviation method, parameters were selected without the benefit of alternative flow-monitoring information.

Parameters were selected by first employing a range of moving standard deviation window lengths to identify likely streamflow events (Figure 8). As shown in Figure 8, the contrast between the thermal amplitude during the presence and absence of streamflow was identifiable using a range of window lengths from one hour to twelve hours. The one-hour standard deviation window was selected over the other window lengths as the most appropriate because of the greater contrast in the moving standard deviation values between the apparent flow and no flow time periods. To improve accuracy, a rain gage near the study site and/or a temperature sensor placed on the dry bank can be used to differentiate between short duration flow events and false positives caused by weather fronts (Figure 8). The reference time was arbitrarily centered within the standard deviation window as it was shown previously that streamflow timing accuracy is insensitive to this choice.

The second step required plotting the mean moving standard deviation temperature to provide a starting point for selecting the threshold parameter. The threshold parameter was then adjusted to a level above the apparent no flow moving standard deviation values.

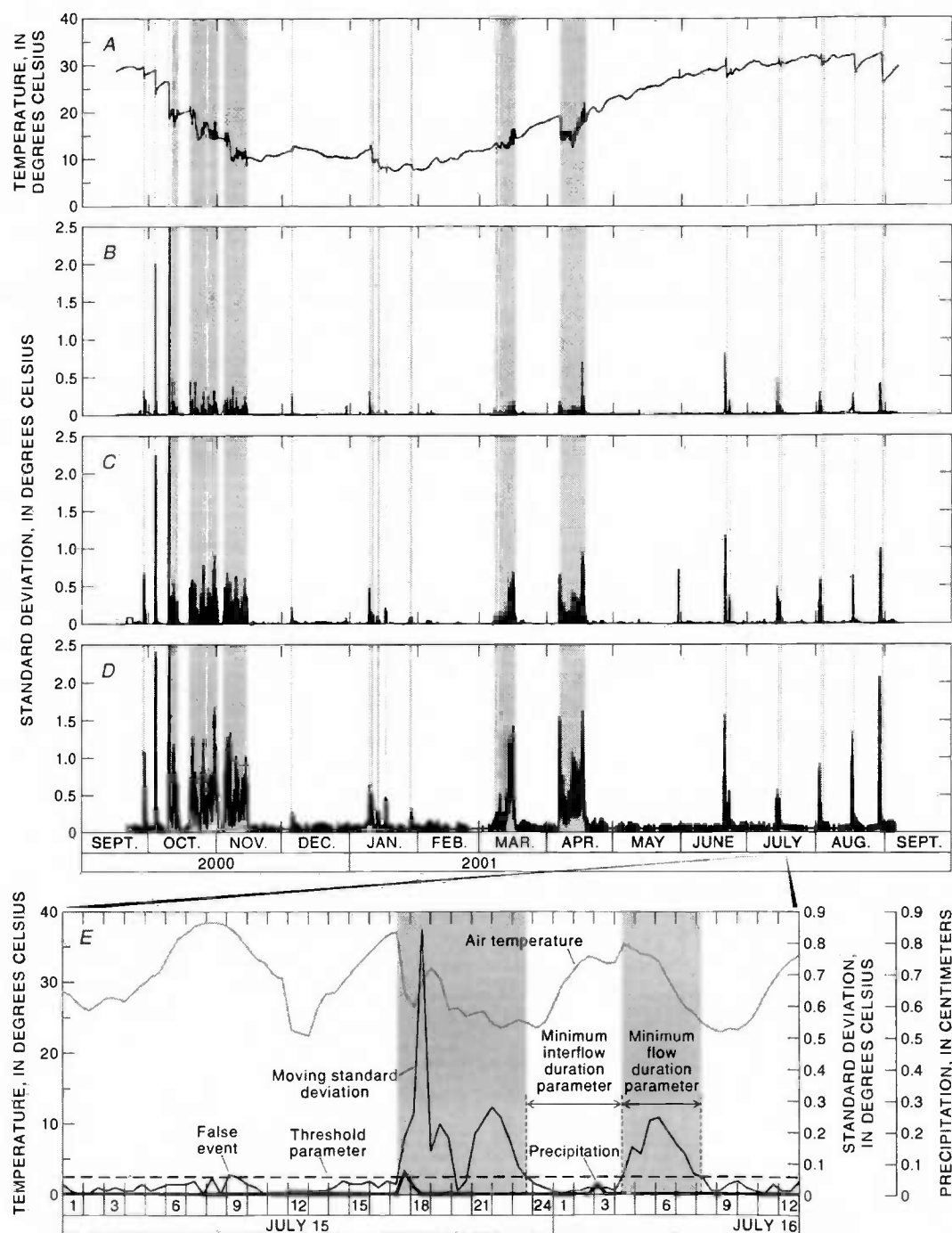


Figure 8. (A) Thermograph from September 16, 2000, through September 15, 2001 for a depth of 0.75 meters, (B) one-hour, (C) four-hour, and (D) 12-hour moving standard deviation windows for temperature data measured at a depth of 0.75 meters. (E) Close-up of two identified events that provide an example of how moving standard deviation parameters can be selected. The gray area denotes periods of identified streamflow events.

Finally, the duration parameters were selected. General knowledge of monsoon season streamflow events within the basin indicated that the localized nature of precipitation produced many of the shortest duration events and events in succession with short interflow periods (Figure 6). Consequently the monsoon time period was considered ideal for establishing the duration parameters. The shortest streamflow event identified during this period was used to define the minimum flow duration parameter (Figure 8). The minimum interflow duration parameter was estimated as the shortest time between two consecutive flow events inferred on the plots. The minimum flow duration and interflow duration occurred during July, 2001.

The optimized parameter set achieved using this calibration technique was a 1-hour window length, a threshold of 1.35 times the mean standard deviation, a minimum flow duration of 150 minutes, and a minimum interflow duration of 600 minutes. When evaluated against the test data, the average timing error associated with these parameters was approximately 95 minutes at the onset of flow and 310 minutes at the cessation per event. Thus, even without the use of alternative flow detection devices it was possible to obtain a suitable parameter set for analysis that is as accurate as visual identification with the benefit of being automated and repeatable.

7. Conclusions

Temperature sensors deployed in streambed sediments can provide a cost-effective alternative for monitoring the timing of streamflow based on heat transport mechanisms

through the water column and sediments. A technique was developed to identify the timing of streamflow based on a statistical analysis of changes in the sediment diurnal temperature wave amplitude. The technique requires the definition of five analysis parameters. The accuracy of streamflow identification is most sensitive to the standard deviation window length and a threshold parameter. Once the analysis parameters are established, either through calibration with independent flow timing measurements or through supporting climate information, identification of the presence or absence of flow is repeatable, objective, and easily automated to process large data sets. Furthermore, the thermal method and analysis technique allows for the use of deeper temperature measurements, which may be advantageous under some field conditions.

References

- Blasch K.W., T.P.A. Ferre, A.H. Christensen, and J.P. Hoffmann, New field method to determine streamflow timing using electrical resistance sensors, *Vadose Zone Journal*, 1, 289-299, 2002.
- Constantz, J., D. Stonestrom, A.E. Stewart, R. Niswonger, and T.R. Smith, Analysis of streambed temperature in ephemeral stream channels to determine streamflow frequency and duration, *Water Resour. Res.*, 37(2), 317-328, 2001.
- Constantz, J. and C.L. Thomas, Stream bed temperature profiles as indicators of percolation characteristics beneath arroyos in the middle Rio Grande Basin, USA, *Hydrological Processes*, 11, 1621-1634, 1997.

- Constantz, J., S.W. Tyler, and E. Kwicklis, Temperature-profile methods for estimating percolation rates in arid environments, *Vadose Zone Journal*, 2, 12-24, 2003.
- Hoffman, J.P., M.A., Ripich and K.E., Ellett, Characteristics of shallow deposits beneath Rillito Creek, Pima County, Arizona, U.S. Geological Survey Water-Resources Investigations Report 01-4257, 51 pp. 2002.
- Stallman, R.W., Methods of collecting and interpreting ground-water data, U.S. Geol. Surv. Water Supp. Paper 1544-H, 36-46, 1963.
- Stallman, R.W., Steady one-dimensional fluid flow in a semi-infinite porous medium with sinusoidal surface temperature, *J. Geophys. Res.*, 70(12), 2821-2829, 1965.
- Stewart, A.E., and J. Constantz, 1999, Measurement techniques to identify spatial and temporal patterns of streamflow in large ephemeral streams, *GSA Abstracts*, Vol. 31(7), p.150-151.
- Stewart, A.E., 2003, Temperature based estimates of streamflow patterns and seepage losses in ephemeral channels, Stanford University Doctoral Dissertation, Stanford, CA, pp. 248.
- Suzuki, S., Percolation measurements based on heat flow through soil with special reference to paddy fields, *J. Geophys. Res.*, 65(9), 2883-2885, 1960.
- Van Wijk, W.R. and D.A. De Vries, "Periodic Temperature Variations in a Homogeneous Soil", in *Physics of Plant Environment* eds. W.R. Van Wijk, Amsterdam, 1963.

APPENDIX B: A NEW FIELD METHOD TO DETERMINE STREAMFLOW TIMING USING ELECTRICAL RESISTANCE SENSORS

Kyle W. Blasch, Ty P.A. Ferré, Allen H. Christensen, and John P. Hoffmann

Vadose Zone Journal, 1: 289-299 (2002)

Abstract

Electrical resistance sensors were constructed to monitor streambed saturation to infer ephemeral streamflow timing. The sensors were evaluated in an ephemeral stream through comparison with temperature-based methods, a stream gage, and soil-water-content sensors. The electrical resistance sensors were more accurate at estimating streamflow timing and the resultant data required less interpretation than data from temperature-based methods. Accuracy was equivalent to timing methods using stream gage and soil-water-content measurements. The electrical resistance sensors are advantageous for use in ephemeral stream channels because they are inexpensive, deployable above or below the sediment surface, insensitive to depth, and do not require connecting wires to an external datalogger or power source. Based on these results electrical resistance sensors may be used to monitor changes in soil water content within the vadose zone. Additionally, the sensors can be used to infer the presence of surface water in diversion canals, storm-water sewers, and in the form of overland runoff.

Introduction

Given the erratic and variable nature of ephemeral and intermittent streamflow in arid and semiarid basins, long-term collection of streamflow timing is necessary for obtaining information on extreme flow events and seasons. Streamflow timing in channels and arroyos is used to accurately model fluid transport through the unsaturated zone beneath ephemeral streams and to constrain channel recharge estimation, a primary component of aquifer replenishment. Additionally, streamflow timing is a necessary component for designing storm-water and flood-control networks in flood-prone environments.

Current methods used to estimate streamflow timing include flow-rated stream gages, velocity meters, soil water-content sensors, and temperature sensors (Latkovich and Leavesly, 1993; Constantz et al., 2001; Blasch et al., in review). These methods have met with varying success depending upon channel morphology, bed sediment characteristics, frequency and duration of streamflow, and other requirements (e.g., magnitude of temperature signal).

Stream gages and velocity meters accurately determine streamflow timing, but generally are not suitable for ephemeral channels that experience changes in channel morphology (Tadayon et al., 2001). Stream gages and velocity meters installed at the bed sediment surface can become buried or damaged by moving sediment or debris. Consequently, streamflow timing sensors deployed within the vadose zone have been shown as advantageous under these circumstances (Constantz et al., 2001).

Soil water-content methods detect infiltration and percolation of water through the sediments, which may be used to infer timing of streamflow (Blasch et al., in review).

Placing sensors in the subsurface reduces the possibility that they will be damaged or lost during flow. Logging instrumentation, however, must be placed on or near the bank with cables extending to the buried sensors.

Temperature methods enable inference of streamflow timing on the basis of the combined transport of heat and fluid within the bed sediments (Constantz and Thomas, 1996, 1997; Ronan et al., 1998; Constantz et al., 2001). Recent development of small ($<10\text{ cm}^3$), inexpensive, waterproof temperature sensors with integrated data storage enable measurement and storage of temperature values without the need for external connecting wires. This advantage enables in situ temperature monitoring in ephemeral channels with unstable beds over large areas with high spatial resolution.

While temperature methods have been used successfully to monitor the timing of streamflow in ephemeral channels, the methods have limitations. Specifically, certain conditions are required for streamflow to produce a readily identifiable thermal signal. For example, water with the same temperature as the channel will not produce an identifiable signal. In ephemeral stream channels subject to repeated scour and deposition, changes in sediment surface elevation complicate the application of numerical methods used for interpretation of the temperature data.

In this investigation, we converted commercially available temperature sensors into electrical resistance sensors (ER sensors) to monitor water content and tested their utility for streamflow detection. Advantages of the electrical resistance approach include: functionality above or below the channel surface, functionality in all streamflow temperatures, lack of connecting wires, and minimal interpretation of data. These same attributes necessary for streamflow timing are also advantageous for monitoring sediment saturation in other similar vadose zone applications such as irrigated fields, fluctuating water tables, and post-burn environments.

Background and Theory

An electrical-resistance measurement in a porous medium can be idealized as a measurement of three resistances in series: the bulk electrical resistance of the medium, which includes solid grains and pore water, (R_m), and a contact resistance at each electrode/medium interface (R_c [two electrical contacts in the circuit; see Figure 1]). Summation of the three resistances in series results in the total electrical resistance, R_t :

$$R_t = R_c + R_m + R_c \quad (1)$$

Bulk Electrical Resistance of a Porous Medium

The bulk electrical conductivity [S/m] of a porous medium, σ , is a measure of the sediment's and pore water's ability to transmit electrical current. The inverse of

electrical resistivity (resistance per unit length) is electrical conductivity. Archie (1942) developed an empirical relation between bulk electrical conductivity, pore-water electrical conductivity [S/m], σ_w , sediment-surface electrical conductivity [S/m], σ_s , and sediment saturation [vol. water /vol. pores], S :

$$\sigma = \sigma_w S^n + \sigma_s = \frac{1}{R_m} \quad (2)$$

where n is a unitless constant that is specific to the sediment type and distribution. For unconsolidated materials, n is approximately 2 (Archie, 1942).

Pore-water electrical conductivity is a measure of a solution's ability to transmit an electrical current and is dependent upon the number of ions present in the solution and their associated charge. Pore-water electrical conductivity is also directly proportional to solution temperature. Sediment-surface electrical conductivity is the ability of the sediments to transmit an electrical current and is primarily dependent upon the clay content of the sediments (McNeil, 1980). In many hydrologic settings of interest, pore-water electrical conductivity is much higher than the sediment-surface electrical conductivity. Because the electrical conductivity of air is practically zero, the electrical conductivity of a medium is strongly dependent on the extent to which it is saturated with water. The normalized electrical conductivity, σ_n , shows a nonlinear dependence on saturation (from equation 2):

$$\sigma_n = \frac{\sigma - \sigma_s}{\sigma_w} = S^n \quad (3)$$

Generally, the electrical conductivity of a coarse-grained medium will be lower than that of a fine-grained medium at the same water soil water potential because the finer-grained material will have a higher water saturation.

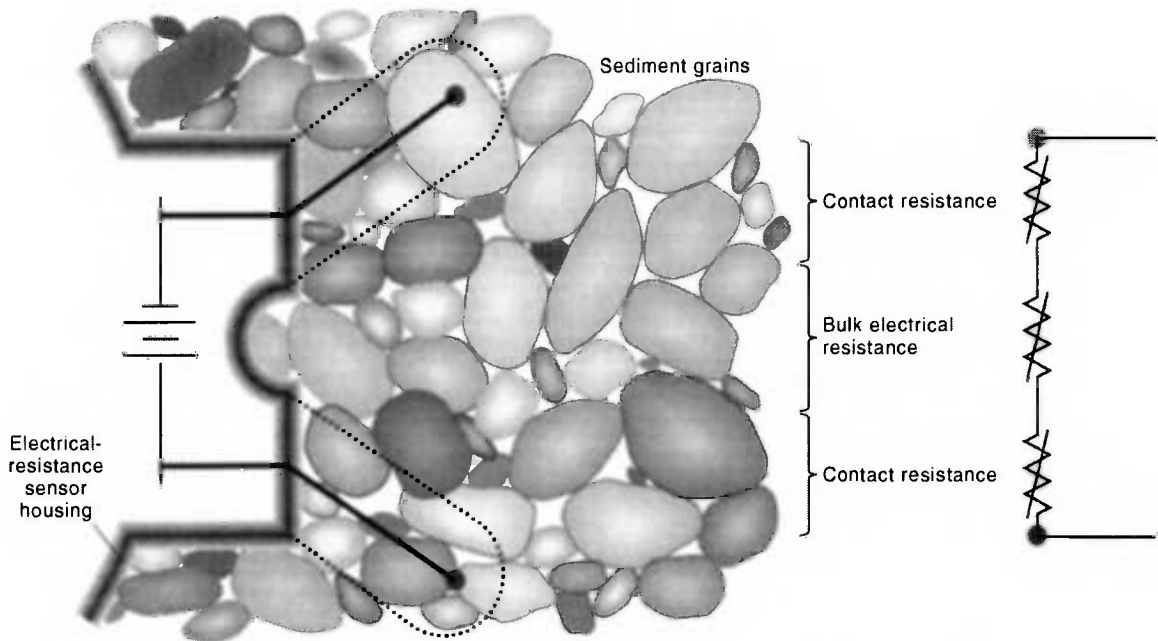


Figure 1. Schematic presentation of bulk electrical and contact resistances of a sediment medium. Dotted lines surrounding the wire leads denote the critical region for determining contact resistance. The remaining regions outside the dotted lines are important for determining the bulk electrical resistance. A measurement of electrical resistance is a combined measure of the bulk electrical resistance of the medium and contact resistance.

Contact Resistance

The inverse of contact resistance, contact conductivity, is the ability of an electrode in a circuit to pass an electrical current to the porous medium. High contact resistance is caused by air-filled gaps (i.e., pores) that exist between the electrodes and the sediment grains (Figure 1). Because of the relatively high electrical conductivity imparted by solutes to pore water, water-filled pores produce low contact resistances. A small diameter pore requires a more negative soil water potential to drain than a large diameter pore. The pores adjacent to an electrode will tend to be smaller in fine-grained materials than in coarse-grained materials. As a result, contact resistance is lower in fine-grained materials than in coarse-grained material at the same soil water potential.

Total Electrical Resistance and Streamflow Timing

At the onset of an ephemeral streamflow event, water rapidly percolates into the sediment pores and replaces air. As the saturation at a given depth increases, the bulk electrical conductivity of the medium increases as well. An electrical resistance (ER) sensor, however, will not measure a significant change in electrical conductivity until a continuous electrical circuit is supported between the electrodes. The level of saturation required for a continuous circuit is defined as the contact resistance threshold. This occurs when saturation of the medium in contact with the electrodes produces a negligible resistance. As the pores near the electrodes and the pores in the bulk medium continue to fill with water, the total electrical conductivity increases to a maximum at full

saturation (i.e., maximum pore water content). Under these saturated conditions, the total electrical conductivity will vary as the pore-water electrical conductivity or the bulk medium temperature fluctuates.

The cessation of streamflow is accompanied by drying of the sediments and a reduction in saturation, causing a decrease in the total electrical conductivity. An ER sensor will show a decline during drying until the contact resistance threshold of the medium surrounding the electrodes is reached, which is marked by a rapid decrease in the measured total electrical conductivity to zero. The soil water potential at which the medium in contact with the electrodes reaches its contact resistance threshold is not always equivalent to the air entry pressure of the medium. The contact resistance threshold will only occur at the air entry pressure of the bulk medium if the pores adjacent to the sensor electrodes are equivalent or greater in size than the largest pores in the bulk medium. If the pores near the electrodes are smaller than those in the bulk medium, then the contact resistance threshold will occur at a lower potential than the air entry pressure of the bulk medium.

Observed changes in saturation at a given depth lag behind the onset and cessation of streamflow because of the time required for a wetting front to reach a given depth or for drainage and evaporation to affect the soil water content at this depth (Blasch et al., in review). This lag increases with depth of observation. At the onset of a streamflow event, the time lag is a function of the hydraulic properties of the sediments and the

antecedent water content. Generally, lag times are shorter for coarse sediments and for sediments having high antecedent water contents. At the cessation of flow, the time lag is a function of hydraulic conductivity of the sediments, pore water redistribution at depth, and evapotranspiration demands.

The advance of a hypothetical wetting front through fine-grained sands and coarse-grained alluvium was modeled using the sediments' contact resistance thresholds determined in column experiments (described in the results) and the sediments' hydraulic properties determined by Fleming (2001) and Hoffmann et al. (2002). A hypothetical streamflow event was simulated to examine possible differences that may be observed in the field between timing of streamflow arrival at the surface and advancement of the infiltrated water at depth. A variably saturated flow model, HYDRUS 1-D (Simunek et al., 1998), was used to simulate the advance of the wetting front, a period of saturated flow, and subsequent drainage. Saturation values were simulated at a depth of 0.20 m in response to a 2-hour streamflow event (Figure 2). Flow was modeled as a constant flux upper boundary with an infiltration rate of 10 cm/h. The initial pressure head was -50 cm throughout the profile. The simulated timing of the streamflow event at 0.20 m depth that would be inferred from ER sensors is also shown.

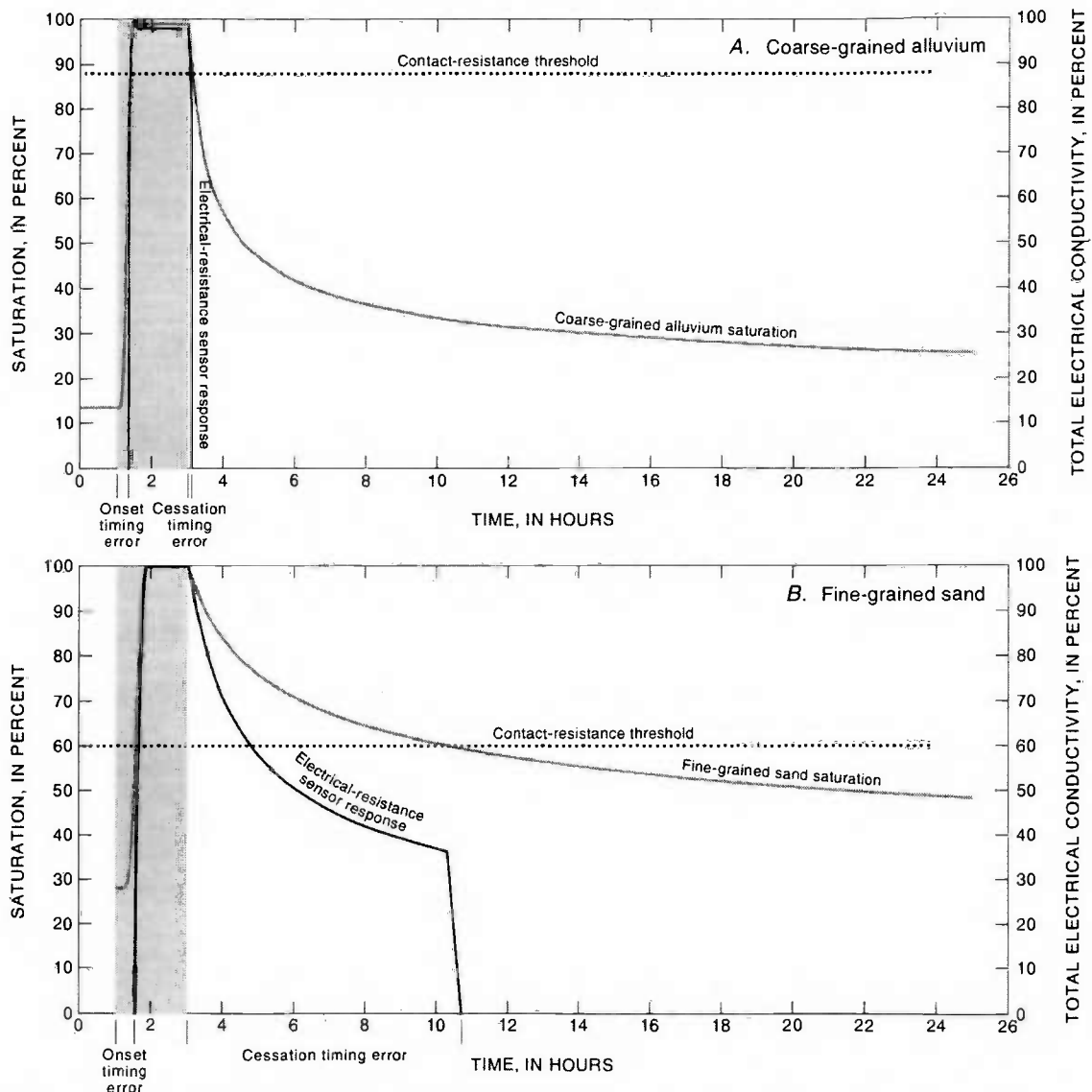


Figure 2. Simulated infiltration of water into fine-grained sand and coarse-grained alluvium during a 2-hour streamflow event. The shaded areas in both A and B denote the period of streamflow. Measured contact resistance thresholds (dotted lines) and conductivity/saturation relations were used to calculate saturation and normalized total electrical conductivity measurements at 0.2 meter. A, shows the saturation response (light solid line) and electrical resistance sensor response (dark solid lines) within the coarse-grained alluvium to the infiltration event and redistribution. B, shows the simulated saturation and electrical resistance response for a sensor in fine-grained sand. The onset timing error is defined as the difference in time between the onset of a streamflow event and the activation of the electrical-resistance sensor. The cessation timing error is defined as the difference in time between the end of the streamflow event and the deactivation of the sensor. Both types of error are shown in A and B.

The onset timing error is the difference in time between the arrival of the streamflow event at the surface and the start time inferred by the ER sensor. The cessation timing error is the difference between the end of the streamflow event and the cessation as indicated by the ER sensor. The magnitudes of the onset and cessation timing errors are dependent upon the contact resistance threshold value, the hydraulic conductivity of the sediments, antecedent water contents, and depth of the sensor. The effect of the contact resistance threshold on streamflow timing error is noticeable in these simulations. For the coarse-grained alluvium the soil water potential of the contact-resistance threshold is similar in magnitude to the air entry pressure of the bulk medium. Thus the ER response declines to zero as soon as the sediments begin to drain. In comparison, the water potential associated with the contact-resistance threshold for the fine-grained sand is much lower than the air entry pressure of the bulk medium, resulting in a decrease in total conductivity before the sharp decrease associated with drainage of the medium around the electrodes. If the timing of this sharp drop is used to identify the end of flow, the timing error will be greater during drainage. To reduce this timing error the time recorded by the ER sensor as the initiation of drainage should be used. This will require an additional step in the analysis of the data.

Materials and Methods

Column experiments were designed to quantify the saturation dependence of the ER sensor output. Field experiments were designed to compare the capabilities of ER sensors with different methods for estimating streamflow timing. Stowaway TidbiT

temperature sensors were modified for this study (Onset Corporation, Bourne, Massachusetts, TidbiT sensors; mention of brand names does not constitute endorsement by the U.S. Geological Survey or the University of Arizona). These sensors contain a thermistor, onboard datalogger, and battery encapsulated in a 10 cm³ plastic housing. The thermistor used has a temperature range of -20° C to 50° C with a precision of approximately 0.1 °C. The TidbiTs were modified by removing the thermistor and stripping the insulation enclosing the electrodes (Figure 3). The average distance of separation between the two electrodes at the housing surface was approximately 0.5 mm. The electrodes were cut to varying lengths ranging from 0.01 mm to approximately 4 mm. The electrodes were bent at a 45-degree angle to prevent contact with each other. During installation in the subsurface, sediment was placed surrounding the electrodes. This was accomplished by lightly sifting the sediment over the ER sensor to ensure coverage of the electrodes.

Column Experiments

The two objectives of the column experiments were to 1) evaluate the ER sensor response during imbibition and drying and 2) quantify contact resistance thresholds for two sediment types. The first sediment was Vinton fine-grained sand (sandy, mixed thermic Typic Torrifluent). The second sediment was coarse-grained alluvium from Rillito Creek (36.2 % gravel, 55.2 % sand, 8.6 % silt and clay). Circular 48 cm diameter x 50 cm tall columns were packed to a bulk density of 1.34 g/cm³ (Figure 4). Columns were instrumented with 4 horizontal time domain reflectometry (TDR) probes, 8 tensiometers,

and 8 ER sensors. The two-rod TDR probes were 20 cm long, and a distance of 3 cm separated the TDR rods. Two TDR probes were placed horizontally at 10 cm depth and the remaining two rods were placed at 20 cm depth. Four ER sensors were placed between the TDR probes at each depth. Four tensiometers were placed at each depth. The column was wetted repeatedly from either the top or bottom with tap water (conductivity = 447.3 microsiemens cm^{-1}) until 5 cm of water was ponded above the soil surface. The ponded condition was maintained for approximately 20 minutes and then the column was allowed to drain. The columns remained undisturbed until the TDR probes indicated that the saturation of the soil was similar to that at the start of the experiment.

A. Temperature sensor

B. Electrical-resistance sensor

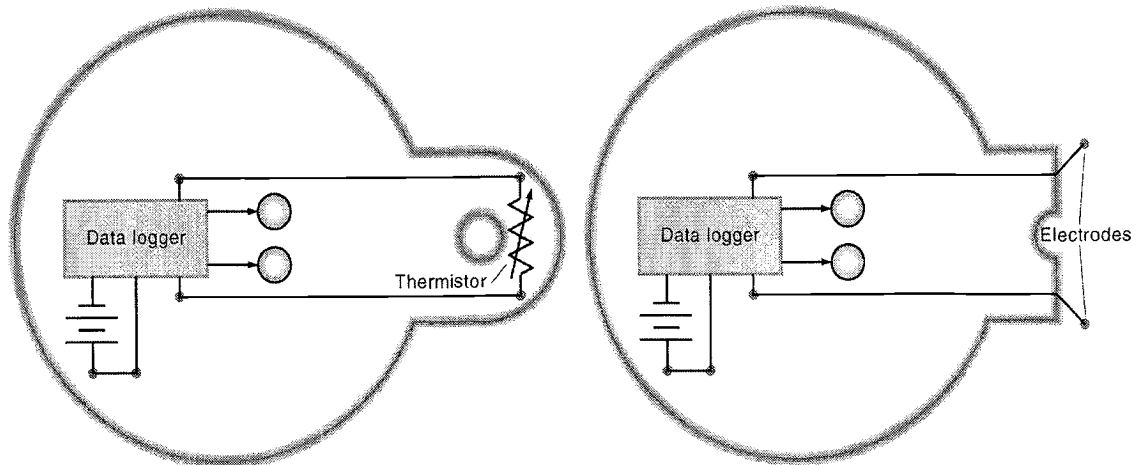


Figure 3. Schematic diagram of a temperature sensor. A, Before modification. B, After conversion to an electrical-resistance sensor through removal of the thermistor.

Ephemeral Channel Experiment

Electrical resistance sensors were installed above and below the sediment surface in Rillito Creek, an ephemeral stream on the north side of Tucson, Arizona (USA), in the same native coarse-grained alluvium used in the column experiments (Figure 5). Rillito Creek is typical of ephemeral streams in the arid and semi-arid southwestern United States. During most of the year, the stream is dry; however, after prolonged or intense periods of rainfall and/or snowmelt, streamflow can exist for several hours to several days along its 20 km length. The aboveground sensors were bolted inside a 5x12 cm polyvinyl chloride (PVC) tube to protect against surface abrasions. The PVC tube remained open at both ends, and about thirty 3 mm diameter holes were drilled into the sides to ensure water flow into the container and to prevent the accumulation of clay and silt particles within the protective enclosure. Three ER sensors were attached to a U.S. Geological Survey stream gage (gaging station 09485700; Tadayon *et al.*, 2000) above the channel surface. To avoid interference with stream-gage operation, the sensors were installed 3 to 5 cm below the stream-gage orifice line. Two additional sensors were deployed 15 cm below the streambed surface within 6 m of a row of 4 TDR probes having specifications similar to those used in the column experiments. The sensors were installed without the protection of the PVC tube to improve soil/sensor contact. The sensors were attached to a PVC plate and cabled to a rebar stake. The sampling frequency was 5 minutes for the sensors, 2 minutes for the TDR probes, and the stream gage operated by the U.S. Geological Survey recorded streamflow data every 15 minutes.

Stream gage and TDR data were post-processed in a similar manner. Timings of flow events were inferred when the stream gage values were greater than zero and volumetric water content values exceeded $0.30 \text{ cm}^3 \text{ cm}^{-3}$. The onset of streamflow was inferred from the ER data when the conductivity values exceeded zero. The cessation of streamflow was identified as a decrease in total electrical conductivity caused by a dewatering of the media. For surface ER sensors this decline was immediate and the values dropped to zero. For the subsurface sensors the initiation of drainage caused a significant drop in total electrical conductivity, but not always to a zero value. The total electrical conductivity did not drop to zero until the contact threshold was reached. However, the initial decline in conductivity signifies the beginning of dewatering and was recorded as the cessation time. This reduced the cessation timing error as previously described in Figure 2.

Two temperature sensors were installed at different depths in the bed sediments within 3 m of the ER sensors for comparison of the temperature method with the electrical-resistance method. A temperature sensor was installed 1.0 m below the sediment surface, a depth determined by Blasch et al. (in review) as optimal for inferring streamflow timing at this study site. A second TidbiT temperature sensor was installed 0.05 m below the sediment surface. Both sensors measured and recorded bed sediment temperatures at 5-minute intervals. The thermographs were post-processed using a 1 hour moving-standard deviation.

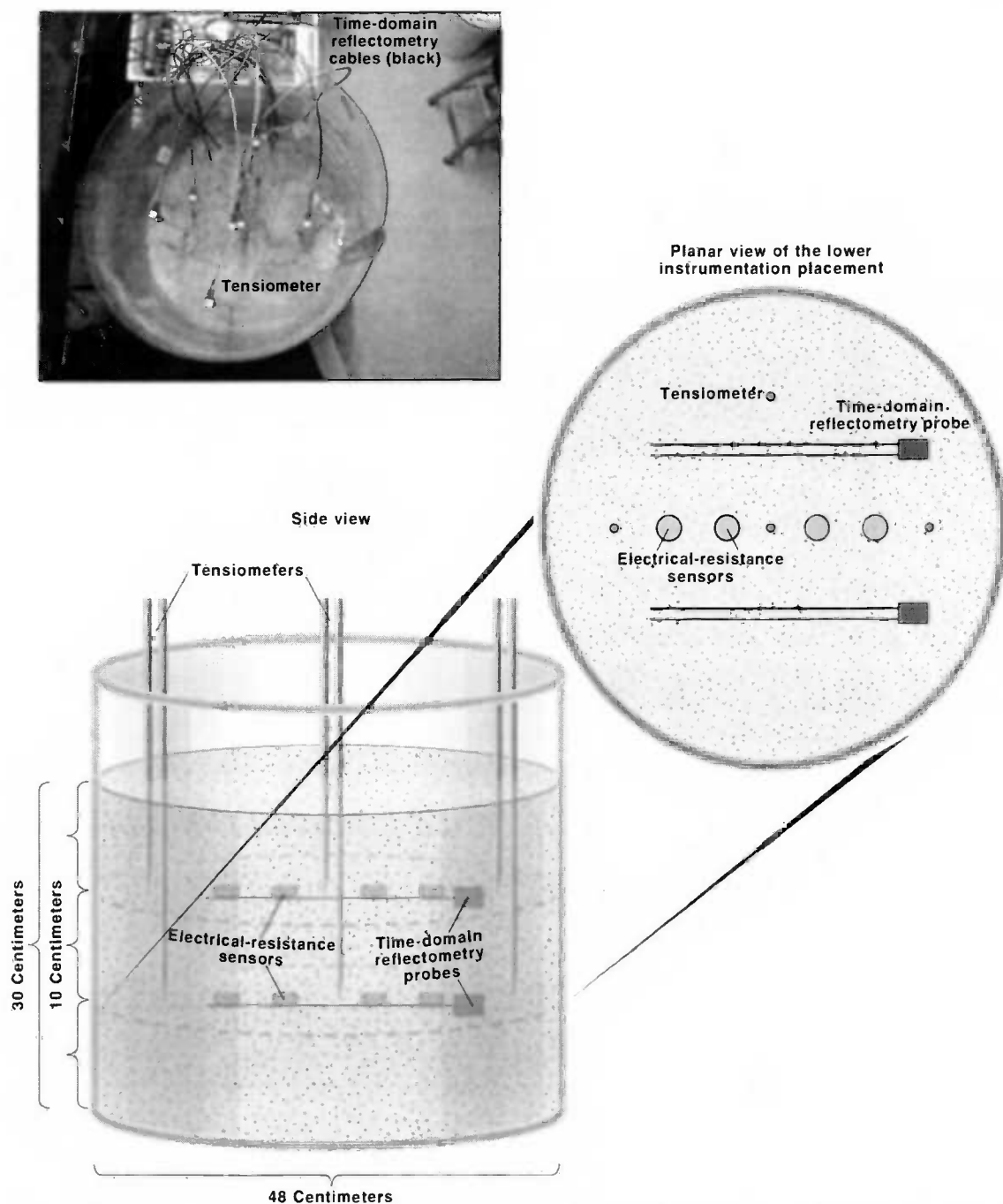


Figure 4. Photograph and schematic diagram of the sensor locations within the laboratory column used to measure the contact-resistance threshold for the fine-grained sand and the coarse-grained alluvium.

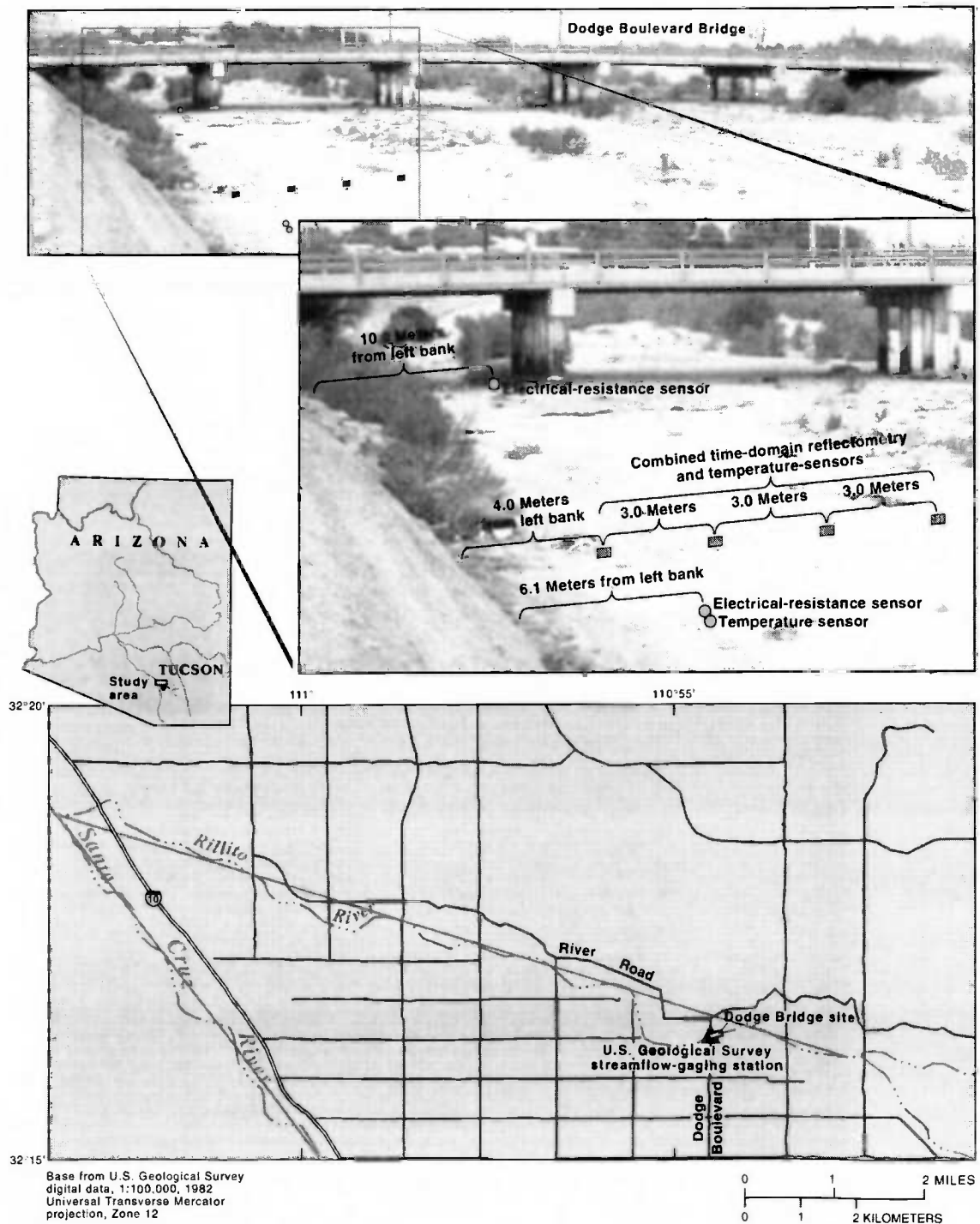


Figure 5. Sensor locations deployed in Rillito Creek, Tucson, AZ (USA).

Results

Column Experiments

Electrode lengths were tested repeatedly in column experiments and during ephemeral streamflow events in Rillito Creek near Tucson, Arizona. A minimum electrode length of 3 mm was required for reliable detection of streamflow conditions. Shorter electrode lengths on sensors installed above the bed sediment surface did not detect all of the streamflow events. Longer electrode lengths in the subsurface provided increased contact with the surrounding media resulting in a lower contact resistance threshold than ER sensors with shorter electrodes. Electrode lengths between 3 and 4 mm were considered optimal for measuring conductivity both above and within the alluvial sediments.

Contact resistance thresholds for the coarse-grained alluvium and fine-grained sand were estimated from the column experiments. Contact resistance thresholds for coarse-grained alluvium and gravel ranged from 81 to 99 % and averaged 88 % saturation (Table 1). For the Vinton fine sand, the threshold ranged from 39 to 91 % and averaged 60 % saturation. The large range for the Vinton fine sand may reflect the differences between the sample volumes of the TDR sensors and the ER sensors. A comparison of the measured total electrical conductivity for one sensor tested in both Vinton fine sand and coarse alluvium is shown in Figure 6. The measured contact resistance thresholds for each sediment type were the same for increasing and decreasing saturation. No hysteresis was observed.

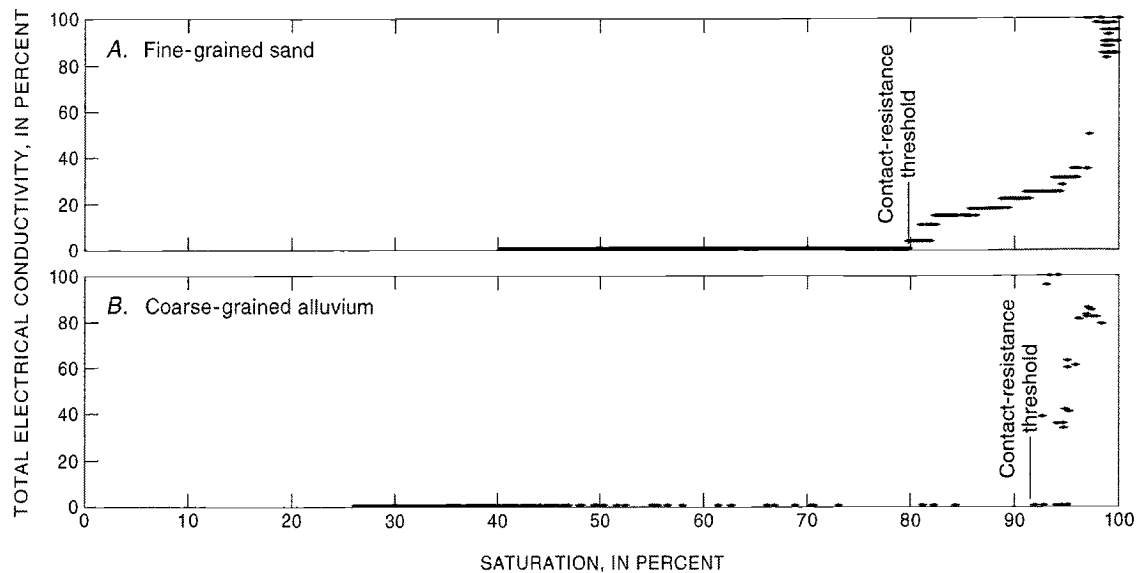


Figure 6. Total electrical conductivity in relation to saturation as determined in column experiments for one of the sensors. A, Fine-grained sand. B, Coarse-grained alluvium. Note the higher contact-resistance threshold for the coarse-grained alluvium.

Table 1. Contact resistance thresholds in fine-grained sand and coarse-grained alluvium.

Soil type	Contact Resistance Thresholds (in percent)				Samples n
	Low	High	Mean	Standard Deviation	
Fine sand	39	91	60	20	16
Coarse alluvium	81	99	88	5.0	44

Ephemeral Channel Experiment

Electrical conductivity data were collected in Rillito Creek from July 10 to September 10, 2001, by ER sensors placed above the streambed surface, and from July 28 to September 10, 2001, by sensors placed 0.15 m below the streambed surface. From July 10 to September 10, there were six streamflow events. Each event was less than 24 hours in duration. Conductivity data from the ER sensors above and below the sediment surface clearly identified the streamflow events (Figure 7 and Figure 8). Streamflow timing

inferred by the ER sensors was compared to timing from the alternate methods, including stream-gage methods, temperature methods, and soil water-content methods. Because of the variability in streamflow path, locations of the sensors, and sediment deposition and erosion, it was difficult to determine an absolute best streamflow-timing method.

Instead, the comparisons were used as a relative means to evaluate the streamflow-timing methods under similar streamflow conditions.

Comparisons of the onset and cessation errors between the streamflow-timing methods are displayed in Table 2. The subsurface-temperature method and electrical-resistance method identified the onset of flow, on average, within 11 minutes of the arrival of the streamflow event as identified by the soil water-content method. At the cessation of flow, however, the temperature method was less accurate than the electrical-resistance method. At a depth of 1.0 m, the temperature method identified the cessation of flow, on average, 108 minutes before the true cessation of flow as identified by the soil water-content method. The 0.05 m temperature sensor underestimated the duration of streamflow by 568 minutes. These errors were attributed to the short durations of the flow events resulting in minimal changes to the diurnal temperature patterns except at the onset of flow. In comparison, the electrical-resistance method identified the end of flow approximately 72.5 minutes after the soil water-content sensors identified the end of flow. A comparison of two water-content sensors 9 m apart, but transverse to the flow path, yielded a difference in onset timing of 5.5 minutes and a cessation timing difference

of 88 minutes. We speculate that these timing differences are a consequence of the heterogeneity of the sediments.

Table 2. Streamflow timing errors at the onset and cessation of flow using the temperature method and the electrical-resistance method. Negative values indicate the method identifies flow preceding the timing of streamflow measured using a conventional method (stream gage for surface timing and soil water content (TDR) for subsurface timing).

Error, in minutes	Method							
	Temperature Sensors (0.05 m depth) [†]		Temperature Sensors (1.0 m depth) [†]		Electrical Resistance Sensors (0.15 m depth) [†]		Electrical Resistance Sensors (surface) [‡]	
	Onset	Cessation	Onset	Cessation	Onset	Cessation	Onset	Cessation
Mean	-7.31	-568	-19.8	-108	3.88	72.5	-12.1	70
St Dev	6.74	118	48.5	250	7.02	40.3	13.4	60

[†] Timing of streamflow compared to conventional method – soil water content measurements

[‡] Timing of streamflow compared to conventional method – stream gage measurements

Measured field values of saturation and electrical conductivity shown in Figure 7 are comparable in appearance to those shown in the modeling exercise of Figure 2 for coarse-grained alluvium. The measured contact resistance threshold ranges from 82% to 91% saturation and averages 88%. During the final event a 5-10 cm layer of silt and clay was deposited on the bed sediment surface. Silt and clay percolated into the sediments and were found with the sediment matrix surrounding the ER sensors. Consequently, dewatering of the sediments differed from the previous events by displaying two contact resistance thresholds. One for the larger pores of the matrix associated with the alluvium and a second for the pores associated with the silt and clay. The authors interpret the dewatering as a two-stage process and cessation of flow occurring at the first threshold. The second threshold occurred at a saturation value of 49%. The diurnal fluctuations in the conductivity values are attributed to the diurnal change in temperature within the porous media.

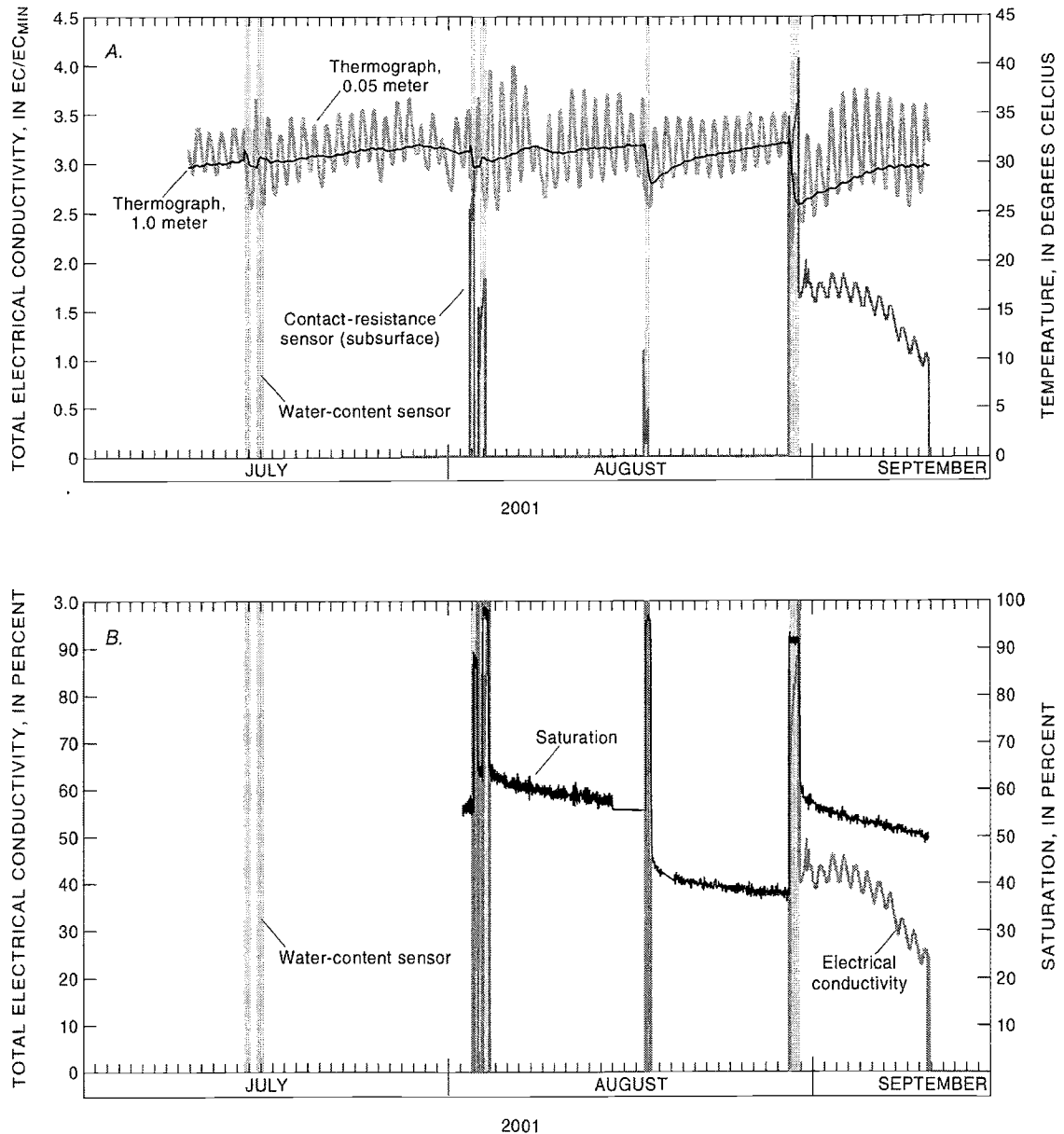


Figure 7. A, Electrical conductivity as measured by an electrical-resistance sensor positioned 0.15 meter below the ground surface and temperature responses measured at depths of 0.05 meter and 1.0 meter. The subsurface electrical-resistance sensor was installed July 28, 2001, after the first two streamflow events. B, Electrical conductivity as measured by an electrical-resistance sensor positioned 0.15 meter below the ground surface and saturation as measured by the water content sensors. The shaded areas denote periods of streamflow as inferred using measured soil water-content data.

The surface ER sensors estimated the timing of flow, on average, 12.1 minutes before the stream gage and estimated the cessation of flow, on average, 70 minutes after the stream gage (Table 2). This discrepancy is likely the result of the ER sensors being installed at an elevation of about 3-5 cm below the stream gage orifice line. At this position, they were triggered at a slightly lower stage than was recorded at the stream gage. The errors should decrease significantly if the stream-gage ports and ER sensors were placed at the same elevation. During the final event, about 5-10 cm of fine silt and clay were deposited on top of the surface ER sensors. The layer of silt and clay deposited around the sensor electrodes produced a slower decrease in saturation compared to earlier events (Figure 8).

Streamflow-timing errors for the subsurface and surface methods show little difference at the onset of a streamflow event. Infiltration of water into the near surface sediments is rapid at the onset of flow. The difference in cessation timing, however, is the critical factor for overall duration timing accuracy. The electrical-resistance method is more accurate than the temperature methods. Analysis of the surface electrical-resistance data and the stream-gage data required the least amount of effort to identify streamflow conditions because the methods record zeros during no flow conditions and nonzero values during the presence of streamflow. The water-content data and subsurface electrical-resistance data required more analysis time to account for travel time of the wetting front and initiation of drainage. Finally, the subsurface method using the

temperature data required the most effort for analysis, even when using the automated moving standard deviation method.

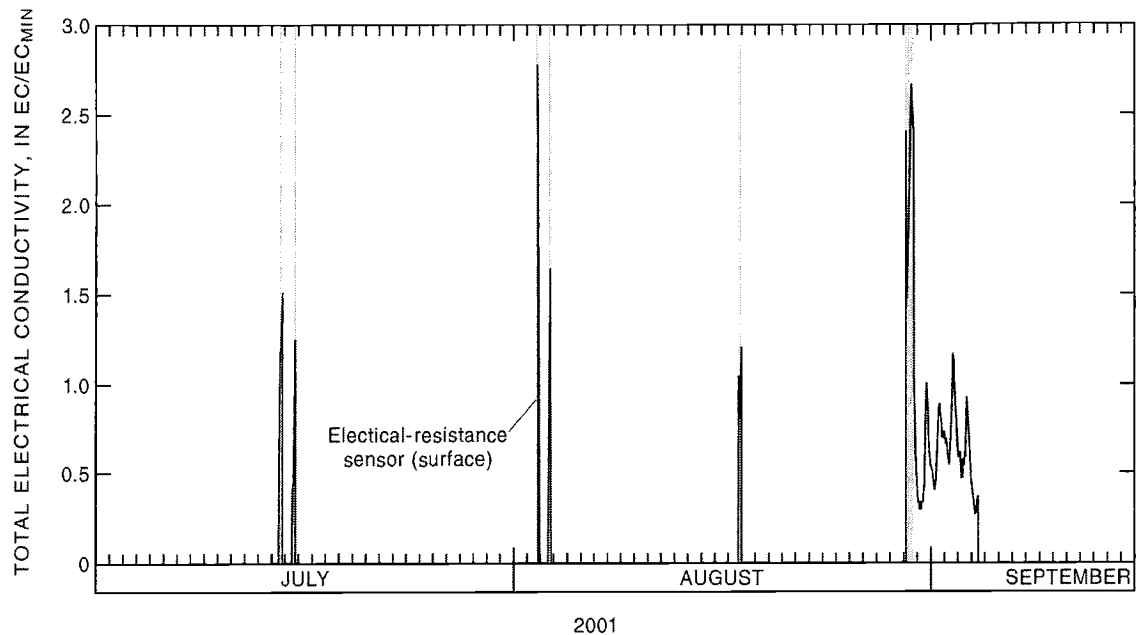


Figure 8. Electrical conductivity as measured by an electrical-resistance sensor positioned at the surface. The shaded areas denote periods of streamflow as measured by a USGS streamflow gage.

Discussion

Correct installation of the ER sensors is important for decreasing streamflow-detection errors. The sensors are most accurate when placed above the stream channel surface to avoid the influence of sediments and to reduce analysis requirements. Caution must be taken when selecting the height of sensor placement. Sensors placed too low can be buried by deposited sediments (Figure 8). If a sensor is placed too high, however, it may fail to detect streamflow at low stages. Sensors placed in the subsurface should be as

close to the sediment surface as possible to reduce streamflow-timing errors while minimizing the risk of sensor damage or removal.

Comparison of the maximum electrical conductivity measured for the streamflow events both above and below the bed surface indicate changes in the electrical conductivity of the water during each event. The variability in magnitudes is attributed to changes in temperature and conductivity of the water, however these values were not measured.

Conclusions

Small, inexpensive, resistance loggers can detect saturated conditions and infer streamflow timing. Estimates of streamflow timing were more accurate when made using the ER sensors rather than the temperature methods and were comparable in accuracy to stream-gage and soil water-content methods. Advantages of electrical resistance sensors include depth independence and reduced analysis requirements. The low cost, ease of implementation, and absence of datalogger connecting wires from the sensor to the stream bank provides a distinct advantage over conventional methods.

Electrical resistance sensors can be used to determine the presence of surface water in ephemeral and intermittent stream channels, storm-water sewers, diversion canals, and in the form of overland runoff. The sensors also can be used to identify the occurrence of saturated soil conditions in the vadose zone; for example, changing water levels, bank storage near streams, and movement of irrigation water in agricultural fields.

References

- Archie, G. E. 1942. The electrical resistivity log as an aid in determining some reservoir characteristics, Trans. AIME, 146, 146, 54-62.
- Blasch, K.B., P.A. Ferré, J.P. Hoffmann. 2001. "Identification of the onset and duration of ephemeral streamflow using streambed temperature," Water Resources Research submitted for review.
- Constantz, J. and C.L. Thomas. 1996. "The use of streambed temperature profiles to estimate depth, duration, and rate of percolation beneath arroyos," Water Resources. Research, 32(12), 3597-3602.
- Constantz, J. and C.L. Thomas. 1997. "Streambed temperature profiles as indicators of percolation characteristics beneath arroyos in the Middle Rio Grande Basin, USA," Hydrological Processes, 11, 1621-1634.
- Constantz, J., D. Stonestrom, A.E. Stewart, R. Niswonger, and T.R. Smith. 2001. "Analysis of streambed temperature in ephemeral stream channels to determine streamflow frequency and duration," Water Resources Research, 37(2), 317-328.
- Dullien, F.A.L. 1992. Porous Media Fluid Transport and Pore Structure 2nd Edition, Academic Press Inc., San Diego.

Ferré, P.A., J.H. Knight, D.L. Rudolph, and R.G. Kachanoski. 1998. "The Sample Area of Conventional and Alternative Time Domain Reflectometry Probes," *Water Resources Research*, 34(11), 2971-2979.

Fleming, J.B. 2001. Applications of the Inverse Approach for Estimating Unsaturated Hydraulic Parameters From Laboratory Flow Experiments: Tucson, University of Arizona, Ph.D. dissertation, p. 289.

Hoffman, J.P., M.A., Ripich and K.E., Ellett, 2002, Characteristics of shallow deposits beneath Rillito Creek, Pima County, Arizona, U.S. Geological Survey Water-Resources Investigations Report 01-4257, 51 pp.

Latkovich, V.J. and G.H. Leavesly. 1993. "Automated Data Acquisition and Transmission" in Handbook of Hydrology, D.R. Maidment, McGraw-Hill, New York, p.25.1-25.21.

McNeil, J.D., 1980, Electromagnetic terrain conductivity measurements at low induction numbers: Mississauga, Ontario, Canada, Geonics Ltd. Technical Note TN-6, 15 pp.

- Ronan, A.D., D.E. Prudic, C.E. Thodal, and J. Constantz. 1998. "Field study and simulation of diurnal temperature effects on infiltration and variably saturated flow beneath an ephemeral stream," *Water Resources Research*, 34(9), 2137-2153.
- Simunek, J., M. Sejna, and M. Th. van Genuchten. 1998. The Hydrus-1D software package for simulating the one-dimensional movement of water, heat, and multiple solutes in variably-saturated media – version 2.0, U.S. Salinity Laboratory, Agricultural Research Service, U. S. Department of Agriculture, Riverside, California.
- Tadayon, S., N.R. Duet, G.G. Fisk, H.F. McCormack, C.K. Partin, G.L. Pope, and P.D. Rigas. 2000. *Water Resources Data for Arizona, water year 2000*, U.S. Geological Survey Water-Data Report AZ-00-1, p. 9-210.

APPENDIX C: TRANSIENT AND STEADY STATE INFILTRATION FLUXES DURING EPHEMERAL STREAMFLOW

Kyle W. Blasch, Ty P. A. Ferré, John P. Hoffmann, and John B. Fleming

Submitted to the *U.S. Geological Society*, 2003

Abstract

Infiltration was simulated for a large coarse-grained alluvial channel experiencing ephemeral flow to determine the relative contribution of transient infiltration at the onset of streamflow to total streambed infiltration. Water content, temperature, and pore pressure measurements were used to constrain a variably saturated water flow and heat transport model. Infiltration fluxes at the onset of streamflow were about 2-3 orders of magnitude higher than steady state fluxes and were inversely proportional to the antecedent water content. The duration of the transient infiltration at the onset of streamflow ranged from 1.8 to 20 hours, compared with steady state flow periods of 231 to 307 hours. Cumulative infiltration during the transient period represented from 10 to 26% of the total cumulative infiltration, with an average relative contribution of approximately 18%. This indicates that cumulative infiltration estimates for large coarse-grained alluvial channels should consider transient infiltration at the onset of streamflow.

Introduction

Infiltration through alluvial channels of ephemeral streams has been identified as an important source of aquifer replenishment in arid and semi-arid environments (Smith, 1910; Davidson, 1973; Hanson and Benedict, 1994). Numerous infiltration and recharge investigations have been conducted to quantify the contributions of streambed recharge to the water budget for resource planning (Wilson, 1980; Ronan, 1988).

Streambed infiltration is a function of the hydraulic gradients beneath the stream, the ability of the underlying sediments to transmit water, and the duration of streamflow. Infiltration beneath ephemeral streams can be separated into infiltration at a varying rate at the beginning of flow followed by a steady state period (Figure 1). Infiltration rates at the onset of streamflow are typically larger than the steady state rate because flow is driven by a combination of gravity and high water pressure gradients within the unsaturated sediments beneath the streambed. In addition, there may be a larger component of lateral flow during this initial, transient period. As the wetting front progresses deeper into the sediments, pressure head gradients diminish and lateral flow contributes proportionately less to the total infiltration. As a result, flow through the streambed can be represented as steady state, one-dimensional vertical infiltration.

Streambed infiltration can be measured using seepage pans, infiltrometers, ponding, or streamflow losses (Babock and Cushing, 1942; Matlock, 1965; Linsley et al., 1992).

However, these standard methods are not suited for measuring the rapidly changing rates of infiltration at the onset of flow. Furthermore, these methods are labor-intensive and difficult to apply to remote ephemeral streams. Due to the variable timing, duration, and magnitude of ephemeral streamflow events, automated, in situ methods are optimal for ephemeral streamflow timing. Unfortunately, in situ methods are susceptible to sediment scour and deposition and to migration of channels (Constantz, 1997; Stephens, 1988).

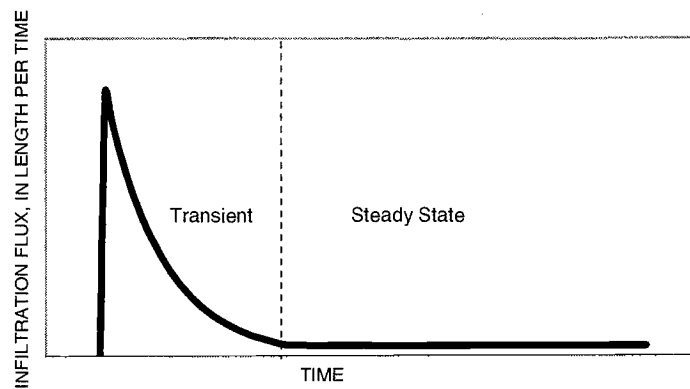


Figure 1. Transient and steady state infiltration fluxes during an ephemeral streamflow event.

In situ streambed temperature monitoring has proved rugged enough to withstand the extreme conditions of ephemeral streams for long-term monitoring (Constantz, 1998; Constantz et al., 2001; Ronan et al., 1998; Bailey 2002). Based on the coupled relationship between energy and fluid transport, numerical models can be constrained with temperature measurements to estimate streambed infiltration rates. To date, these methods have been applied to estimate infiltration rates through saturated bed sediments during periods of constant streamflow well after the onset of streamflow. Only Ronan et al. (1998) estimated infiltration rates at the onset of streamflow using temperature

profiling methods. But, this study lacked the data needed to validate the numerical modeling results during the transient period.

The relative contributions of cumulative infiltration at the onset of flow and cumulative steady-state infiltration depend on the magnitudes of the infiltration rates and durations of each flow period. Steady state infiltration rates during sustained flow are simpler to measure than transient infiltration rates at the onset of flow. As a result, these values have been reported more widely (Wilson, 1980; Katz, 1987; Linsley et al, 1992).

Typically, total infiltration is determined as the product of the steady-state infiltration rate and the duration of flow, including both the transient and steady-state periods. This leads to a systematic underestimation of the total infiltration beneath ephemeral streams. The objectives of this investigation were: to develop an expression to relate cumulative infiltration at the onset of flow to total infiltration; to use a combination of hydrologic and thermal *in situ* monitoring methods to construct a continuous infiltration hydrograph throughout a streamflow event; and to determine whether the use of steady-state infiltration rates to estimate total streambed infiltration gives rise to significant errors in the estimated cumulative infiltration.

Theory

Infiltration rates at the onset of streamflow can vary several orders of magnitude over a short duration of time. As a result, it is technically more difficult to monitor infiltration at the onset of flow than during steady state flow after the onset of flow. It would be

useful to determine whether the cumulative infiltration throughout a flow event can be represented reasonably using the steady-state infiltration flux, thereby supporting this simplified analysis. Owing to non-uniform water contents of sediments and heterogeneous conditions, quantitative analysis of transient unsaturated flow into heterogeneous streambed sediments requires the use of multidimensional, variably saturated numerical flow models to represent the movement of water. While such models have been applied previously to estimate infiltration fluxes at the onset of streamflow (Ronan et al, 1998), they typically require large amounts of data to build and calibrate. We develop a simplified representation of cumulative infiltration. This treatment is not intended to replace a quantitative analysis if sufficient data are available. Rather, we provide a method to identify whether it is likely that infiltration during transient flow makes a significant contribution to total streambed infiltration, thereby warranting monitoring during transient flow and more comprehensive analysis of streambed infiltration.

Cumulative infiltration per unit length along the axis of the stream, I [L^2/T], can be defined as:

$$I = \int i(t) W(t) dt , \quad (1)$$

where $i(t)$ [L/T] is the instantaneous rate of infiltration and $W(t)$ [L] is the wetted length across the stream. For simplicity, we assume that the wetted length is constant for all

time during a flow event. With this assumption, Equation 1 can be separated into transient and steady state components as:

$$\frac{I}{W(t)} = \int i_t(t) dt + \int i_{ss} dt . \quad (2)$$

If the wetting front is hydraulically disconnected from the water table for the duration of steady-state flow, the steady-state flow component is proportional to the saturated effective hydraulic conductivity of the sediments, K_{ss} [L/T], and the duration of the steady-state flow period, τ_{ss} [T] (Youngs, 1964; Philip, 1969; Kirkham and Powers, 1972; Warrick, 2003). For these conditions, Equation 5-2 can be rewritten as:

$$\frac{I}{W(t)} = \int i_t(t) dt + K_{ss} \tau_{ss} . \quad (3)$$

The relative contribution of infiltration during the onset of streamflow to the total infiltration during streamflow, R [-], is:

$$R = \frac{\int_0^{\tau_r} i_t(t) dt}{\int_0^{\tau_r} i_t(t) dt + K_{ss} \tau_{ss}} * 100 . \quad (4)$$

where τ_t is the time to reach steady-state flow.

The percent error in cumulative infiltration that arises due to the assumption that infiltration occurs at a rate equal to the steady-state infiltration rate over the entire flow event, E [-] is:

$$E = \frac{\int_0^{\tau_r} i_t(t) dt - K_{ss} \tau_r}{\int_0^{\tau_r} i_t(t) dt + K_{ss} \tau_{ss}} * 100 . \quad (5)$$

Several analytical solutions have been developed to represent infiltration into variably saturated sediments (Green and Ampt, 1911; Philip, 1957; Youngs, 1964; Parlange, 1971; Warrick, 2003). These solutions to Richards' equation were derived for one-dimensional infiltration into a homogeneous profile with a constant flux and a uniform antecedent water content profile. These conditions rarely describe infiltration into streambeds. However, these solutions can provide insight into the hydrologic parameters that most directly influence the rate and duration of transient infiltration. For example, Warrick (2003) presented a linearized solution for Richards' equation:

$$i(t) \approx (\theta_{sat} - \theta_{in}) \left(\frac{D}{\pi t} \right)^{0.5} . \quad (6)$$

If $i(t)$ is assumed to be equal to the steady-state rate of infiltration, K_{ss} , then the transient flow duration can be approximated as:

$$t \approx \left(\frac{D}{\pi} \right) \left(\frac{\theta_{sat} - \theta_{in}}{K_{sat}} \right)^2. \quad (7)$$

The relative contribution of infiltration during the transient period, R , is small if the steady state period, τ_{ss} , is much longer than the transient period, τ_t . The steady-state period can be determined from flow gages or using temperature methods (Constantz and Thomas, 1996; Ronan et al., 1998). The transient flow duration is directly proportional to the moisture deficit at the onset of flow and to the soil water diffusivity, D , [L^2/T] and is inversely proportional to the effective saturated hydraulic conductivity. That is, if the antecedent water content is low, the soil water diffusivity is high, and the effective saturated hydraulic conductivity is low, then the transient flow period will be relatively long producing a large relative contribution to total infiltration. In contrast, if the antecedent moisture content is high, the transient period will be short and the transient infiltration rate will be similar to the steady-state infiltration rate, leading to a small relative contribution of infiltration during the transient period. Then, the decision to instrument a stream to account for infiltration at the onset of flow can be based on a user-defined acceptable error in cumulative infiltration estimate, E .

The simplified analysis presented here has been developed for a uniform subsurface. Frequently, ephemeral stream channels are comprised of more than one sediment layer. Considering the profile beneath a streambed to be comprised of two layers (e.g., a

streambed layer and an underlying geologic layer) comparisons between infiltration into a one layer system and a two layer system can be evaluated. The impact of the upper layer thickness on infiltration will depend upon the cumulative length of infiltration into the sediments and the antecedent water content within the layers. That is, in general, if the available storage, expressed as a length of water within the upper layer, is significantly larger than the total cumulative infiltration of the streamflow event, the system can be treated as a single layer (Table 1) and the transient contribution for the event will be the same as a single layer approximation. However, if the available storage of the upper layer is larger than the cumulative infiltration during transient infiltration, but not larger than the total cumulative infiltration, the values of R and E will depend on the permeabilities and the upper layer thickness. If the streambed sediments are less permeable than the underlying sediments, then R will depend primarily on the hydraulic conductivity of the streambed layer and will be relatively insensitive to the hydraulic conductivity of the underlying sediments (Colman and Bodman, 1944; Wang et al., 1999). Two-layer systems with a more permeable upper layer will tend to have higher R and E values than a single layer approximation because K_{ss} of the two-layer system will be smaller than K_{ss} of the single layer approximation.

Table 1. Evaluation of Cumulative Onset Infiltration for a Two-Layer System

	Representation	$K_{up} > K_{low}$	$K_{up} < K_{low}$
$\int i_t(t) dt + K_{ss} \tau_{ss} < L(\theta_{sat} - \theta_{in})$	Single Layer	$R = R_{1-Layer}^*$ $E = E_{1-Layer}$	$R = R_{1-Layer}$ $E = E_{1-Layer}$
$\int i_t(t) dt < L(\theta_{sat} - \theta_{in}) < \int i_t(t) dt + K_{ss} \tau_{ss}$	Double Layer	$R > R_{1-Layer}$ $E > E_{1-Layer}$	$R > R_{1-Layer}$ $E > E_{1-Layer}$
$L(\theta_{sat} - \theta_{in}) < \int i_t(t) dt$	Double Layer	$R ? R_{1-Layer}$ $E ? E_{1-Layer}$	$R ? R_{1-Layer}$ $E ? E_{1-Layer}$

* Values denoted by a subscript of 1-Layer represent the case of a single homogenous layer with the same initial water content; L is the depth of the upper layer, θ_{sat} is the saturated water content, and θ_{in} is the antecedent water content

Site Description

Rillito Creek is an ephemeral stream in southern Arizona with a drainage area of 2,256 square kilometers (Figure 2). The Dodge Boulevard study site is underlain by a layer of recent stream-channel deposits and a second deeper layer of basin-fill deposits that are Pleistocene in age or older (Davidson, 1973). The recent deposits, consisting of fine- to coarse-grained alluvium, are about 10 m thick and derived from the surrounding mountain ranges. The alluvium consists predominantly of sand and gravel and contains less than 10 percent clay and silt. The underlying basin-fill deposits are finer grained and extend to depths of several hundreds of meters (Davidson, 1973). Both deposits are loosely compacted within the study area. Depth to the regional water table is about 42 m at the site. The elevation of the stream channel over the entire 60-meter cross section varies by less than 0.75 m. Cores were collected to a depth of 45 m and analyzed for physical, hydraulic, and thermal properties (Hoffmann et al., 2002). Cores were obtained 30 days after the cessation of a streamflow event. The effective saturated hydraulic

conductivities of the two sediment layers were calculated using the core samples collected at the field site. The effective saturated hydraulic conductivities of the upper layer stream channel sediments and the lower basin fill deposits were 2.2 m/day and 0.22 m/day, respectively.

The porosity of the channel sediments determined from core values was $0.35 \text{ m}^3/\text{m}^3$ and the antecedent volumetric water content was $0.22 \text{ m}^3/\text{m}^3$. This latter value was used as an approximation of the field water content. Therefore, the storage capacity at the onset of streamflow was 1.3 m. Previously measured infiltration rates within Rillito Creek at the onset of streamflow were on the order of 50 m/d (Blasch et al., 2000). Using equations 5-6 and 5-7 we can set K_{ss} to the core derived value of 2.2 m/d to solve for the duration of the onset period. The time to steady state is approximately 8.9 hours and the cumulative infiltration is 1.6 m. This suggests that R and E will not be affected by the properties of the lower layer for flow events less than 8.9 hours in duration, but that R and E will be underestimated for longer flow events.

Rillito Creek has two primary seasons of streamflow; summer North American Monsoon (July- September) and winter (December-March). Summer flows typically result from localized, short-duration convective storms, whereas longer-duration frontal storms and snowmelt produce winter flows. During the months of October and November, precipitation from tropical storms or changes in weather patterns caused by periodic climate fluctuations can cause periods of streamflow. However, these events are less

common than the summer and winter events. A U. S. Geological Survey (USGS) streamflow-gaging station, 09485700 (Tadayon et al, 2000), is located 45 m downstream from the study site. Typical flows are less than 28 cubic meters per second (m^3/s); a maximum discharge of about 680 m^3/s occurred during the 1993 El Niño season (Tadayon et al., 2000). Over the last decade, the average number of annual streamflow events was 14, and the typical duration of the events was less than 24 hours (Figure 3). The median streamflow event duration was approximately 8 hours and the average durations was 55 hours.

Investigators have attempted to quantify stream channel infiltration and recharge along reaches of Rillito Creek for almost a century (Smith, 1910). Using seepage runs, Turner (1943) estimated stream channel infiltration rates ranging from 0.34 to 1.1 m/d for a snowmelt event. The lower rate coincided with a shallow water table where a surface/ground water connection impeded vertical infiltration through the stream channel alluvium. Matlock (1965) estimated an average infiltration rate of 1.1 m/d during a continuous four-month long snowmelt event in the spring of 1962. Katz (1987) estimated streamflow loss values of 0.5 m/d within Rillito Creek by measuring streamflow and wetted perimeter during a 119-day event from December 1984 through April 1985.

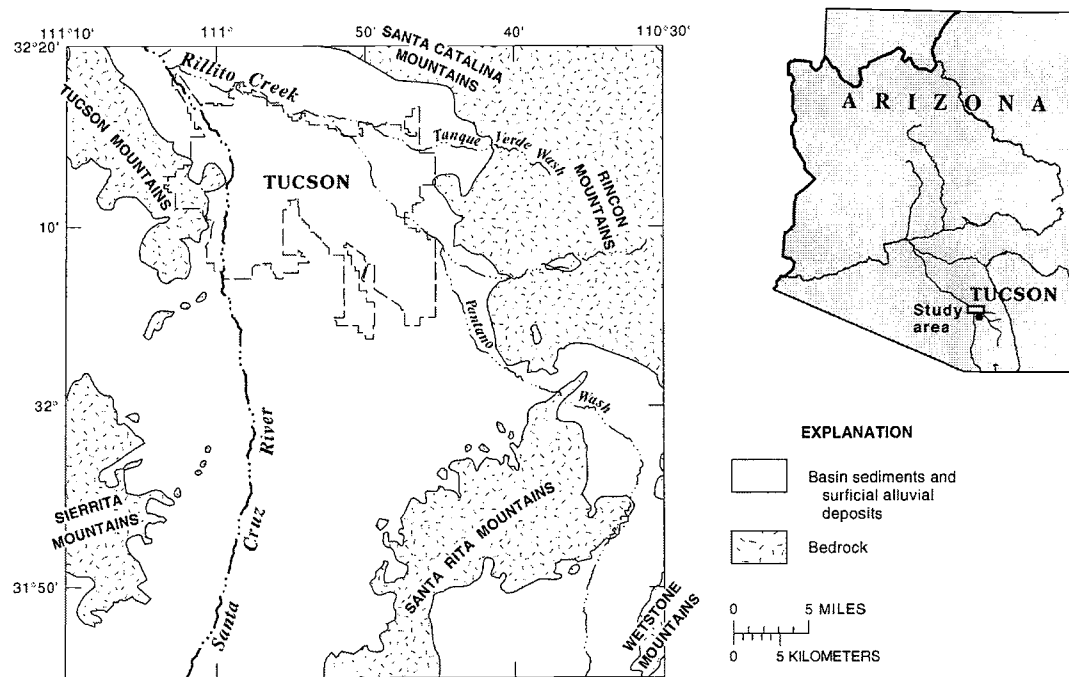
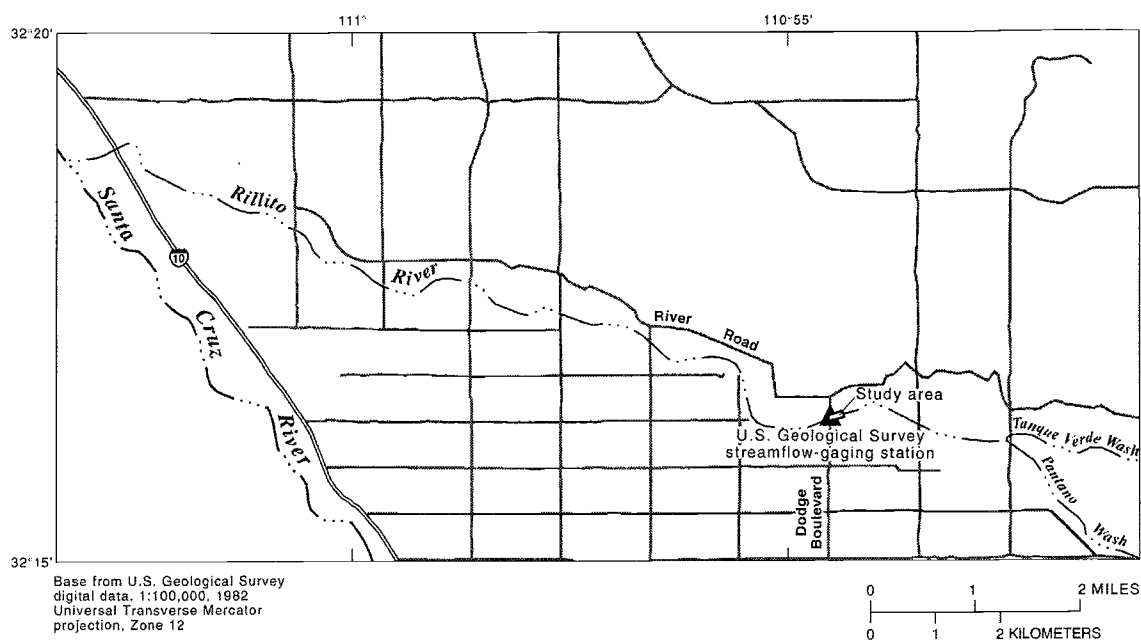


Figure 2. Location of Rillito Creek study area and view of Rillito Creek within the Tucson Basin, Tucson, Arizona.

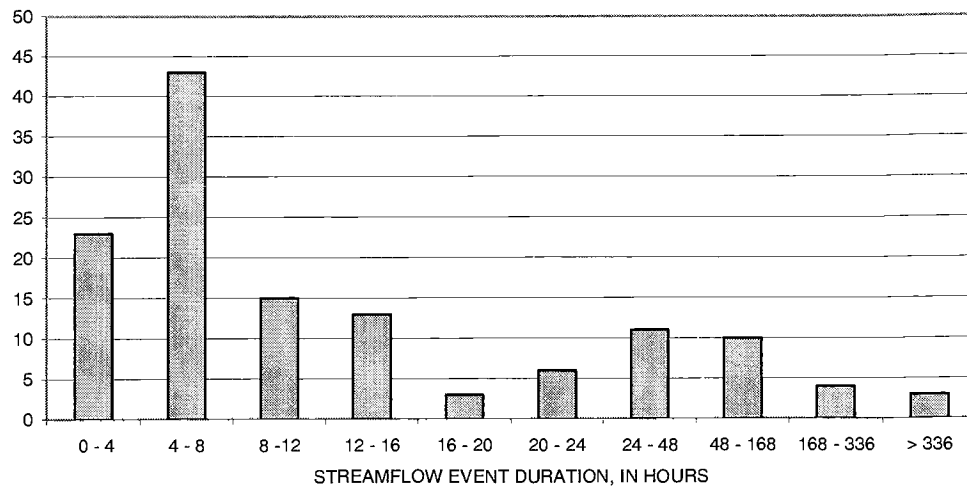


Figure 3. Ephemeral streamflow event durations for Rillito Creek, Tucson, Arizona at study site (1990-2002).

Methods

Stream-channel sediments were instrumented perpendicular to flow with a two-dimensional vertical array of 28 thermocouples and 28 time-domain reflectometry probes (Figure 4). Sensors were arranged in four vertical profiles, spaced 3 m apart. The southernmost instrument profile was installed at the point of lowest elevation in the channel cross section, approximately 4 m from the south bank and about 56 m from the north bank. Pairs of temperature and water-content sensors were located at depths of approximately 0.50, 0.75, 1.0, 1.25, 1.50, 2.0, and 2.5 m below the stream channel surface.

Type T copper-constantan thermocouples were installed and programmed to measure temperature every 5 seconds and to record a time-averaged temperature at 5-minute intervals with a precision of 0.1 °C. TDR probes adjacent to each thermocouple

measured and recorded volumetric water content at 2-minute intervals with a precision of approximately $0.03 \text{ cm}^3 \text{ cm}^{-3}$. A Campbell Scientific TDR100 time domain reflectometer was used in conjunction with a Campbell Scientific CR10X datalogger to transmit, receive, and convert waveforms into water content. TDR probes contained two stainless steel wave-guides 0.20 m in length, spaced 0.03 m apart. Probes were constructed and calibrated in-house using RG-8 coaxial cable to minimize signal transmission loss between the probes and the TDR100 instrument. Cable lengths ranged from 11 to 26 m. Three pore pressure sensors were installed within the trough to measure pressure gradients (Carpenter et al., 2001). One pore pressure sensor was placed between profiles 2 and 3 at a depth of 1.5 m and the remaining two sensors were installed in profile 2 and profile 3 at a depth of 0.7 m. Because of the large number of cobbles in the soil, the instruments could not be inserted directly into the walls of the trench. Rather, the instruments were placed in the trough and sediments were backfilled around them. Data were collected from July 2000 through December 2001.

The ground surface was surveyed after each streamflow event to determine the amount of scour and deposition. About 0.25 m of sediment was scoured after the first 3 events. Profiles 1 and 2, nearest the southern bank, became the lowest points in the cross section. Scour and deposition associated with later streamflow events were less than 0.1 m.

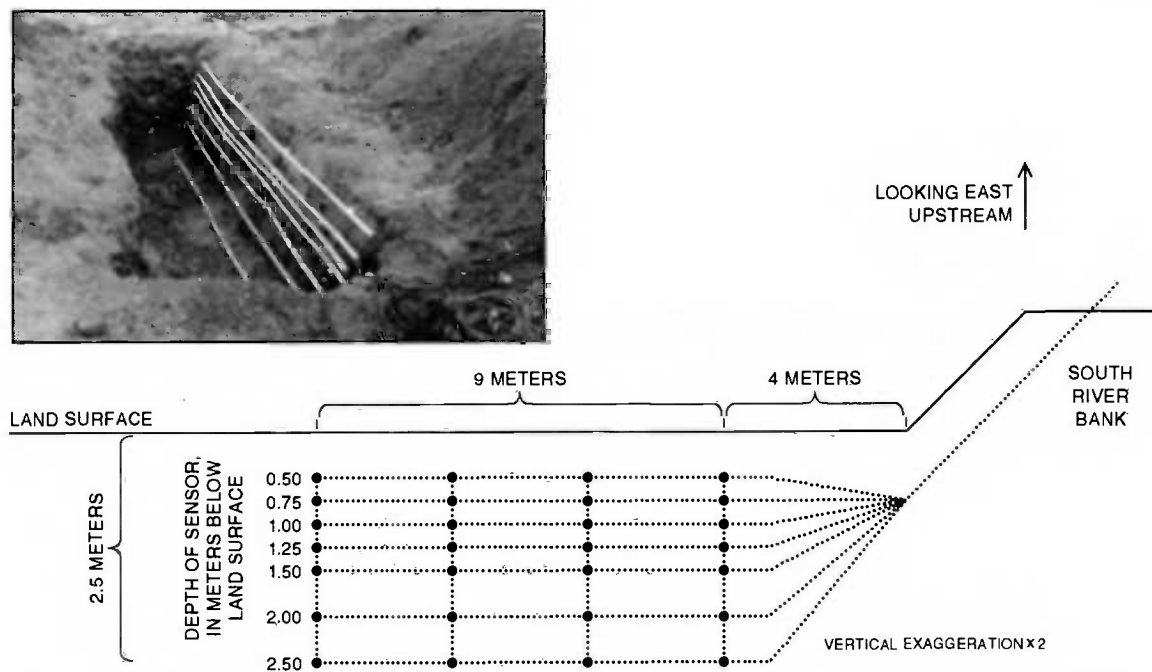


Figure 4. Photograph and schematic of the two-dimensional array of sensors within the stream-channel deposits. Each black circle represents a temperature and soil-water sensors.

Steady-state infiltration rates were estimated using a two-dimensional variably saturated heat and fluid transport model, VS2DH (Healy and Ronan, 1996). This model has been employed successfully in previous investigations to estimate stream channel infiltration (Ronan, 1998; Constantz, 1998). The two longest flow events (10-11 days) recorded during the monitoring period were used to calibrate the thermal (sediment heat capacity and saturated thermal conductivity) and hydraulic (saturated hydraulic conductivity and porosity) parameters within the model. PEST (Watermark Computing, 1994) was used for nonlinear parameter estimation. A one-dimensional model was created for each profile using the measured initial and boundary conditions to provide a more accurate measure of the flux through the near surface sediments. The model was approximately 2

m in depth with 30 vertical cells equal in size. The 0.5 m-depth thermocouple was used as the upper temperature boundary condition and the 2.5 m-depth thermocouple was used to define the lower temperature boundary condition. The remaining five thermocouples were used as observation points. The parameter set that minimized the sum of least squares between the simulated and observed temperatures was selected as the optimum. Simulated temperatures at all five depths were equally weighted. The pressure measurements were used to calculate a pressure gradient. This gradient was extended over the entire profile to define upper and lower constant head boundary conditions. Steady state infiltration rates were estimated for the November 2000 and April 2001 events. Profiles 1-4 were analyzed for the November event. However, because streamflow did not extend over the entire cross-section for the April 2001 streamflow event only profiles 1 and 2 were analyzed. Infiltration fluxes simulated using a two-dimensional model were comparable to those simulated using four independent one-dimensional models, indicating that flow could be represented as one-dimensional. Parameter values for the sediments obtained through calibrations were similar determined using cores (Table 2).

Table 2. Comparison of calibrated and core-measured thermal and hydraulic properties of the channel sediments

	Porosity $\text{m}^3 \text{ m}^{-3}$	Hydraulic Conductivity (saturated) m d^{-1}	Specific Heat Capacity $10^6 \text{ J m}^{-3} \text{ }^\circ\text{C}^{-1}$	Thermal Conductivity (saturated) $\text{W m}^{-1} \text{ }^\circ\text{C}^{-1}$	Thermal Conductivity (dry) $\text{W m}^{-1} \text{ }^\circ\text{C}^{-1}$
Simulated	0.357	2.95	1.64	1.21	0.2
Core	0.35	2.2	1.4	1.05	0.26

The period of sediment dewatering after the cessation of streamflow was used to calibrate the unsaturated hydrologic parameters for the profiles. Soil-water contents and temperatures for the middle five depths were used to calibrate the unsaturated zone parameters (Figure 5 & 6). With the parameters of the model calibrated, three ephemeral streamflow events were simulated. Soil-water contents were used to define the antecedent moisture conditions. Temperature and pressure measurements were used to represent the boundary conditions.

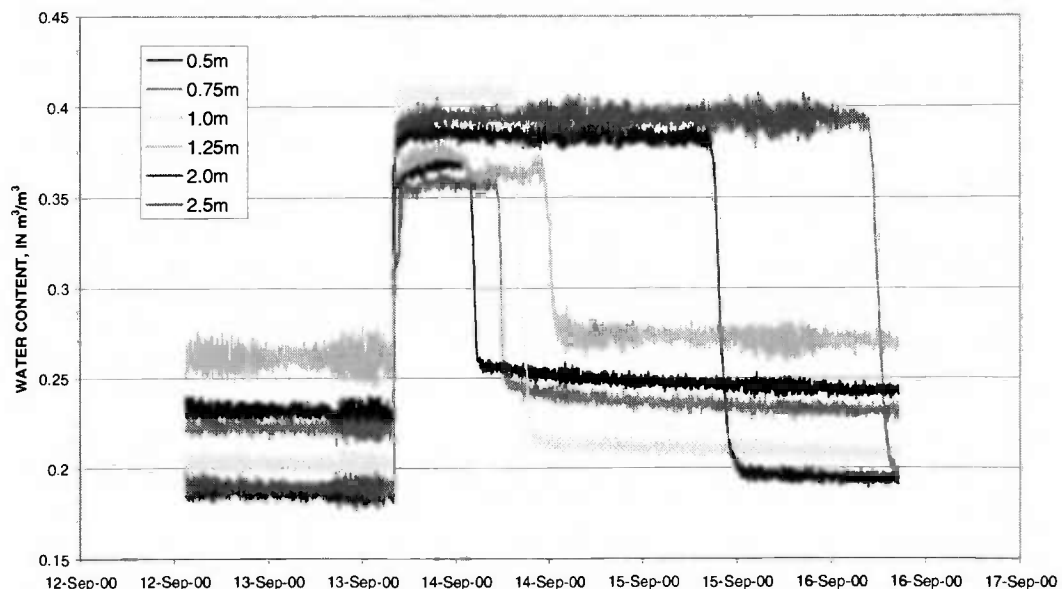


Figure 5. Water content data showing rapid increases at the onset of streamflow; a stabilization of water content during the event; and subsequent dewatering after streamflow is over.

Wetting front velocities and infiltration fluxes at the onset of infiltration were calculated using the water content measurements from 0.5 to 2.5 m (Figure 5). Infiltration was assumed to have begun when the water content at 0.5 m depth increased by $0.05 \text{ cm}^3/\text{cm}^3$ above the initial condition. Even for the sharp wetting fronts observed in the coarse-

grained sediments, water could still have exited the lower boundary before the lower layer reached full saturation. Therefore, to avoid underestimating the contribution of flow at the onset of infiltration, we quantified the infiltration rate until the volumetric water content of the lowest layer reached $0.30 \text{ cm}^3/\text{cm}^3$, rather than full saturation. The average variance of residuals for the November profile simulations was 0.097°C and ranged from $0.06 - 0.12^\circ\text{C}$. The average variance of residuals for the April profile simulations was 0.635°C and ranged from 0.2 to 1.07°C .

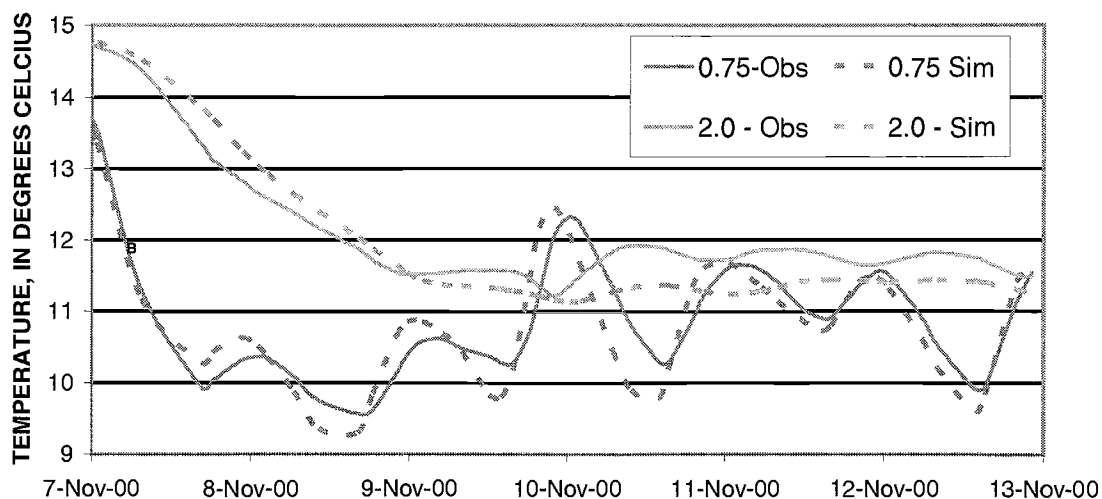


Figure 6. Representative observed and simulated thermographs for two depths, November 2000.

Results and Discussion

There were 26 streamflow events recorded over the measurement period. Events varied in duration from 2 hours to 11.6 days. Sixteen of the events were less than 1 day in duration and only 3 events were longer than 7 days. The median event lasted 12 hours. Peak discharge ranged from 0.03 to $180 \text{ m}^3/\text{s}$ with a median of $3 \text{ m}^3/\text{s}$. The interflow period between streamflow events ranged from 6 hours to 67 days. Eleven streamflow

events began before the sensor profile had fully dewatered to field capacity ($\sim 0.20 \text{ cm}^3/\text{cm}^3$). The three longest events were used to determine stream channel fluxes. These events occurred on 4-15 November 2000, 9-15 March 2001, and 6-17 April 2001 and were 11, 7, and 12 days in duration, respectively. The November event occurred within 2.7 days of the end of the previous flow event. The lowest 0.5 m of the profile was still saturated. The onset of the March event began 0.6 days after the end of the previous flow event. The lowest 2.0 m of the profile was still saturated. The onset of the April event started 15 days after the end of the previous flow event, and the profile had drained to field capacity.

The calculated onset infiltration fluxes using were 38 m/d and 67 m/d for the November and April events, respectively. There were insufficient data to estimate the onset infiltration flux for the March event because it was nearly saturated at the onset of flow. The transition from the transient period to the steady state period was defined as the time at which the simulated infiltration fluxes varied by less than $1 \times 10^{-9} \text{ m}^3/\text{s}^2$. For the November event this was approximately 4.19 hours (Figure 7). The duration of the March event was 1.8 hours. For the April event the transient duration was about 20 hours (Table 3). The events displays two steady infiltration periods. For example, the first constant infiltration period for the April event occurs 0.9 hours after the onset of flow and lasts for nearly 17 hours. The infiltration rate during this period is approximately 1.23 m/d, which is similar to the effective hydraulic conductivity of the channel sediments. The second constant infiltration period begins 20 hours after the

onset of flow. This behavior may be explained by the impacts of the layered streambed structure. Specifically, the available storage in the upper layer is larger than the cumulative transient infiltration. Therefore, constant infiltration occurs within the first layer within an hour (case 1, Table 1). But, as the wetting front approaches the lower, less permeable layer, the rate of infiltration decreases until steady-state infiltration is established throughout the profile. For this case, cumulative transient infiltration was summed until the end of the second transient period. In contrast to the April 2001 event, antecedent moisture contents were so high for the March event that steady state infiltration rates were immediately influenced by the lower layer (case 3, Table 1).

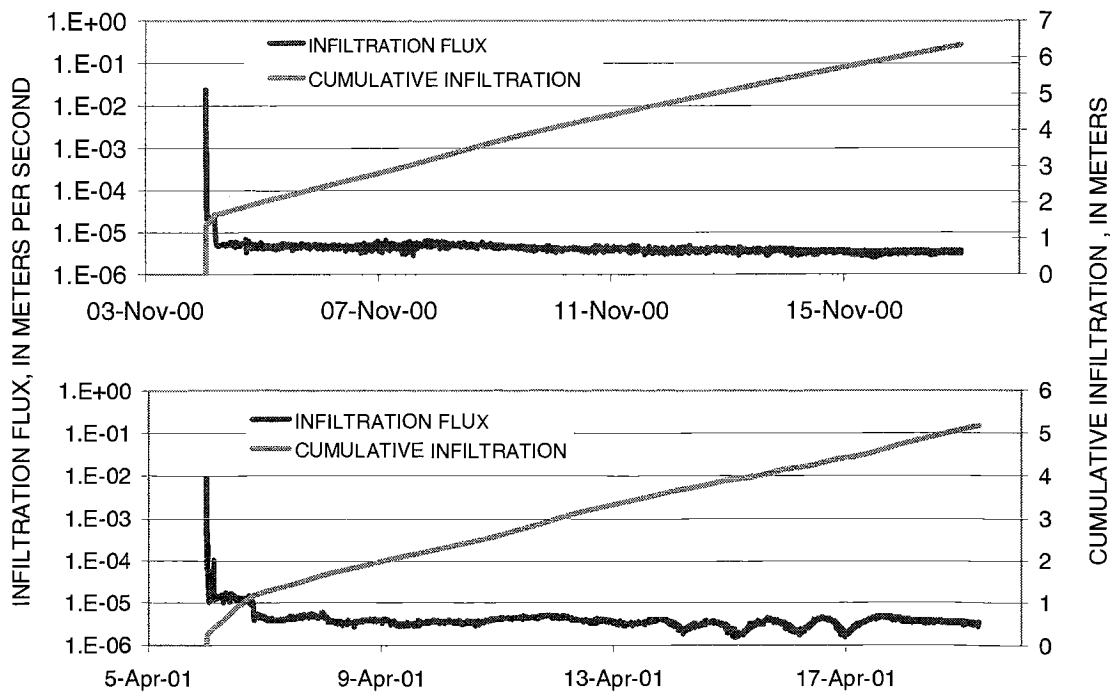


Figure 7. Infiltration fluxes and cumulative infiltration for A) 4 November 2000 and B) 6 April 2001.

The concept of steady state infiltration is convenient for representing streambed infiltration beneath ephemeral streams. However, our measurements do not show that constant infiltration was reached during streamflow. Rather, infiltration fluxes determined using VS2DH (Figure 7) showed a general decline over the period of the event (Figure 8). The decline may be attributed to a reduction in the pressure gradient as the wetting front extends farther from the surface, a reduction in the effective hydraulic conductivity of the basin fill sediment, or the development of an impermeable layer at the surface (Bailey, 2002). The simulations also show several higher frequency perturbations. The November event shows an increase in the flux about three days into the event, which coincides with an increase in discharge from approximately $0.85 \text{ m}^3/\text{s}$ to about $75 \text{ m}^3/\text{s}$ and an increase in stage from about 0.15 m to over 0.61 m. The March and April events show a diurnal variation in infiltration rate, which may be attributed to temperature changes at the surface (Ronan et al., 1998). This diurnal variation is not seen in the November event, which experienced smaller diurnal variations in surface temperature. The average infiltration flux for the November 2000 event was 0.39 md^{-1} and ranged from 0.3 m/d to 0.45 m/d. The steady state flux measured using seepage measurements for an event 4 days before the November event was 0.28 m/d. The average steady state value for the March event was 0.28 m/d and ranged from 0.14 to 0.40 m/d. The average steady state infiltration value for the April 2001 event was 0.32 m/d and ranged from 0.17 m/d to 0.43 m/d. While the concept of steady-state infiltration is flawed, these results show that the simulated steady-state infiltration rates can be

estimated using the effective hydraulic conductivity determined for the lower layer cores, as suggested by Hillel (1998) and Leconte et al. (2001).

The cumulative infiltration during the transient period for the November event was 1.65 m (Table 3). The cumulative lengths of infiltration during the transient period for the March and April events were 0.32 m. and 0.9 m, respectively. The November steady state period contributed 4.69 m of water. The values of relative transient contribution, R , and the infiltration error, E , for this event were 0.26 and 25%. The simulated transient contribution for the March event was 0.3 m while the steady state period contributed 2.72 m, producing an R of 0.10 and an E of 9%. For the April event the simulated transient cumulative infiltration was 0.9 m and the steady state total was 4.28m, giving R and E values of 0.17 and 13%. It should be noted that the three longest flow events were selected for this analysis to enable computation of the steady state infiltration fluxes and to more accurately calibrate the model. Accordingly, the infiltration error, E , calculated in this analysis is likely an underestimate of the true infiltration error for the stream channel because the transient contributions, R , increase for shorter duration events.

Table 3. Description of ephemeral streamflow infiltration events

Event	Transient Infiltration (m)	Steady State Infiltration (m)	Time to Steady State (hr)	Steady State Average Flux (m d^{-1})	Transient Infiltration (w/ SS rate) (m)	R (%)	E (%)
November	1.65	4.69	4.2	0.39	0.06	26	25
March	0.3	2.72	1.8	0.28	0.02	10	9
April	0.9	4.28	20	0.32	0.2	17	13

Given the importance of stream channel infiltration reporting for incorporation into various hydrologic investigations we suggest one of two approaches to improve the estimation and reporting of streambed infiltration beneath ephemeral streams. Infiltration rates based on steady state infiltration can be reported with an estimate of the likely underestimation error. Or, a general estimate of the cumulative infiltration during the transient period can be developed and applied on a site-specific basis.

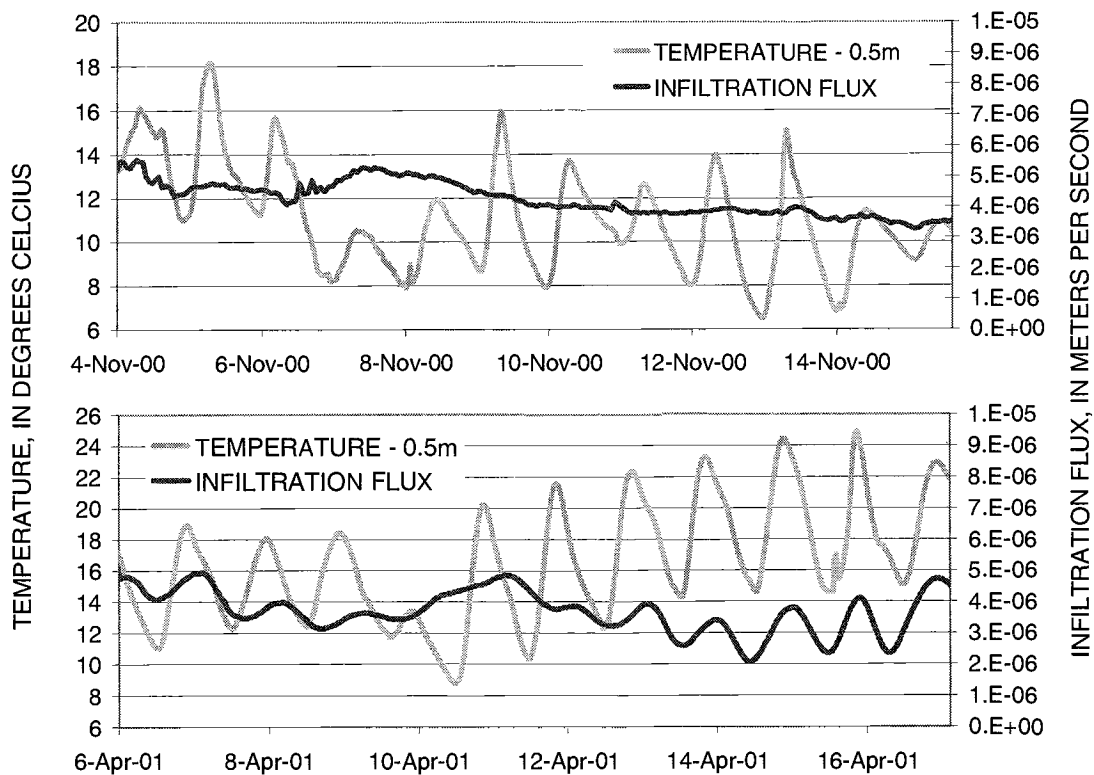


Figure 8. Steady state infiltration fluxes and thermal boundary conditions for A) 4 November 2000 and B) 6 April 2001.

Conclusion

Temperature and water content measurements were used to calculate infiltration fluxes throughout the duration of three ephemeral streamflow events in a large ephemeral stream with a higher conductivity alluvial layer overlying a lower conductivity alluvial material. Average infiltration rates at the onset of the events were 2-3 orders of magnitude larger than steady state infiltration rates. Transient periods were 1.8 to 20 hours in duration, in inverse proportion to the antecedent moisture content. Steady-state infiltration rates were related to the effective hydraulic conductivity of the underlying basin fill layer. The multi-layer system produced two observable transient and steady-state periods. The lengths of the transient and steady state periods were dependent on the antecedent water content profiles. Use of steady state infiltration rates to estimate cumulative infiltration underestimated simulated values by 18%, demonstrating the need to consider transient infiltration to improve streambed infiltration estimates for aquifer recharge investigations.

References

Babcock, H.M and E.M. Cushing, 1942. Recharge to ground water from floods in a typical desert wash, Pinal County, Arizona: Transactions, American Geophysical Union, v.23, pt.1, Reports of Papers, p.49-56.

- Bailey, M., 2002. Analysis Of One-Dimensional Vertical Infiltration Using Heat As A Tracer In Rillito Creek, Tucson, Arizona, University of Arizona, Masters Thesis, 130 pp.
- Bartolino, J.R. and R.G. Niswonger, 1999. Numerical Simulation of Vertical Ground-Water Flux of the Rio Grande from Ground-Water Temperature Profiles, Central New Mexico, U.S. Geological Survey Water-Resources Investigations Report 99-4212, 34 pp.
- Carpenter, M.C., Cluer, B.L., Smith, G.R., Wick, E.J., Lockett, J.L., and Brockner, S.J., 2001, Field trials monitoring sand deposition and erosion on a razorback sucker spawning bar on the Green River near Jensen, Utah, and operational description of load-cell scour sensors, *in* Seventh Federal Interagency Sedimentation Conference, Proceedings, March 25–29, 2001, Reno, Nevada USA, p. Poster 12–15.
- Colman, E.A. and G.B. Bodman, 1944, Moisture and energy conditions during downward entry of water into moist and layered soils, Soil Science Society of America, 9, p.3-11.
- Constantz, J. and C.L. Thomas, 1996. The use of streambed temperature profiles to estimate the depth, duration, and rate of percolation beneath arroyos, *Water Resources Research.*, 32(12), p. 3597-3602.

Constantz, J. and C.L. Thomas, 1997. Streambed temperature profiles as indicators of percolation characteristics beneath arroyos in the Middle Rio Grande Basin, USA, *Hydrol. Process.*, 11, p. 1621-1634.

Constantz, J., 1998. Interaction between stream temperature, streamflow, and groundwater exchanges in alpine streams, *Water Resources Research*, 34(7), p. 1609-1615.

Constantz, J., D. Stonestrom, A.E. Stewart, R. Niswonger, and T.R. Smith, 2001, Analysis of streambed temperature in ephemeral stream channels to determine streamflow frequency and duration, *Water Resources Research*, 37(2), p. 317-328.

Davidson, E.S., 1973, Geohydrology and water resources of the Tucson basin, Arizona: U.S. Geological Survey Water-Supply Paper 1939-E, 81 pp.

Green, W.H. and G.A. Ampt. 1911. Studies on soil physics, Part 1, Flow of air and water through soils, *J.Agr.Sci* 4, p.1-24.

Hanson, R.T. and Benedict, J.F., 1994 , Simulation of ground-water flow and potential for land subsidence, Upper Santa Cruz basin, Arizona: U.S. Geological Survey, Water-Resources Investigations Report 93-4196, 47 pp.

Hillel, D., 1998. Environmental Soil Physics, Academic Press San Diego, p.404.

Hoffman, J.P., M.A., Ripich and K.E., Ellett, 2002. Characteristics of shallow deposits beneath Rillito Creek, Pima County, Arizona, U.S. Geological Survey Water-Resources Investigations Report 01-4257, 51 pp.

Healy, R.W. and Ronan, A.D. 1996. Documentation of computer program VS2DH for simulation of energy transport in variably saturated porous media – Modification of the U.S. Geological Survey's computer program VS2DT: U.S. Geological Survey Water-Resources Investigations Report 96-4230, 36 pp.

Katz, L.T., 1987. Steady State Infiltration Processes Along the Santa Cruz and Rillito Rivers, Ph.D. Dissertation, University of Arizona, Tucson.

Kirkham, D. and W.L. Powers, 1972. Advanced Soil Physics, Wiley-Interscience, New York, 534 pp.

Leconte, R and F.P. Brissette, 2001. Soil Moisture Profile Model for Two-Layered Soil Based on Sharp Wetting Front Approach, *Journal of Hydrologic Engineering*, 6(2), p. 141-149.

Linsley R.K., J.B. Franzini, D.L. Freyberg, and G. Tchobanoglous, 1992. Water Resource Engineering 4th Edition, McGraw-Hill, Inc. New York., 334pp.

Matlock, W.G., 1965. The effect of silt-laden water on infiltration in alluvial channels, Ph.D. Dissertation, University of Arizona, Tucson.

Parlange, Jean-Yves., 1971. Theory of water-movement in soils: II. One-dimensional infiltration. *Soil Science*, 111, p.170-174.

Philip, J.R., 1957. The theory of infiltration. 1. The infiltration equation and its solution. *Soil Science*, 83, p.345-357.

Philip, J.R., 1969. Theory of Infiltration, in *Advances in Hydrosience*, 5. Academic Press, New York.

Rawls, W.J., L.R. Ahuja, D.L. Brakensiek, and A. Shirmohammadi, 1993. Infiltration and Soil Water Movement, in Handbook of Hydrology, eds. Maidment, D.R., McGraw-Hill, New York, p. 5.38.

Ronan, A.D., D.E. Prudic, C.E. Thodal, and J. Constantz, 1998. Field study and simulation of diurnal temperature effects on infiltration and variably saturated flow beneath an ephemeral stream, *Water Resources Research*, 34(9), p. 2137-2153.

- Smith, G. E. P., 1910. Groundwater supply and irrigation in the Rillito Valley: Tucson, AZ, Bulletin No. 64, University of Arizona Agricultural Experiment Station, p. 81-243.
- Stephens, D.B., W. Cox, and J. Havlena, 1988. Field study of ephemeral stream infiltration and recharge, Tech. Completion Report, 228, 188 pp., water Resources Research Institute, New Mexico State University, Las Cruces.
- Tadayon, S., N.R. Duet, G.G. Fisk, H.F. McCormack, C.K. Partin, G.L. Pope, and P.D. Rigas. 2000. Water Resources Data for Arizona, water year 2000, U.S. Geological Survey Water-Data Report AZ-00-1, 210 pp.
- Turner, S.F., and others, 1943, Ground-water resources of the Santa Cruz basin, U.S. Geological Open File Report.
- Wallace, D.E., and Lane, L.J., 1978. Geomorphic features affecting transmission loss potential on semiarid watersheds, *in* Hydrology and Water Resources in Arizona and the Southwest—Proceedings of the 1978 Meetings of the Arizona Section, American Water Resources Association and the Hydrology Section, Arizona Academy of Science, Flagstaff, Arizona: Tucson, Arizona, Arizona Section, American Water Resources Association, 8, p. 157-164.

Wang, Q. M. Shao, and R. Horton, 1999. Modified Green and Ampt Models for Layered Soil Infiltration and Muddy Water Infiltration, *Soil Science* 164(7), p. 445-53.

Warrick, A.W., 2003. Soil Water Dynamics, Oxford University Press, New York 391 pp.

Watermark Computing, 1994. PEST Model-Independent Parameter Estimation Manual, Brisbane, Australia, 160 pp.

Wilson, L.G., K.J. DeCook, and S.P. Neuman, 1980. Regional Recharge Research for Southwest Alluvial Basins, Water Resources Research Center, University of Arizona, Tucson.

Youngs, E.G., 1964. An Infiltration Method Measuring the Hydraulic Conductivity of Unsaturated Porous Materials,” *Soil Science*, 97, p.307-311.

**APPENDIX D: COMBINED USE OF HEAT AND SOIL-WATER CONTENT TO
DETERMINE STREAM/GROUND-WATER EXCHANGES, RILLITO CREEK,
TUCSON, ARIZONA**

John P. Hoffmann, Kyle W. Blasch, and Ty P.A. Ferré

Published in U. S. Geological Circular, *Using Heat as a Tracer for Examining Stream
Exchanges with Ground Water*, September 2003

Introduction

The City of Tucson and surrounding communities obtain virtually all their municipal, agricultural, and industrial water from ground water that is withdrawn from thick alluvial aquifers underlying the desert basins. A large fraction of this ground water entered the aquifers as recharge after percolating through channel deposits along ephemeral streams (Matlock and Davis, 1972; Davidson, 1973; Hanson and Benedict, 1994). Most of the ground water in the underlying aquifers is thousands of years old (Kalin, 1994), and the amount of water that recharges the aquifers is insufficient to meet current and future demands. The resultant ground-water deficit, which will grow as the population increases, is manifested in water-level declines of more than 60 meters since the middle of the 20th century. To help mitigate the deficit, an in-stream recharge facility has been proposed in the Rillito Creek channel on the north side of Tucson. The source of water for the recharge facility is likely to be Colorado River water, transported from Lake

Havasu and delivered to the Tucson area through the Central Arizona Project aqueduct.

Infiltration of streamflow is known to occur in ephemeral streams in the southwestern United States; however, a better understanding of the infiltration processes can improve the effectiveness of in-stream recharge facilities. This chapter describes one component of an investigation designed to improve our understanding of infiltration processes in ephemeral-stream alluvium. In particular, we discuss the variability of infiltration rates during a streamflow event and show how temperature methods in conjunction with soil-water content measurements can be used to evaluate potential sites for recharge facilities.

In this chapter, we show examples of how numerical simulations using temperature methods are used to estimate rates of infiltration in the shallow Rillito Creek stream channel deposits during an ephemeral streamflow event. Water content changes measured at several depths are used to estimate the rapid infiltration rate at the onset of streamflow. The variation in infiltration rates during a streamflow event is examined. Drainage rates at the cessation of streamflow, determined on the basis of soil-water content measurements, are compared to estimated infiltration rates near the end of streamflow for each profile. These estimated infiltration rates and drainage rates are compared with previous estimates of these rates obtained by other techniques.

Rillito Creek

Rillito Creek has a drainage area of 2,256 square kilometers at the streamflow-gaging

Rillito Creek at Dodge Boulevard (09485700) and has two major tributaries: Tanque Verde Creek and Pantano Wash (Figure 1). The creek is typical of ephemeral streams in the arid and semiarid Southwestern United States. During most of the year, the creek is dry; however, after prolonged or intense periods of rainfall and (or) snowmelt, it has flowed for several hours to several days along its 20-kilometer length. Precipitation runoff and snowmelt from the Santa Catalina Mountains to the north and the Rincon Mountains to the east, as well as urban runoff from the northeastern suburbs of Tucson, contribute most of the flow to Rillito Creek. Rillito Creek is a losing stream along its westward course toward its confluence with the Santa Cruz River.

Rillito Creek is underlain by recent stream-channel deposits and Pleistocene or older basin-fill deposits (Anderson, 1987). The channel deposits, which were derived from the surrounding mountain ranges, comprise fine- to coarse-grained alluvium and are about 10 meters thick. They predominantly are sand and gravel and contain less than 10 percent clay and silt, indicating that streambed infiltration is rapid. The underlying basin-fill deposits generally are finer grained and extend to depths of several hundreds of meters. Both deposits generally are loosely compacted but the basin fill can be moderately compacted. Depth to ground water beneath Rillito Creek typically ranges from less than 3 meters in the upper reach near the confluence of Tanque Verde Creek and Pantano Wash to about 45 meters near the confluence with the Santa Cruz River to the west.

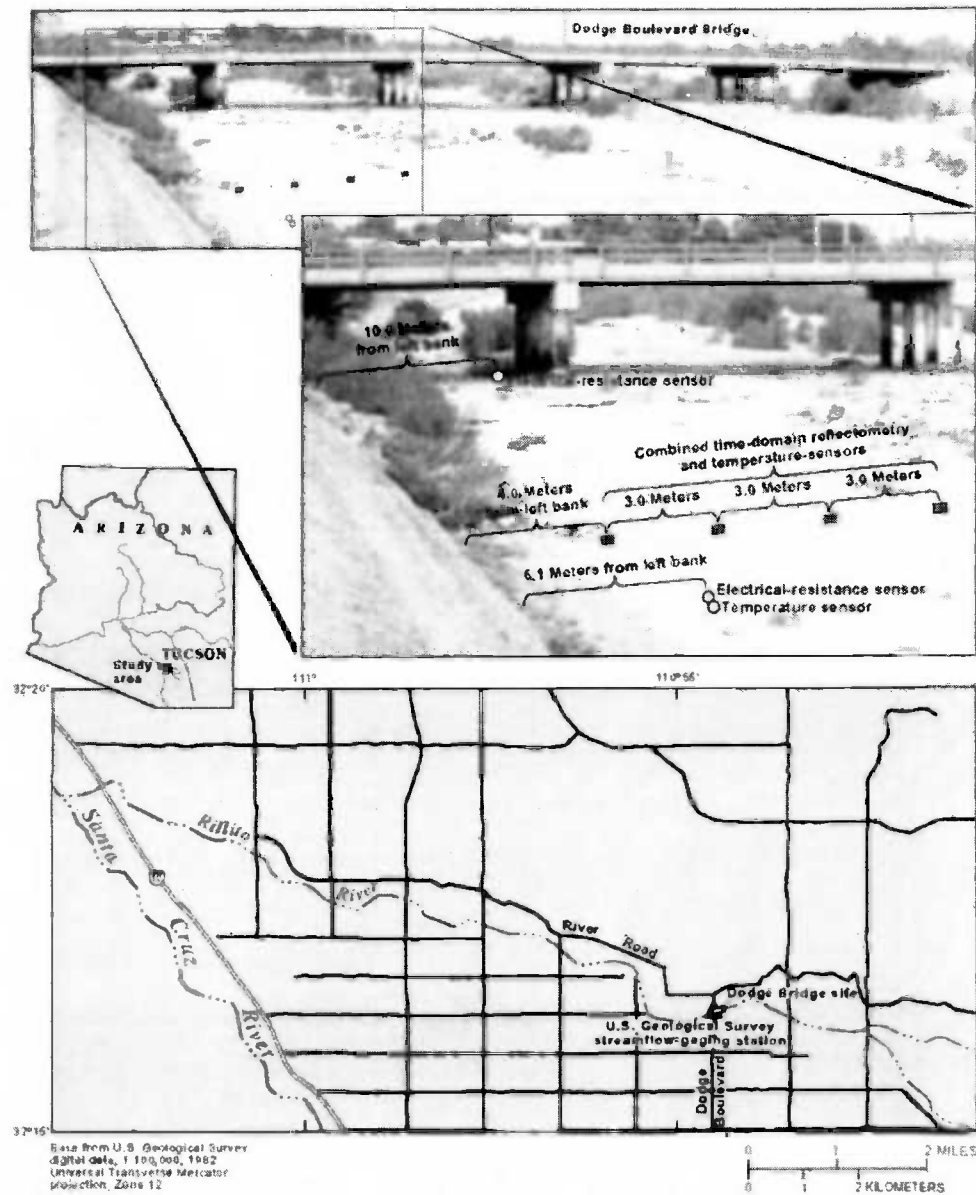


Figure 1. Location of study area showing position of instrumentation relative to streambank.

Field Instrumentation

The streambed was instrumented with a two-dimensional vertical array of 28 paired thermocouples temperature probes and time-domain reflectometry (TDR) moisture probes placed perpendicular to flow (Figure 2). The thermocouples used measure temperature with a precision of about 0.1 degree Celsius; TDR probes measure volumetric water content with a precision of about 3 percent (see Appendix A for discussion of thermocouple accuracy). The paired probes were arranged in four columns (profiles C1, C2, C3, and C4 in Figure 2) spaced 3 meters apart. There are seven rows (depths) within the array at depths of about 0.50, 0.75, 1.0, 1.25, 1.50, 2.0, and 2.5 meters below the stream-channel surface. Depths of the probes varied by as much as 0.25 meters owing to deposition and erosion during flow events. A near-surface temperature sensor also was placed adjacent to the paired two-dimensional array at a depth of 0.05 m. Depth to the regional water table is about 42 m at the site. The U.S. Geological Survey (USGS) streamflow-gaging station Rillito Creek at Dodge Boulevard is 45 meters downstream from the site.

Temperature Data

As discussed in chapter one, heat can be transferred through sediments by advection and conduction. Although both advective- and conductive-heat transport occur during infiltration, advective-heat transport is more prevalent in high water flux settings, whereas conductive-heat transport is more prevalent in static or very low water flux

conditions. For most hydrologic applications related to infiltration through alluvial sediments, advection is the primary mechanism for the transport of heat by flowing water and conductive heat transport is regarded as a negligible component of heat transfer.

Subsurface temperatures change rapidly at the onset of streamflow (Figure 3) because heat transport is coupled directly with water flow through advection. The temperature changes are reduced in amplitude and show an increasing lag time with depth.

Temperature changes occur in both the horizontal and vertical dimensions (Figure 4).

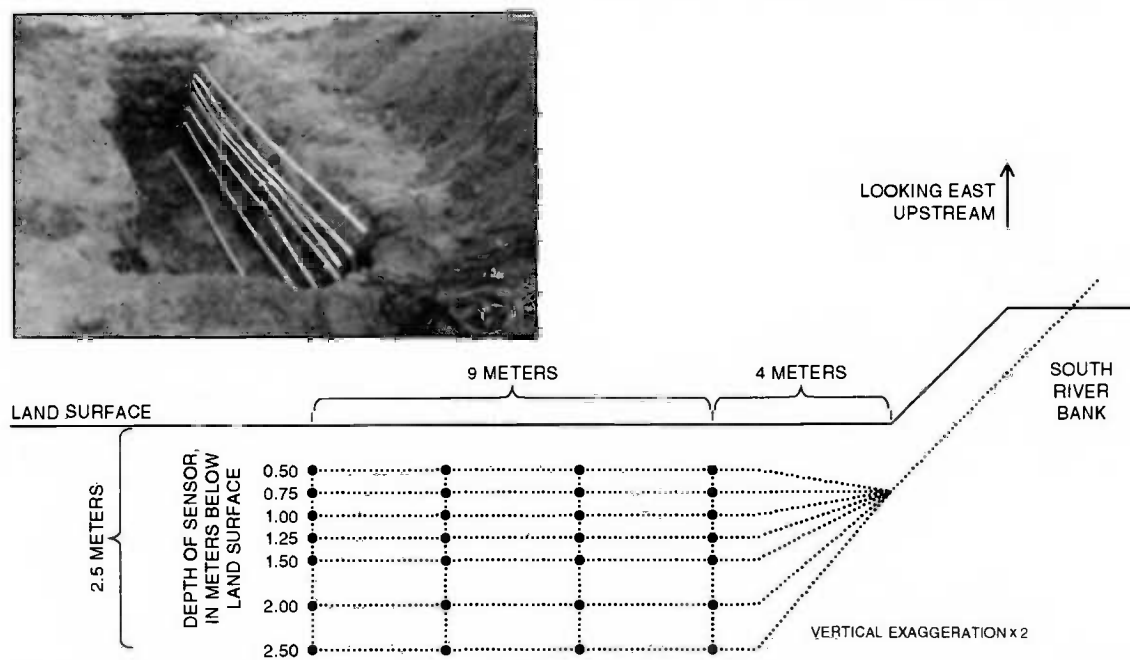


Figure 2. Photograph and schematic of the two-dimensional array of sensors within the stream-channel deposits. Each black circle represents a temperature and soil-water sensor. Refer to Figure 1 for location of array within Rillito Creek.

Soil-water content data

The highly transient conditions that exist at the onset of streamflow are difficult to

simulate numerically; therefore, a direct analysis of water-content measurements probably is the most accurate method of estimating initial infiltration rates. Infiltration rates at the onset of streamflow can be estimated using wetting-front arrival times at successive TDR probes. Once streamflow ends, the water that has infiltrated into the subsurface continues to redistribute vertically and horizontally. The rate of drainage depends on the distribution of water throughout the subsurface at the end of streamflow. Drainage rates, similar to infiltration rates, are determined from the elapsed time between sharp decreases in water content at each depth (Figure 5). Drainage rates through the Rillito Creek stream-channel deposits typically are between 0.5 and 1.0 meters per day (Blasch and others, 2000).

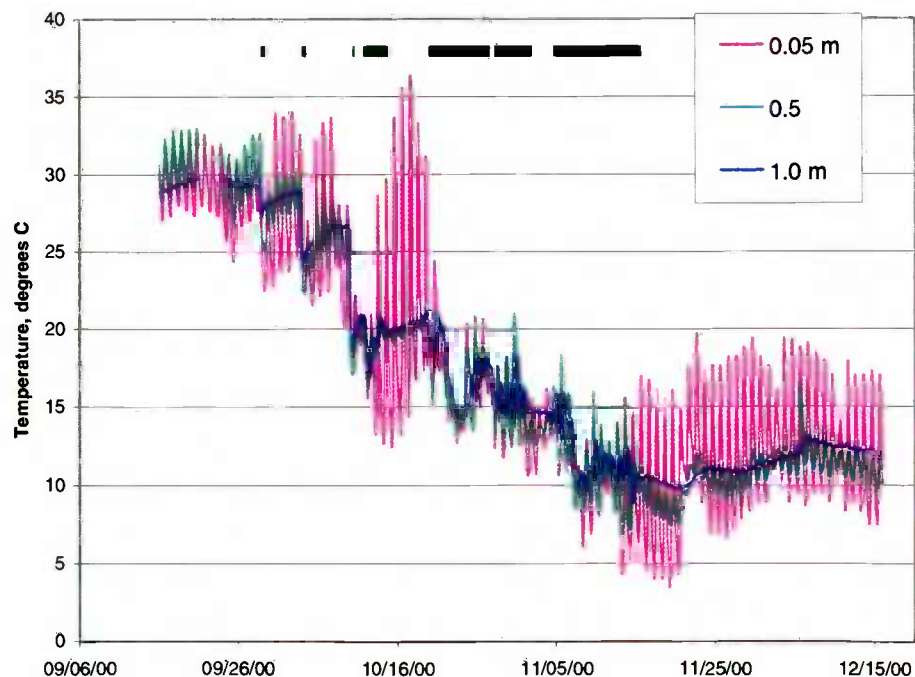


Figure 3. Thermograph of Rillito Creek sediments at depths of 0.05, 0.5 and 1.0 meters. Periods of streamflow are shown by solid bars above thermographs.

Water-content data show rapid changes at the onset of streamflow (Figure 5). Volumetric water content increases from about 20 percent to 40 percent within minutes of the onset of streamflow. These initial infiltration rates were as high as 3.5 millimeters per second, which if sustained would be equivalent to 300 meters per day. The high rates are likely

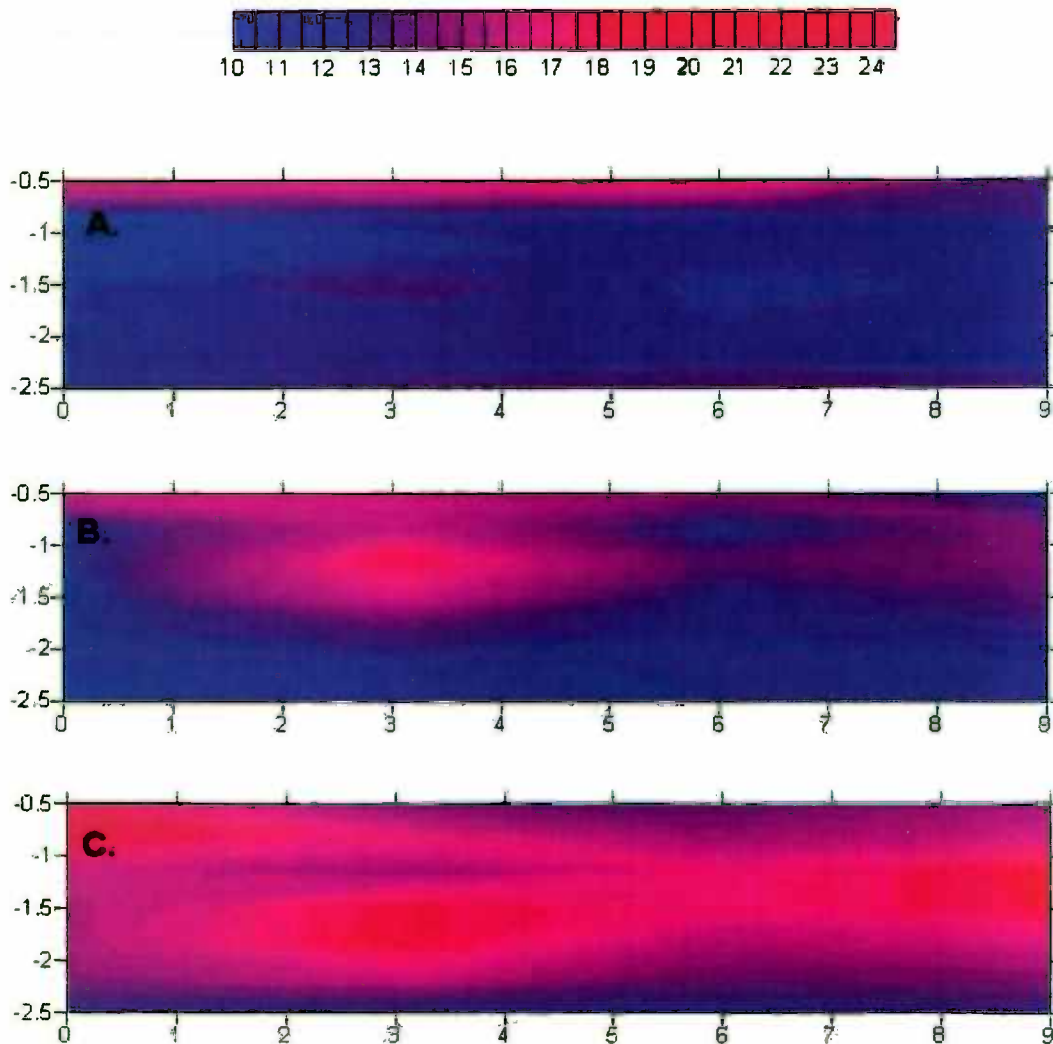


Figure 4. Two-dimensional temperature distribution within stream-channel deposits. (A) Thermal transport through conduction before the onset of a streamflow event. (B) Thermal transport through combination of advection and conduction at the onset of a streamflow event. Multidimensional percolation through the sediments. (C) Combined advection and conduction thermal transport to the deeper sediments several hours into a flow event.

to include vertical and lateral flow components. Similar to the temperature data, the water-content data indicate that infiltration occurs in both the horizontal and vertical directions at the onset of streamflow (Figure 6). Drainage rates determined from water-content measurements after the cessation of flow for the same event for which modeled simulations are presented in this chapter were about 0.46 m/d.

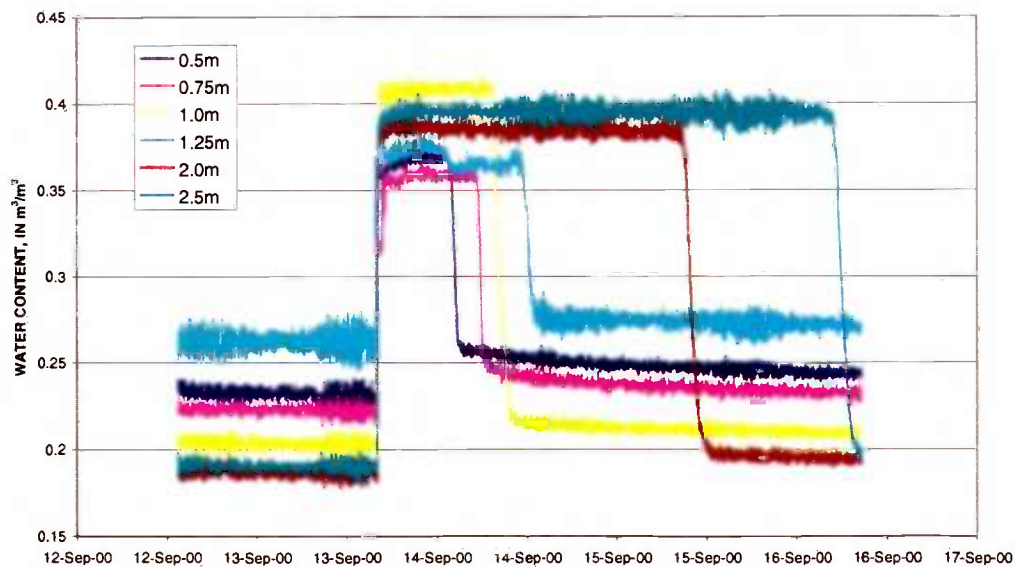


Figure 5. Water-content data showing rapid infiltration at the onset of streamflow; a stabilization of water content during the streamflow event; and subsequent drainage after the streamflow is over.

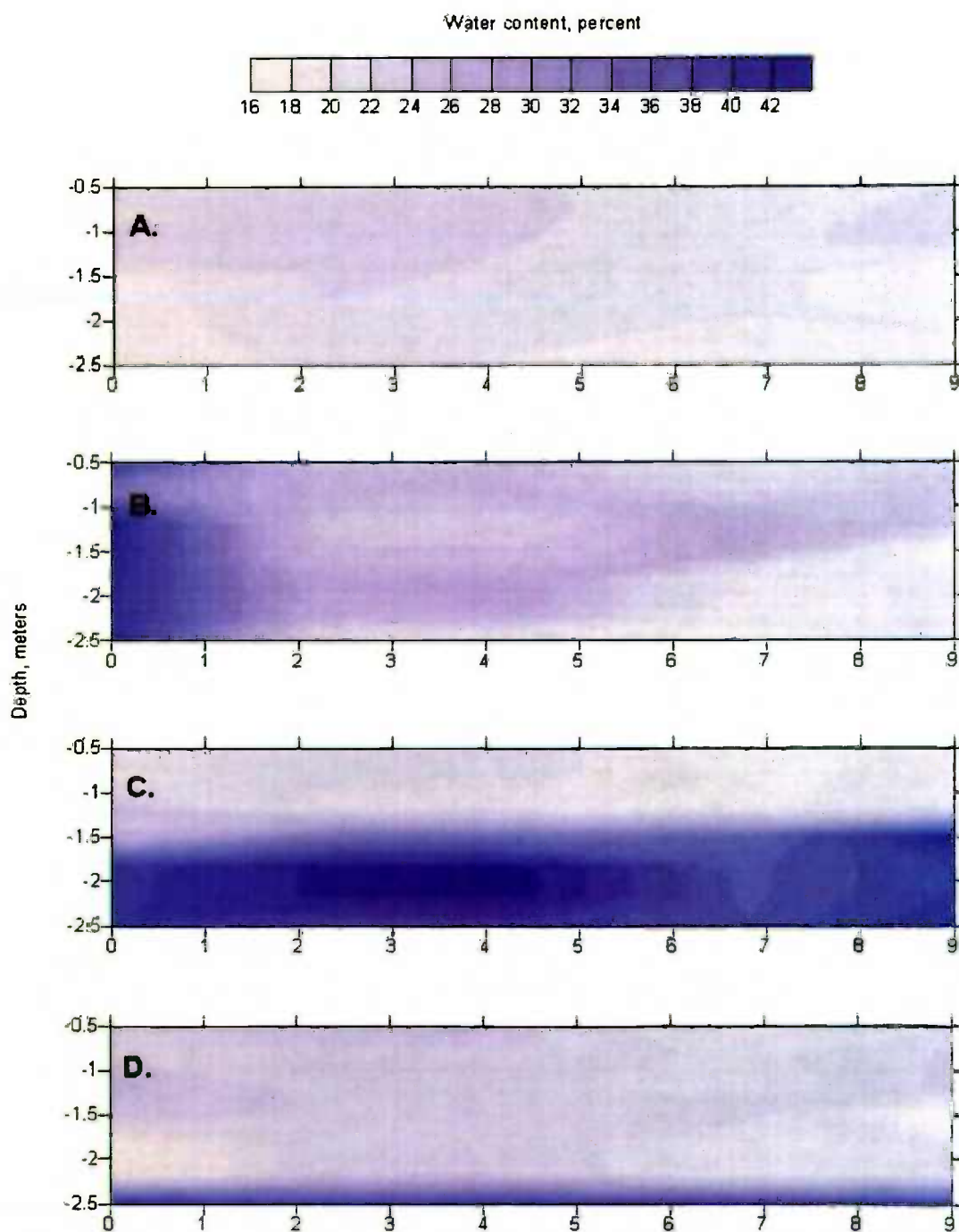


Figure 6. Two-dimensional water-content distribution in sediments beneath Rillito Creek. (A) Soil-water content before the onset of streamflow. (B) Soil-water content 5 minutes after the onset of streamflow. (C) One-dimensional dewatering immediately after the cessation of flow. (D) One-dimensional dewatering approximately 2 days after the cessation of streamflow

One-dimensional simulation results

As discussed in chapter one, temperature and water-content measurements are interpreted using numerical models that describe water flow and heat transport. Multidimensional flow simulations are required to accurately represent infiltration into a heterogeneous medium, such as layered stream channel deposits, and near the margins of the wetted perimeter of the advancing wetting front where capillary flow dominates. However, infiltration is predominantly vertical near the center of streamflow in a homogeneous medium after a period of sustained flow. Infiltration was assumed to be predominantly vertical within the relatively homogeneous stream-channel deposits of Rillito Creek; therefore, simplified one-dimensional model simulations were used. The time from the onset of flow required for predominantly vertical infiltration to occur varies depending on streamflow conditions and the texture of the streambed material. For instance, small braided ribbon flows over fine-grained material may never result in predominantly vertical infiltration, whereas large bank-to-bank flows of coarse-grained material may produce predominantly vertical infiltration beneath the streambed within minutes.

Thermographs predicted by numerical simulations are fitted to measured thermographs from the field by adjusting model parameters within appropriate ranges until the best match is found between simulated and measured thermographs. A typical set of measured Rillito Creek thermographs and the best-fit numerically simulated thermographs are shown in Figure 7. Numerical simulations shown in this chapter are for a bank-to-bank flow event in April 2001. Vertical flow is assumed since temperature changes were

measured predominantly in the vertical direction. Although the simulated and measured thermographs are in general agreement, significant departures exist. Simulated temperatures can differ from measured temperatures for several reasons, such as incorrectly defined boundary conditions, incorrect hydraulic and thermal property assignments, or an inability for a one-dimensional model to represent multidimensional infiltration. In the case of the latter, multidimensional simulations might yield thermographs that are in closer agreement to field data than those shown in Figure 7.

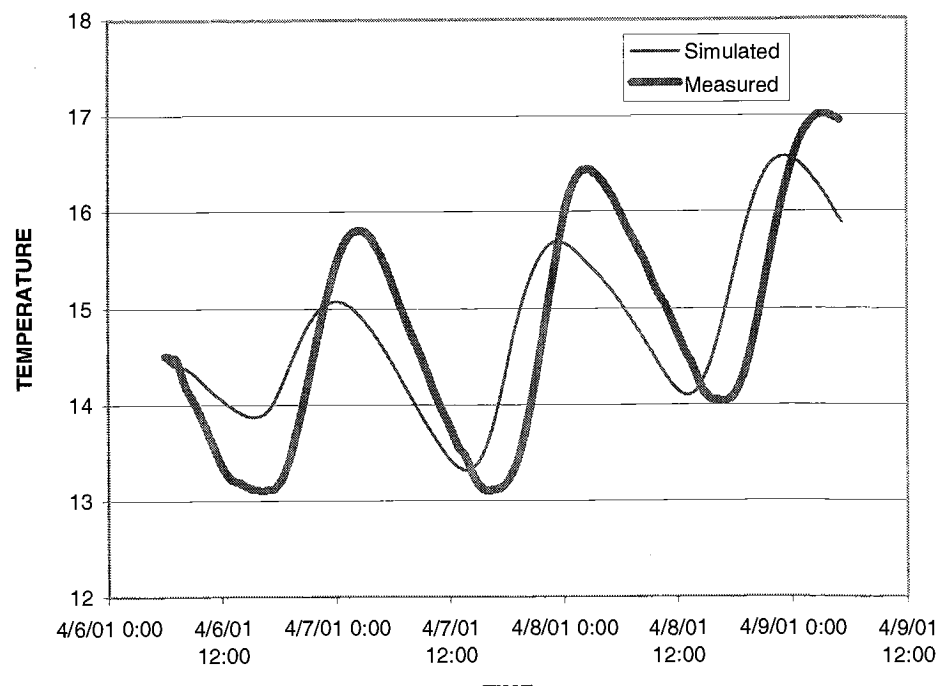


Figure 7. Measured and simulated thermographs ($^{\circ}\text{C}$) at a depth of 0.75 meter, column 3.

An example of simulated thermographs that best match the measured thermographs at 0.75 meter depth in two profiles is shown in Figure 8. There is general agreement

between simulated and measured thermographs. The predicted infiltration rates vary from less than about 0.35 to about 0.39 m/d throughout the two-day flow period (Figure 9). This represents a variation in predicted infiltration rates of less than 10 percent among the four columns, indicating that infiltration was uniform and predominantly vertical. The infiltration rate generally declines as the streamflow event proceeds.

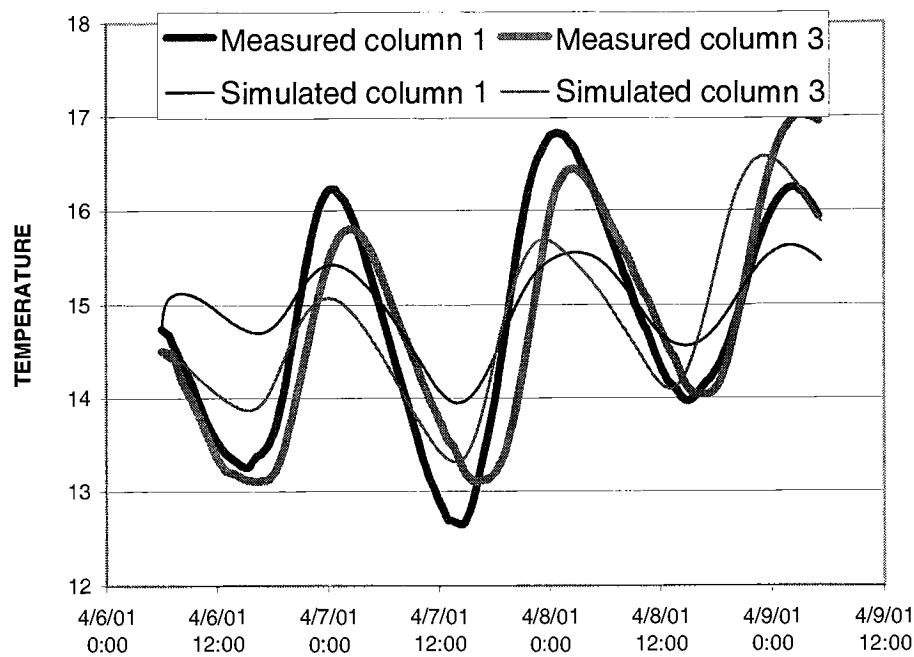


Figure 8. Set of measured and simulated thermographs ($^{\circ}\text{C}$) for two adjacent columns

Discussion

Ground-water recharge is a critical component of the hydrologic cycle. Currently, many areas in the Southwestern United States pump more ground water than is naturally recharged. Current and future artificial recharge sites will become increasingly important in achieving sustainable water supplies. The potential exists to use water-content

measurements and temperature measurements to evaluate the potential suitability of in-stream recharge facilities and to provide guidance on citing such facilities.

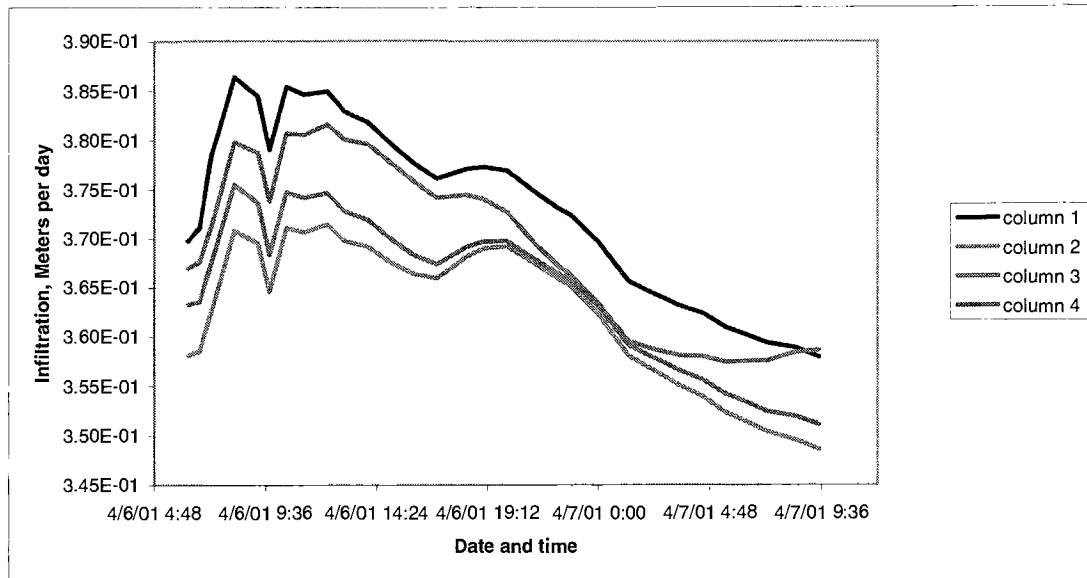


Figure 9. Simulated infiltration rates at columns 1,2,3, and 4 during a streamflow event.

Infiltration rates can be estimated from temperature measurements; these estimates may be complimented by initial infiltration and drainage rate estimates from water-content measurements. The water-content measurements enable better estimates of rapid infiltration rates associated with the onset of streamflow. In Rillito Creek, initial instantaneous rates were estimated to be as high as 3.5 millimeters per second, which included both vertical and lateral flow components that occurred only during the onset of streamflow.

Within several minutes after streamflow has been established, the stream channel deposits become fully saturated and remain so during subsequent flow. For this reason,

temperature measurements are more useful for estimating infiltration rates during streamflow than are water-content measurements. One-dimensional analyses of temperature measurements collected during a streamflow period in April 2001 show that infiltration rates through the Rillito Creek stream deposits were sustained at about 0.37 meter per day; however, there was a general decline in infiltration rate over time during a flow. A decline in infiltration during streamflow events in the Rillito has been recognized using temperature methods by other investigators (Bailey and others, 2000a, b). They attributed this decline to the accumulation of a fine-grained surface layer that effectively clogged the streambed. One of their simulations required a change in the hydraulic conductivity of the shallow streambed sediments during streamflow to reproduce the observed subsurface thermographs. Another set of simulations showed that the hydraulic conductivity of this shallow streambed material changed four orders of magnitude between two sequential streamflow events.

An estimated sustained infiltration rate of about 0.37 meter per day during streamflow agrees well with the estimated post-streamflow drainage rate of 0.46 meter per day. These rates show general agreement with estimates ranging from 0.41 to 0.50 meter per day made by other investigators along Rillito Creek (Burkham, 1970; Lane, 1983; Katz, 1987). The good agreement among these independent measures provides confidence that the temperature method enables accurate estimates of infiltration. As such, vertical arrays of temperature probes can be located along stream reaches to estimate the potential for in-stream recharge and to provide guidance on siting recharge facilities. However, high

infiltration rates at shallow depths are not sufficient to ensure that water can be recharged at a high rate. Generally, the primary constraints on recharge rates are the total amount of water that infiltrates into the subsurface over time and the rate at which that water can move down through the entire subsurface into an aquifer. To estimate potential recharge rates, long-term vertical infiltration rates need to be estimated. Infiltration rates determined from shallow measurements should be considered an upper limit of the potential recharge rate for a particular site.

References

- Anderson, S.R., 1987, Cenozoic Stratigraphy and geologic history of the Tucson basin, Pima County, Arizona: U.S. Geological Survey Water-Resources Investigations Report 87-4190, 20 p., 3 plates
- Bailey, M.A., Ferre, P.A., and Hoffmann, J.P., 2000a, Numerical simulation of measured streambed-temperature profiles and soil hydraulic properties to quantify infiltration in an ephemeral stream [abs.], in American Geophysical Union, 2000 Fall Meeting, December 15-19, 2000, San Francisco, California, supplement to EOS Transactions, vol. 81, no. 48, November 28, 2000, p. F501-F502.

Bailey, M.A., Hoffmann, J.P., and Ferre, P.A., 2000b, Investigation of subsurface variations to quantify infiltration in an ephemeral stream, Tucson, Arizona [abs.], in Geological Society of America 2000 Annual Meeting, Abstracts with Programs, November 13-16, 2000, Reno, Nevada, p. A-185.

Blasch, K.W., Fleming, J.B., Ferre, P.A., and Hoffmann, J.P., 2000, One- and two-dimensional temperature and moisture-content profiling of an ephemeral stream channel in a semiarid watershed [abs.], in American Geophysical Union, 2000 Fall Meeting, December 15-19, 2000, San Francisco, California, supplement to EOS Transactions, vol. 81, no. 48, November 28, 2000, p. F502.

Burkham, D.E., 1970, Depletion of streamflow by infiltration in the main channels of the Tucson basin, southeastern Arizona: U.S. Geological Survey Water-Supply Paper 1939-B, 36 p.

Davidson, E.S., 1973, Geohydrology and water resources of the Tucson basin, Arizona: U.S. Geological Survey Water-Supply Paper 1939-E, 81 p.

Hanson, R.T., and Benedict, J.F., 1994, Simulation of ground-water flow and potential land subsidence, upper Santa Cruz basin, Arizona: U.S. Geological Survey Water Resources Investigations Report 93-4196. 47 p.

Kalin, R.M., 1994, The hydrogeochemical evolution of the groundwater of the Tucson basin with application to 3 dimensional groundwater flow modeling: Tucson, University of Arizona, Ph.D. dissertation, 510 p.

Katz, L.T., 1987, Steady state infiltration processes along the Santa Cruz and Rillito Rivers: Tucson, University of Arizona, unpublished master's thesis, 119 p.

Lane, L.J., 1983, National Engineering Handbook, U.S. Department of Agriculture, Soil Conservation Service, Section 4, Chapter 19, Transmission Losses, 21 p.

Matlock, W.G., and Davis, P.R., 1972, Groundwater in the Santa Cruz Valley, Arizona: Tucson, Technical Bulletin 232, University of Arizona Agricultural Experiment Station, 59 p.

**APPENDIX E: DETERMINING TEMPERATURE AND THERMAL PROPERTIES
FOR HEAT-BASED STUDIES OF SURFACE-WATER GROUND-WATER
INTERACTIONS**

David A. Stonestrom and Kyle W. Blasch

Published in U. S. Geological Circular, *Using Heat as a Tracer for Examining Stream
Exchanges with Ground Water*, September 2003

Introduction

Advances in electronics leading to improved sensor technologies, large-scale circuit integration, and attendant miniaturization have created new opportunities to use heat as a tracer of subsurface flow. Because nature provides abundant thermal signals at the land surface, heat is particularly useful in studying stream-groundwater interactions. This appendix describes methods for obtaining the thermal data needed in heat-based investigations of shallow subsurface flow.

Techniques for measuring temperature have evolved considerably since 1714, when German physicist Gabriel Daniel Fahrenheit introduced the sealed mercury-in-glass thermometer as an improvement over Galileo's alcohol-in-glass thermometer (Star, 1983). The Galilean thermometer, being open to air, also responded to barometric fluctuations. The temperature scale that bears Fahrenheit's name pays tribute to the

significance of solving the long-standing problem of creating an accurate and readily transferable unit of temperature. Swedish astronomer Anders Celsius introduced a water-based, power-of-ten scale shortly after that was later adopted by the Swedish Academy of Sciences as the basis of the metric temperature scale (Kant, 1984). On adoption, the academy wisely reversed Celsius' original assignments of 0 °C and 100 °C, respectively, to the boiling and freezing points of water. Development and linkage of the Celsius scale to the thermodynamically based Kelvin scale paved the way for quantitative theories of heat flow and transformation during the 1800's that formalized the concepts of heat capacity and thermal conductivity. Mathematicians, physicists, and engineers who developed the conceptual framework included such notables as Jean Baptiste Joseph Fourier, James Prescott Joule, and William Thompson (Lord Kelvin). Their work spurred scientific investigations into the thermal behavior of matter that continues today (Lienhard and Layton, 1988).

Industry, government, and other technical organizations publish periodic compendia of temperature-measurement techniques (for example, ASTM, 1993; CSIRO, 1998; Herzfeld, 1962; Schooley, 1982). These works include elaborate and special-purpose techniques for specific applications. The focus here is on practical methods employed in hydrologic investigations. These methods are relatively inexpensive and accurate, and comprise the thermal measurement techniques used in case studies of this circular.

Types and Characteristics of Temperature Sensors

Applications that use heat as a tracer of subsurface flow usually require multiple measurements of temperature through time at relatively inaccessible locations. This requirement generally limits suitable sensors to those that convert temperature to some form of electronic signal. The sensors most often employed are thermocouples (Constantz and Thomas, 1996) and thermistors (LeCain, Lu, and Kurzmack, 2002). Resistance temperature devices (RTDs) and integrated-circuit (IC) sensors can also be used (Paluch, 2002). Figure 1 shows characteristic response curves of these sensors together with main advantages and disadvantages of each. Due to their small thermal masses, all of the sensors in Figure 1 respond quickly to changes in temperature.

Thermocouples are the least expensive and most easily deployed sensor (Figure 1A).

They can be fabricated as needed from thermocouple cable with little more than a soldering tool and wire stripper. Thermocouples operate on the principle, discovered by Thomas Seebeck in 1821, that dissimilar metals in a circuit develop a voltage proportional to the temperature difference between their junctions (Finch, 1962).

Thermocouples are more stable than thermistors but less stable than RTDs. Being self-powered, they are not subject to self-heating effects like thermistors, RTDs, and IC sensors. Of common thermocouple pairs, type T (copper-Constantan) is best suited for hydrologic applications due to its high sensitivity (relative to other thermocouple types) and corrosion resistance. Thermocouples require linearization and measurement of reference-junction temperatures. Linearization and reference circuitry is often integrated

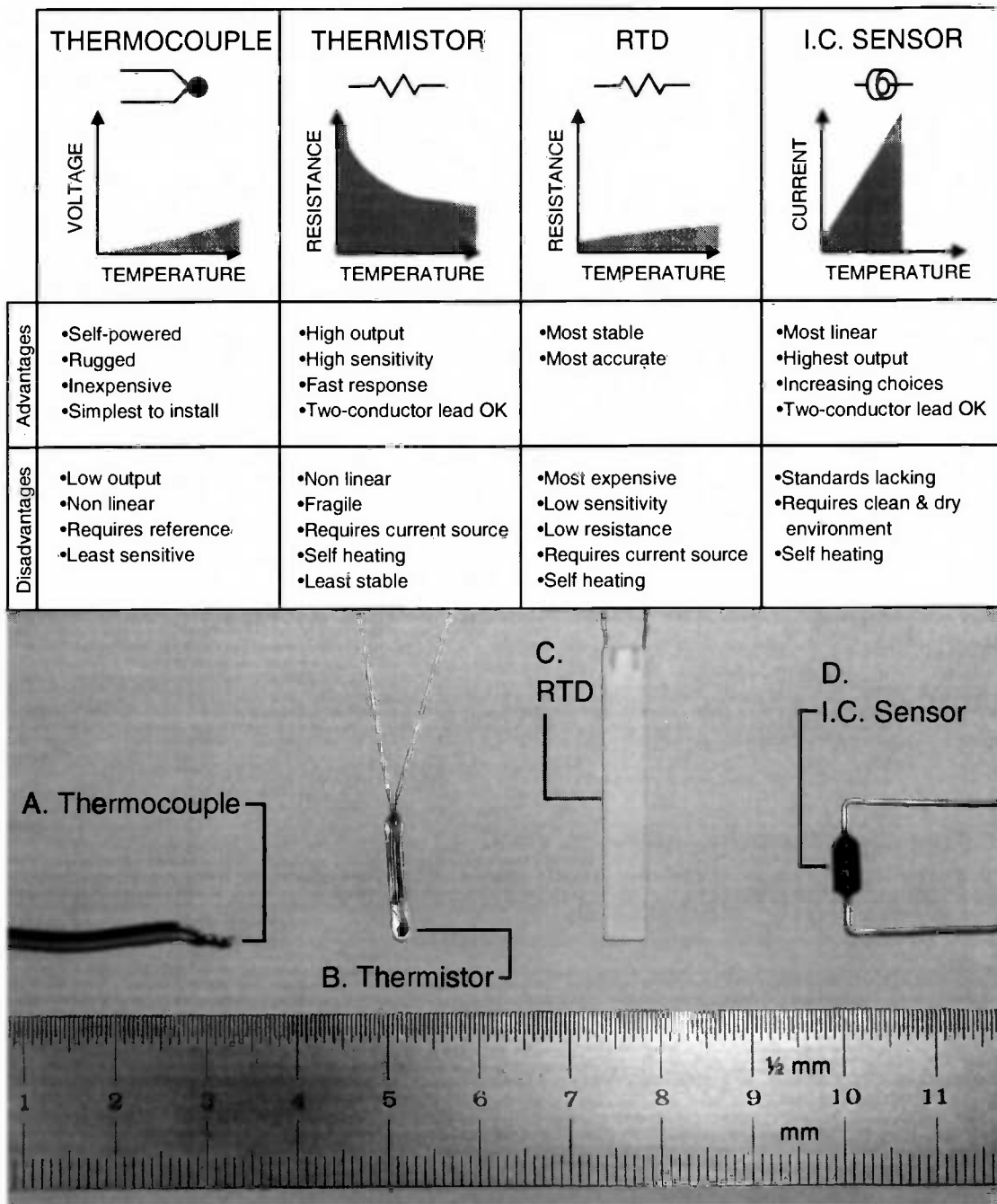


Figure 1. Common electronic temperature sensors with schematic symbols, response characteristics, and advantages and disadvantages of each type (adapted from Hewlett Packard, 1983). RTD and IC are industry acronyms for resistance temperature device and integrated circuit, respectively.

into data-acquisition systems, making thermocouples suitable for multi-point sampling arrays. An important consideration with thermocouples is that their output voltages are small, placing stringent demands on signal-conditioning equipment. A type T thermocouple generates only 0.04 millivolt per °C temperature difference between reference and measuring junctions, requiring the data-acquisition system to resolve four millionths of a volt (0.000,004 V) to detect a 0.1-°C change in temperature. Stray currents in poorly configured systems can cause common-mode (error) voltages much larger than this (Horowitz and Hill, 1989; Morrison, 1998). Another consideration stems from the fact that any error in the reference-junction temperature produces an equal error in the indicated subsurface temperature. Such errors may represent a time-invariant bias common to all subsurface temperature values, with perhaps little consequence on inferred transport. But if the reference junction is even a few millimeters from the reference-temperature measurement point, thermal transients in the data-acquisition system can produce time-varying errors that are on the same order of magnitude as the signal of interest. Isolation of the data-acquisition system from thermal transients, usually by insulating and burying it, is essential for avoiding these errors.

The other commonly deployed sensor is the thermistor. Thermistors are temperature-dependent resistors made from transition-metal oxides (Hewlett-Packard, 1983). They have a large base resistance, typically on the order of 2000 ohms at 20 °C, and a (nonlinear) sensitivity on the order of -10 to -20 ohms °C⁻¹. Thermistors are usually embedded in glass or other material for chemical protection (Figure 1B). Thermistors can

be made to microscopic dimensions, trading off calibration stability for thermal mass. But all thermistors drift with time, requiring periodic calibration (CSIRO, 1998). This becomes a consideration for long-term deployments in inaccessible locations.

Resistance temperature devices (RTDs) have highly stable calibrations even in harsh environments. Figure 1C shows a platinum RTD embedded in a ceramic body. Platinum RTDs are sufficiently stable to serve as calibration-transfer standards in metrology laboratories (Klock and Sullivan, 1962; Morris, 2002). The temperature sensitivity of RTDs is positive, slightly nonlinear, and small relative to thermistors (Figure 1). The relative insensitivity of RTDs, typically $0.04 \text{ ohms } ^\circ\text{C}^{-1}$ for platinum, limits their use to settings with relatively large thermal gradients. Because of their low base resistance (typically 100 ohms at 0°C), RTDs require redundant leads and active compensation for lead-wire resistance. RTDs are also the most expensive of the common sensor types.

IC sensors are based on a semiconductor resistor embedded in an integrated circuit for conversion to a linear electrical output (Figure 1D). Current-output IC sensors require only two wires for connection to data-logging equipment, making them relatively easy to deploy (Sheingold, 1980). Unfortunately, most IC sensors are designed for dry environments, and have relatively short times-to failure in moist environments. IC sensors are actively being developed, and may soon emerge as an advantageous choice for field deployments.

Single-channel temperature loggers offer an alternative to multiplexed sensor installations. Available from various manufacturers, these devices contain a thermistor or thermocouple integrated with signal-conditioning circuitry, a real-time clock, a memory unit, and an optical or infrared interface to provide access by computer or portable data shuttle. Figure 2A shows an example of one such device. Response times are longer than the sensors in Figure 1, but short enough to track most hydrologic signals of interest (Figure 2B). Self-contained devices have the advantage of not needing an external data logger or connecting wires. The user retrieves the devices to obtain data.

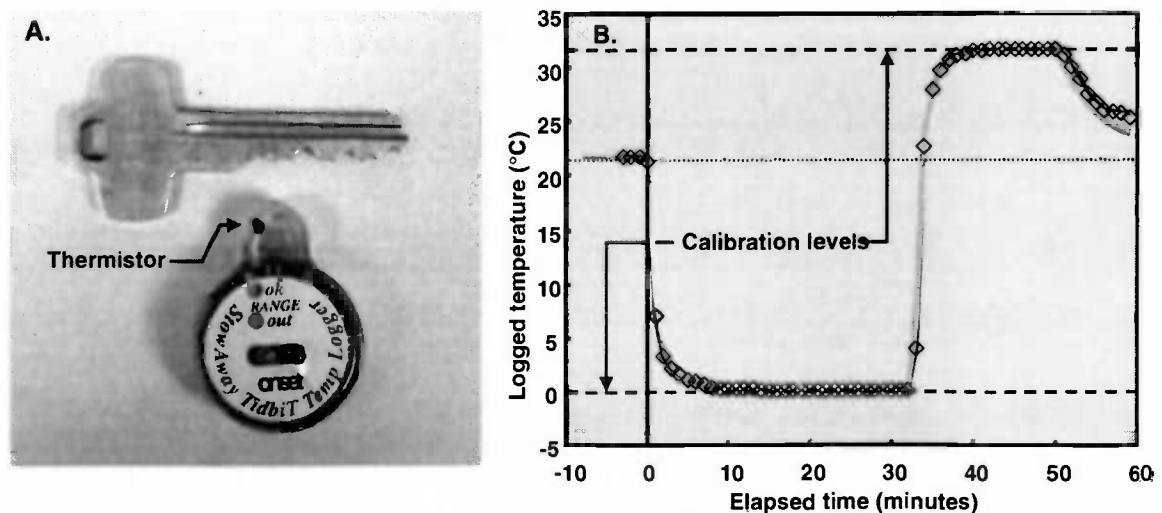


Figure 2. (A) Self-contained temperature logger is about 3 cm in diameter. Note thermistor in mounting eyelet. (B) Dynamic response of four self-contained temperature loggers during calibration tests. Loggers, initially at room temperature, were immersed in a 0°C bath, followed by a 32°C bath. The average 95% response time of the loggers was about 5 minutes. Data sets are color coded. To avoid clutter, individual data points are shown for only one of the loggers.

Specific Heat Capacity, Thermal Conductivity, and Thermal Diffusivity

The thermal properties of soils and sediments can be obtained from literature values, laboratory analysis of field samples, or field measurements. As explained in Chapter 1, thermal properties vary over a much narrower range than do analogous hydraulic properties. Because of this, estimates of water flux are relatively insensitive to errors in thermal properties relative to errors in hydraulic properties (Appendix B). Temperature is often the only thermal parameter measured in the field.

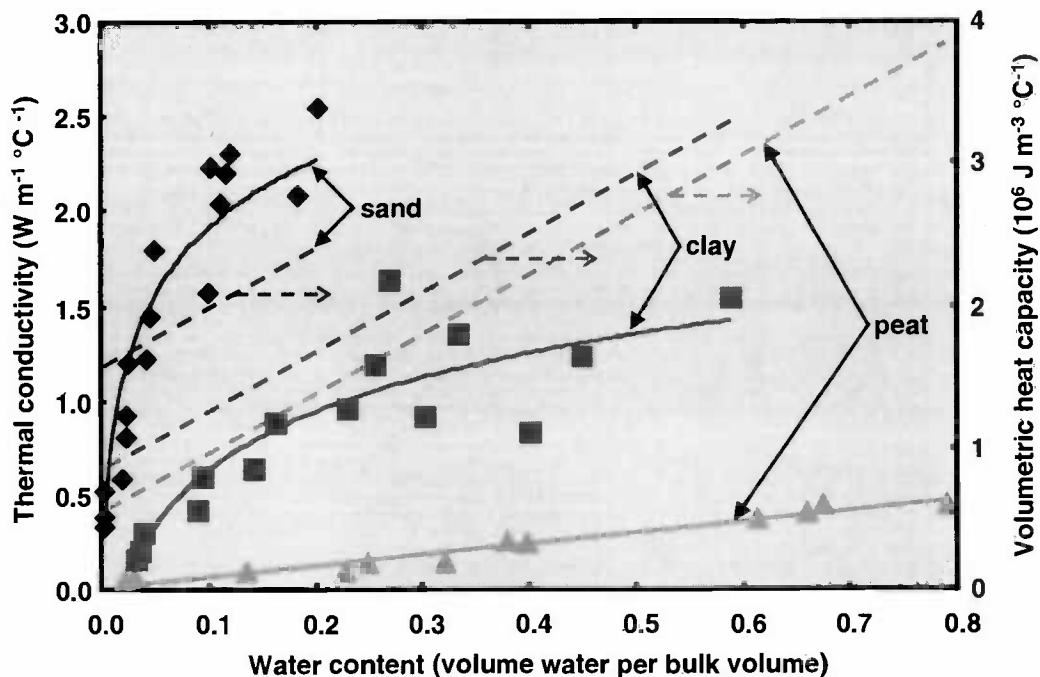


Figure 3. Dependence of volumetric heat capacity and thermal conduction on water-content for selected materials. Dashed lines are volumetric heat capacities calculated as described in the text, using data from Table 1A. Points are experimentally determined thermal conductivities, from DeVries (1966). Solid curves are empirical fits to the thermal-conductivity data.

Specific heat capacity is the amount of heat absorbed or released per mass of material when the material's temperature increases or decreases by a small amount, operationally defined as one degree Celsius ($^{\circ}\text{C}$). Multiplying specific heat capacity by density (mass per unit bulk volume) gives volumetric heat capacity, the change of heat per unit volume of material per unit change in temperature. Units of volumetric heat capacity are joules per cubic meter per degree Celsius ($\text{J m}^{-3} ^{\circ}\text{C}^{-1}$). Heat capacities of relevant phases fall in the order: [liquid water] > [organic solids] > [mineral solids] >> [soil gases] (Table 1A). Heat capacities of porous materials depend on their composition and bulk density, and vary linearly with water content (Table 1B, Figure 3).

Heat capacities of unconsolidated materials can be determined in the laboratory with a calorimeter, which is an insulated chamber equipped with a stirrer and precision thermometer. The method of Taylor and Jackson (1986) determines heat capacity by mixing slurry made from the porous medium with water at a different temperature. The heat capacity of the sediment is calculated from the masses and temperatures of the initial slurry, added water, and final slurry. In practice, heat capacities are more often calculated from the volume-weighted sum of heat capacities of the constituents making up the material, using literature values (de Vries, 1966). Denoting volume fraction as x and heat capacity as c the volumetric heat capacity of the bulk material C_s is approximately

$$C_s = X_w C_w + X_o C_o + X_m C_m + X_a C_a, \quad (1)$$

where subscripts w, o, m, and a denote water, organic solids, mineral solids, and air, respectively.

Table 1A. Thermal properties of selected materials -- Individual phases

Individual phase	Density (10^6 g/m^3)	Volumetric heat capacity ($10^6 \text{ J/m}^3 \text{ }^\circ\text{C}$)	Thermal conductivity ($\text{W/m } ^\circ\text{C}$)	Thermal diffusivity ($10^{-6} \text{ m}^2/\text{s}$)
Air ¹	0.001	0.001	0.024	19
Liquid water ¹	1.0	4.2	0.60	0.14
Ice ²	0.9	1.9	2.2	1.2
Quartz ³	2.7	1.9	8.4	4.3
Average, soil minerals ³	2.7	1.9	2.9	1.5
Average, clay minerals ⁴	2.7	2.0	2.9	1.5
Average, soil organic matter ³	1.3	2.5	0.25	0.10

Table 1B. Thermal properties of selected materials -- Porous media

Porous medium	Bulk density (10^6 g/m^3)	Porosity ($V_{\text{pores}}/V_{\text{bulk}}$)	Water content	Volumetric heat capacity ($10^6 \text{ J/m}^3 \text{ }^\circ\text{C}$)	Thermal conductivity ($\text{W/m } ^\circ\text{C}$)	Thermal diffusivity ($10^{-6} \text{ m}^2/\text{s}$)
Tottori sand ⁵	1.83	0.31	saturated	2.6	2.2	0.85
Clarion sandy loam ⁶	1.38	0.48	saturated	3.2	1.8	0.55
Harps clay loam ⁶	1.21	0.54	saturated	3.2	1.4	0.42
Sandfly Creek sand ⁷	1.50	0.43	dry	1.3	0.25	0.18
Yolo silt loam ⁸	1.30	0.51	dry	1.1	0.26	0.23
Clarinda clay ⁷	1.16	0.56	dry	1.2	0.18	0.15
Snow ⁹	0.46	0.50	dry	1.0	0.71	0.68
	0.73	0.80	dry	0.4	0.13	0.36
	0.87	0.95	dry	0.1	0.06	0.60

Sources

- 1 Carslaw and Jaegger, 1959, p. 497. 6 Ren, Kluitenberg, and Horton, 2000.
 2 van Wijk and de Vries, 1966a, p. 40. 7 Bristow, Kluitenberg, and Horton, 1994.
 3 van Wijk and de Vries, 1966b, p. 105. 8 Wierenga, Nielsen, and Hagan, 1969.
 4 de Vries, 1966, p.210. 9 van Wijk and de Vries, 1966b, p. 110.

Thermal conductivity, κ_s , is a measure of a material's ability to conduct heat. It is defined as the amount of heat transmitted per unit time per unit area per unit temperature gradient. Units of thermal conductivity are watts (joules per second) per square meter, per degree Celsius per meter ($\text{W m}^{-1} \text{ }^\circ\text{C}^{-1}$). The thermal conductivity of porous materials

depends upon the composition and arrangement of the solid phase. Coarse-grained materials generally have higher thermal conductivities than fine-grained materials. Also, because water conducts heat much better than air, thermal conductivity depends strongly on water content (Table 1A and B, Figure 3). Due to the complexities of pore geometry, this dependence is non-linear and difficult to predict (Wierenga, Nielsen, and Hagan, 1969). In practice, empirical equations can be used to fit measured thermal-conductivity data over limited ranges of water content (Hopmans, Simunek, and Bristow, 2002).

Thermal conductivities of porous media can be measured using steady-state or transient-state methods (Jackson and Taylor, 1986). Steady-state methods facilitate testing of Fourier's law, which is almost universally assumed to govern heat conduction (Carslaw and Jaeger, 1959). Maintaining a thermal gradient in moist materials, however, induces fluid flow along temperature and density gradients. Fluid flow complicates the measurement of thermal conductivity because advection as well as conduction transfers heat. In partly saturated media, latent heat transfer (that is, heat associated with vapor-liquid and liquid-vapor transitions) may also be important. Water contents in partly saturated media become non-uniform when temperature gradients are maintained. To avoid complications associated with these processes, rapid transient-state methods have been developed for measuring thermal conductivities in moist materials. The pulsed cylindrical-heat-source method (also known as the pulsed thermal-probe method; described below), is the most commonly used transient method for measuring thermal

conductivities in both field and laboratory applications (de Vries, 1952; Jackson and Taylor, 1986; Shiozwa and Campbell, 1990; Wierenga, Nielsen, and Hagan, 1969).

Thermal diffusivity is the ratio of thermal conductivity to volumetric heat capacity. The units of thermal diffusivity are meters squared per second ($\text{m}^2 \text{s}^{-1}$). Thermal diffusivity is a measure of how quickly an imposed change in temperature is transmitted through the material. Air has a large thermal diffusivity, despite having a low thermal conductivity, because its volumetric heat capacity is small (Table 1A). With almost no capacity for storing or releasing heat, temperature signals travel quickly through air.

Jackson and Taylor (1986) described a method for direct determination of thermal diffusivities of soils and sediments. The method entails analyzing transient temperatures within a sample as heat is applied to its boundary through a copper plate. The method, while relatively simple, is difficult to apply outside the laboratory. Recent advances in the pulsed thermal-probe method have produced field-deployable probes that simultaneously determine various combinations of heat capacity, thermal conductivity, and thermal diffusivity (Bristow, Kluitenberg, and Horton, 1994; Campbell, Calissendorff, and Williams, 1991; Hopmans, Simunek, and Bristow, 2002; Kluitenberg, Bristow, and Das, 1995). These techniques apply heat-pulse theory to cylindrical probes made from hypodermic-needle tubing. One probe contains a heater. Parallel to this probe are one or more auxiliary probes for measuring temperature responses. Pulses of heat induce changes in surrounding temperatures measured by auxiliary probes. Analytical or

numerical analyses of the temperature histories produce estimates of thermal properties. Pulsed thermal probes have been combined with time-domain-reflectometry probes for simultaneously measuring thermal properties, water content, and bulk electrical conductivity (Noborio, McInnes, and Heilman, 1996; Ren, Noborio, and Horton, 1999).

Sensor Deployment and Data Acquisition

A pipe driven into loose sediments can provide a temporary casing while sensors are deployed to desired depths. The sediments collapse around the wires as the pipe is withdrawn (Figure 4A, B, and C). To avoid induced preferential flow, intervals between sensors can be grouted with swelling clay (Nielsen and Sara, 1992) or expanding foam (Faybishenko, 2000). These materials are emplaced through the temporary casing as the casing is withdrawn. Proper grouting is required in cohesive soils and sediments. To minimize disruption of sedimentary layers and soil structures, sensors can be installed through holes that slant diagonally beneath the study area or extend horizontally from an adjacent access point (Faybishenko, 2000). Wires connecting streambed sensors to remote data loggers need to be deeper than the maximum depth of scour. Conduit anchored to the streambed can help protect wires. Deploying a precision temperature reference on the wiring panel can reduce reference-junction errors. A thermally conductive strip on the wiring panel minimizes temperature offsets between the reference junction and reference-junction temperature measurement. Burial of loggers in watertight containers that are packed in thermal insulation can further reduce errors from temperature transients (Figure 4D and E).

Self-contained temperature loggers can be buried directly in the ground (with or without protective housings) or deployed in access tubes. Directly buried loggers in stream channels usually have housings that are tethered to anchors driven into the channel upstream of the measurement point (Figure 4F). Access tubes need to be grouted to prevent preferential flow down the annular space around the tube (Figures 4H-J). Baffles inhibit thermally induced advection (Figure 4L). In addition to the self-contained temperature loggers, figures 4G-L also show external thermocouples on moveable arms that were pulled against the surrounding sediments after the access tube was lowered into position. The two-component expanding foam that grouted the annular space locked the arms into position as it hardened (Figure G-J).

Design of Temperature-Measurement Arrays

Success of thermal methods for quantifying surface-water ground-water exchanges is dependent on appropriate placement of temperature sensors. Appropriate placement depends on hydraulic and thermal properties of the sediments, climatic conditions (which determine the nature of thermal forcing), anticipated pore-water velocities, and practical considerations such as depth of scour. Experimental design includes frequency of data collection. While the overall design will be dictated by the purpose of the study, standard principles of experimental design should be considered at every level of detail (Garcia-Diaz and Phillips, 1995). In large-scale projects, formalized data-quality objectives can lead to efficient measurement designs (USEPA, 2000).

Preliminary modeling is useful for selecting measurement locations and frequencies (Constantz, Stonestrom, and others, 2001). Fluid flow modulates the transmission of thermal signals into the profile (Silliman, Ramirez, and McCabe, 1995; van der Kamp and Bachu, 1989). Fluid flow can thus be determined by the departure of temperatures from a purely conductive pattern (Constantz and Thomas, 1996; Silliman and Booth, 1993). To guide sensor placement, theoretical temperature patterns can be predicted from numerical solutions of the coupled transport equations. For simple cases, theoretical temperature patterns can also be predicted from analytical solutions. The analytical solution for pure thermal conduction in a deep, uniform profile with sinusoidal heating at the land surface is (Carslaw and Jaeger, 1959)

$$\Delta T(z,t) = A \cdot e^{-z/D} \cdot \sin[(2 \pi /P)(t-t_0)-(z/D)], \quad (2)$$

where ΔT is the departure of temperature from its average value, z is depth, t is time, A is the amplitude of the surface temperature, D is the damping depth, P is the period of the surface temperature, and t_0 is the time at which ΔT equals zero. The damping depth D is equal to $(P\alpha/\pi)^{-1/2}$, where α is the thermal diffusivity.

Daily and annual temperature fluctuations imposed at the land surface are roughly periodic. As periodic diurnal temperature waves move into a profile, the energy stored and released by the conducting medium attenuates the signal as it propagates away from

the boundary. In consequence, the magnitude of periodic temperature perturbations decreases with depth. The depth below which cyclic surface fluctuations of a given magnitude have no measurable effect depends on the period of the fluctuations, the velocity of subsurface fluid flow, and the precision and accuracy of the temperature measurements. For the purely conductive case, the depth D at which daily temperature fluctuations are damped 63% ($= 1 - e^{-1}$), is approximately 0.08 m in dry sand and 0.14 m in wet sand (van Wijk and de Vries, 1966b). Damping depths increase in direct proportion to the square root of the period of fluctuations. Damping depths for annual fluctuations are thus roughly 19 times ($= 365^{-1/2}$) greater than their diurnal equivalents. Damping depths for annual fluctuations (again, in the absence of fluid flow) are about 1.5 m in dry sand and 2.7 m in wet sand. Downward movement of water increases the apparent damping depth; upward movement decreases it. Instruments used for recording temperatures in field installations typically have resolutions ≥ 0.01 °C and accuracies ≥ 0.1 °C. The maximum depth to which annual temperature cycles are resolvable is usually about 10-15 meters.

Temperature sensors need to be located within the thermally active zone for studies of surface water-ground water exchanges. Depending on the requirements of the study, sensors can be placed at uniform-depth increments, exponentially increasing increments, or according to stratigraphy or other hydrogeologic feature. Multi-dimensional arrays of sensors allow assessment of heterogeneity and lateral flow. Multiple sensors at the same

location, possibly of different types, can reduce uncertainty and provide insurance against sensor failure.

In conclusion, an increasing variety of techniques are becoming available for measuring temperature and even thermal properties in field settings. These techniques enable the use of heat as a tracer of exchanges between surface water and ground water. As sensors and data-acquisition systems continue to develop and come onto the market, instrumentation costs should continue to decrease while the number and quality of options improves. Thermal techniques are providing increasingly useful information about surface water-ground water interactions and related hydrologic processes.

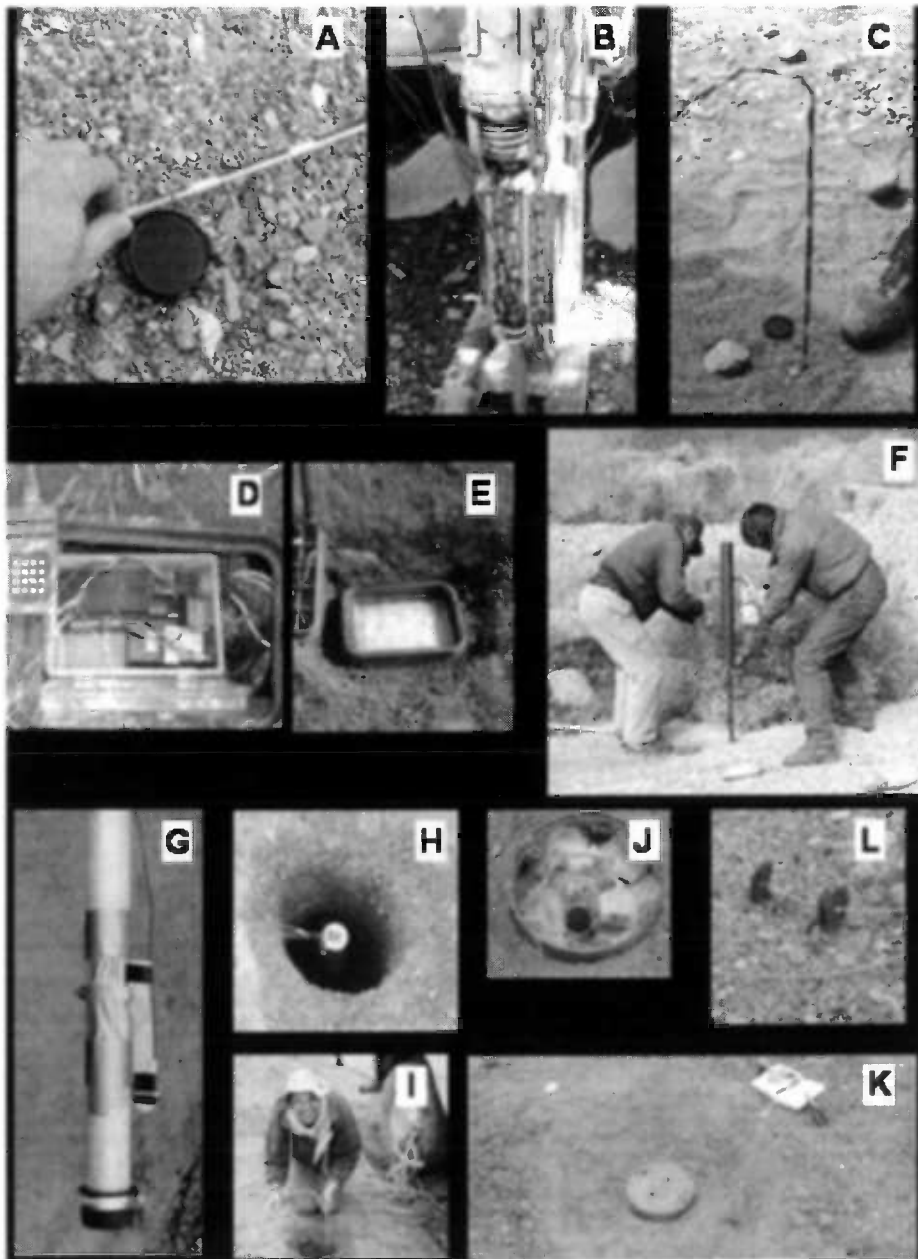


Figure 4. Field deployment of temperature-measuring equipment. (A,B,C) Installation of thermocouple sensors in a stream channel. (D,E) Data logger for thermocouple installation. (F) Installation of stream-bed sensor. (G) Swing-out thermocouple arm on access tube. (H) Top of access tube prior to grouting. (I) Grouting access tube with two-component foam. (J,K) Access-tube enclosure at channel surface. (L) Single-channel temperature logger on cable for suspension in access tube. Foam baffles on either side of logger prevent advection. See text for additional explanation

References

- ASTM, 1993, Annual Book of ASTM Standards, Vol. 14.03: Temperature Measurement: West Conshohocken, Pennsylvania, American Society for Testing and Materials, 502 p.
- Bristow, K.L., Kluitenberg, G.J., and Horton, R., 1994, Measurement of soil thermal properties with a dual-probe heat-pulse technique: *Soil Sci Soc Am J*, v. 58, p. 1288-1294.
- Campbell, G.S., Calissendorff, K., and Williams, J.H., 1991, Probe for measuring soil specific heat using a heat-pulse method: *Soil Sci Soc Am J*, v. 55, p. 291-293.
- Carslaw, H.S., and Jaeger, J.C., 1959, *Conduction of Heat in Solids* (2nd ed.): New York, Oxford University Press, 510 p.
- Constantz, J., and Thomas, C.L., 1996, The use of streambed temperature profiles to estimate the depth, duration, and rate of percolation beneath arroyos: *Water Resources Research*, v. 32, no. 12, p. 3597-3602.
- Constantz, J.E., Stonestrom, D.A., Stewart, A.E., Niswonger, R.G., and Smith, T.R., 2001, Analysis of streambed temperatures in ephemeral channels to determine streamflow frequency and duration: *Water Resources Research*, v. 37, no. 2, p. 317-328.
- CSIRO, 1998, *Handbook of Temperature Measurement*: New York, Springer Verlag, 3 v., 400 p.
- de Vries, D.A., 1952, A non-stationary method for determining thermal conductivity of soil in situ: *Soil Science*, v. 73, p. 83-89.

_____1966, Thermal properties of soils, in van Wijk, W.R., ed., Physics of Plant Environments.

**APPENDIX F: PROCESSES CONTROLLING RECHARGE BENEATH
EPHEMERAL STREAMS IN SOUTHERN ARIZONA**

Kyle Blasch, Ty P.A. Ferré, John Hoffmann, Donald Pool, Matthew Bailey, and Jeffrey Cordova

Accepted for Publication in the American Geophysical Union Monograph Series,
Recharge and Vadose-Zone Processes: Alluvial Basins of the Southwestern United States, June 2003

Abstract

Recharge beneath ephemeral streams in southern Arizona (USA) has been a focus of investigation for many years because of its importance for continued replenishment of subsurface reservoirs. Combined hydrological, geophysical, and isotopic methods were used to monitor the transport of water within ephemeral streams and through their underlying sediments. Previous studies were reviewed to assess processes controlling recharge beneath ephemeral streams in southern Arizona. Sediment permeability and clogging of pores had a significant influence on streamflow transmission losses. Scour and deposition of surface sediments caused permeability values to vary by as much as four orders of magnitude between streamflow events. Multidimensional flow in the channel sediments was characteristic at the onset of a streamflow event, and transitioned during the event to unidirectional vertical flow. Continued redistribution of water through

the unsaturated zone and mounding at the water table were measured using isotopic and thermal methods. Long-term precipitation and streamflow measurements within the Tucson Basin provided evidence of the dynamic nature of channel recharge. Channel infiltration losses increased from 1933 until 1999. Seasonal fluctuations in channel losses indicated that annual recharge rates and empirical equations based on uniform coefficients may not be suitable for computing long-term recharge.

Introduction

Recharge to aquifers within alluvial basins of the southwestern United States may occur through infiltration of precipitation directly through the basin floor (Gee et al., 1994), infiltration from irrigation and municipal returns, and seepage losses through stream channels. In the semiarid regions of southern Arizona, diffuse infiltration of precipitation through the basin floor is considered the smallest component of total recharge owing to limited precipitation in comparison to evapotranspiration (Scott et al., 2000; Walvoord and Scanlon, 2003). For instance, daily evaporation and precipitation rates measured in the Tucson Basin, Arizona, from 1991-2002 indicate that on average the precipitation rate exceeded the evaporation rate 25 days per year. Additionally, depth to ground water in alluvial basins can be hundreds of meters, which provides ample opportunity for storage of infiltrated water. Because of these environmental conditions, concentrated infiltration repeated over time within the same channel reaches or recharge basins is often necessary for recharge to occur. For example, repeated incidental recharge comprised of irrigation return flows from agriculture, golf courses, and green belts, and municipal return flows,

such as treated effluent, can represent a significant source of basin recharge. Within the Tucson Basin, incidental recharge accounts for about 15 to 30 percent of the total recharge (Hanson and Benedict, Table 1, pages 8-9, 1994; Galyean, 1996).

Channel recharge consists of localized infiltration of streamflow along perennial, ephemeral, and intermittent streams. Where streams flow over areas with a high water table, the stream and aquifer can be connected hydraulically and continually exchange water. Perennial streams that are connected hydraulically to an underlying unconfined aquifer can control the elevation of the water table in the aquifer by acting as a drain when ground-water levels are high, and as a source when ground-water levels are low. Ground-water withdrawals from alluvial aquifers can increase the vertical hydraulic gradient below streams and increase recharge from perennial streams (Theis, 1940). In the extreme case, ground-water pumping will cause stream infiltration losses to equal discharge, and the stream will become ephemeral. Historical demands for ground water and surface water in populated basins within the Southwest, including the Tucson Basin, have transformed many perennial reaches of streams into ephemeral reaches; thus, the fraction of recharge attributed to ephemeral stream channels is increasing (Anderson et al., 1992). As this recharge component increases in significance, an improved understanding of the processes controlling recharge is needed for effective management of the surface-water and ground-water resources.

Ephemeral streams vary widely in their physical and hydrologic characteristics (Wilson et al., 1980; Lerner et al., 1990; Anderson et al., 1992). Streams that originate near mountain fronts may flow over thick alluvial valleys and lose hydraulic connection with the underlying aquifer so that they are ephemeral in their lower reaches. In many basins of the Southwest, such as the Tucson Basin, streams originating at higher elevations coalesce downstream to form higher order ephemeral streams. In contrast, streams such as those draining Vicee Canyon (Nevada), originate as single channels along the mountain front and fan out into lower order channel or disperse as braided channels, and eventually terminate as unbounded channels (Maurer and Fischer, 1988). Underlying many of these ephemeral mountain-front streams is coarse-grained stream-channel deposits that overlie basin-fill deposits. Coarse-grained stream-channel deposits characteristically have a higher permeability that enables high infiltration rates (Anderson et al., 1992; Hanson and Benedict, 1994; Hoffmann et al., 2002.) The depth to regional aquifers underlying ephemeral channels can vary from a few meters to tens of meters (Anderson et al., 1992; Hoffmann et al., 2002). Although depth to water can vary substantially, depths are usually shallower in the upper reaches near the mountain fronts than in the lower reaches (Anderson et al., 1992; Hoffmann et al., 2002).

The amount of water flowing in ephemeral channels, and therefore available for recharge, is primarily related to precipitation frequency, distribution, and intensity, as well as to spring discharge and basin/channel runoff characteristics. The temporal distribution of flow in ephemeral streams can be highly variable and includes monthly and decadal

oscillations (Webb and Betancourt, 1992). Because of this, ephemeral channels present particular difficulties in estimating or predicting recharge rates on the basis of limited temporal observations. The objective of the following discussion is to review a series of investigations primarily focused on ephemeral channel recharge in southern Arizona that have been completed within the past two decades. This review is not intended to be comprehensive, nor does it provide a chronology of channel recharge literature from its inception. Rather it is meant to augment existing introductions to ephemeral recharge (Smith, 1910; Wilson and DeCook, 1968; Freeze, 1969 and 1970; Wilson et al., 1980; Lerner et al., 1990.)

Recharge Theory

Infiltration is defined as the flow of water from above ground into the subsurface, whereas recharge is defined as the positive downward flux of water across the regional water table. Infiltration can lead directly to recharge if the wetting front crosses the water table during surface flow. Alternatively, water can infiltrate into the subsurface and then cross the water table during redistribution, long after surface flow ends.

During an ephemeral flow event, the stream channel surface is quickly saturated and a positive pressure head, equal to the stream stage, is exerted at the channel boundary (Freyberg et al., 1980). The flux, q (LT^{-1}), across the ground surface in response to a constant pressure head applied at the ground surface, Ψ_0 (L), can be expressed as:

$$q = -K_s \frac{\psi - \psi_0 - z_f}{z_f} \quad (1)$$

where K_s is the saturated hydraulic conductivity of the medium (LT^{-1}), z_f is the depth of the wetting front (L), and ψ_f is the pressure head at the wetting front (L). The velocity of the wetting front, v_f (LT^{-1}), can be expressed as:

$$v_f = \frac{q}{\theta_s - \theta_a} = -K_s \frac{\psi_f - \psi_0 - z_f}{z_f (\theta_s - \theta_a)} \quad (2)$$

where θ_s is the saturated volumetric water content (L^3L^{-3}) and θ_a is the antecedent volumetric water content (L^3L^{-3}). Integrating this expression gives an expression similar to that developed by Green and Ampt (1911) that defines the time, t , at which the wetting front will have advanced to a depth, z_f , as:

$$t = \frac{(\theta_s - \theta_a)}{K_s} \left(z_f + (\psi_f - \psi_s) \ln \left(1 + \frac{z_f}{(\psi_s - \psi_f)} \right) \right) \quad (3)$$

For a given water table depth, z_{wt} (L), if the time, t , determined using the previous expression is less than the duration of a streamflow event, then the wetting front will cross the water table during the flow event. The higher the initial water content, the faster the wetting front will progress. In addition, the wetting front will progress more slowly through media with lower K_s values. Finally, closer examination of the above expression shows that the rate of advance of the wetting front is highest initially, when

the distance from the channel surface to the wetting front is smallest, because this leads to the highest overall pressure head gradient. After the wetting front has progressed away from the surface, the pressure gradient becomes small and gravity dominates infiltration. The rate of advance of the wetting front eventually decreases to a constant value of $K_s/(\theta_s - \theta_i)$. Should it be $K_s/(\theta_s - \theta_i)$? For most natural systems it is likely that the saturated water content, the antecedent water content, and the saturated hydraulic conductivity will vary with depth.

Once streamflow ceases, the water that has infiltrated into the subsurface continues to redistribute both vertically and horizontally. This stored water will either remain in storage until it is displaced by a later infiltration event, continue to drain across the water table, or it may be removed through evapotranspiration (Walvoord and Scanlon, 2003). The rate of drainage across the water table depends on the distribution of water in the unsaturated zone and the degree of fluctuation of the water table elevation in response to recharge. In general, if the water content is high from the surface to the water table, the initial recharge rate will be high and recharge will continue for a long period. If, however, the wetting front only reaches a shallow depth, the infiltrated water may redistribute during drainage without reaching the water table.

The preceding discussions have focused on simplified, one-dimensional, vertical infiltration through a single-layer homogenous soil and a constant head at the surface. Although this representation may be applicable for some ephemeral channels,

multidimensional, variable flow beneath channels must be considered as a possibility owing to heterogeneity of the subsurface media and fluctuating streamflow depth (Freyberg et al., 1980). A complete discussion of the effects of heterogeneity and fluctuating heads on infiltration through variably saturated soil is beyond the scope of this discussion; however, it is important to understand how multidimensional flow can change the amount and distribution of subsurface water storage following a streamflow event. Specifically, with the addition of lateral, capillary-dominated flow at the edges of a streambed, more water must flow into the subsurface to achieve the same depth of advance of the wetting front. The additional influx is stored near the ground surface and near the margins of the stream. These effects will increase the path length that infiltrating water must travel to reach the water table and lead to variability in the horizontal distributions of water storage in the vicinity of the stream channel.

Ephemeral Channel Recharge

For the purposes of this review, water movement beneath ephemeral streams is characterized as infiltration at the onset of streamflow, infiltration during streamflow, or redistribution following streamflow.

Infiltration at the Onset of Streamflow

At the onset of flow, infiltration into the channel sediments is primarily a function of input discharge within the channel, the channel sediment properties, and antecedent

moisture content. The leading wave of an ephemeral flow event typically originates as a thin trickle within the channel; however, intense precipitation and environments conducive to high runoff factors can produce immediate bank-to-bank flow conditions. The distance that the streamflow surface wave travels downstream and the speed at which it progresses is related to the slope of the streambed or the alluvial fan, volume of water entering the channel, and amount of water seeping into the underlying sediments. If the rate of streamflow exceeds the rate of water flow into the sediments, the leading wave will continue to travel downstream. Streamflow in highly braided or wide channels, which have greater wetted perimeters and therefore greater access to infiltration pathways and subsurface storage, will generally lead to more infiltration than in a stream confined primarily to a narrower channel (Rohwer and van Pelt Stout, 1948; Guzman et al., 1989).

The speed and magnitude of the surface wave will decrease as the wave passes along stream reaches that are conducive to infiltration. Materials lining the channels that have low-permeability, such as bedrock, cobbles and boulders, or fine-grained sediments, will reduce the transmissivity of the surface sediment, and the flow front will progress at a faster rate. Swelling of colloidal sediments can decrease pore sizes, which results in decreased infiltration rate at the channel surface (Knighton and Nanson, 1994).

Ephemeral streamflow that entrains large amounts of sediment and organic matter, such as runoff from high intensity rainfall, can cause increases in bed sediment clogging (Wilson et al., 1980). Infiltration can be reduced at the channel surface even in coarse-grained alluvium if the pores become clogged during streamflow (Wilson et al., 1980).

Clogging of pores also occurs from growth of microbial flora. This biotic process is more common in artificial recharge ponds, but has been observed in ephemeral channels containing return flow from effluent and gray water. During an investigation of the Santa Cruz River within the Tucson Basin, long-term, low-magnitude discharge of effluent increased accumulation of biotic organisms and surface armoring (Lacher, 1996). Surface armoring reduced the hydraulic conductivity over a 6-month interstorm period from 37 mm/h to 11 mm/h. High intensity, erosive flows were required to remove the surface accumulation and increase infiltration.

Reductions in fluid and bed sediment temperatures increase the fluid's dynamic viscosity as well as the fluid density. The changes in fluid properties result in an overall decrease in hydraulic conductivity and increase in surface tension reducing infiltration and extending the streamflow terminus (Constantz et al, 1994; Ronan et al., 1998). Additionally, scour holes and side pools along the channel can store large portions of the flow and thereby reduce the extent to which the stream terminus will travel.

Infiltration at the onset of streamflow is often multidimensional as the wetting front travels both downward, transverse to, and along the channel. As an example, water content measurements within the bed sediments of Rillito Creek, Tucson, Arizona, showed a multidimensional progression of infiltration into the stream channel sediments with lateral flow velocities nearly as large as vertical flow velocities at the onset of streamflow (Blasch et al., 2000, Hoffman et al., 2003).

Infiltration During Streamflow

After the initial onset of streamflow, a typical hydrograph will show an increase in discharge often leading to increased stages, head gradients, and wetted perimeters. Generally, low-flows are confined to a primary channel, whereas larger flows can produce overbank flow and inundation of flood-plain sediments. The hydraulic conductivity of the flood-plain sediments will determine the infiltration rate during these flood events. Bank stabilization is used in communities in southern Arizona to contain large flows and minimize channel migration. Application of impermeable surfaces to the banks and channel bottoms decreases vertical and lateral infiltration rates, which reduces the potential for recharge at these locations while increasing flow velocities and streamflow extent (Guzman et al, 1989).

Following the work of Constantz (1998), Constantz et al. (2002) and Ronan et al. (1998), Bailey (2002) estimated infiltration rates along Rillito Creek by using temperature monitoring and inverse simulation of heat and water transport through stream sediments. Through a numerical sensitivity analysis of the advection-dispersion equation and a non-linear form of Darcy's law, Bailey (2002) showed that vertical fluid transport during streamflow is more sensitive to the hydraulic conductivity of the streambed than to stage. In addition, modeling of two sequential streamflow events showed that the hydraulic conductivity of the streambed surface layer changed by four orders of magnitude. During one of the events, the hydraulic conductivity changed by two orders of magnitude

resulting from the redistribution of sediments. Maurer and Fischer (1988) observed similar fluctuations in the infiltration rate between events owing to changes in the permeability caused by deposition at the end of the first event.

Redistribution Following Cessation of Streamflow

After streamflow in the channel ceases, subsurface sediments lose stored water through redistribution and evapotranspiration. Factors affecting the rate and pattern of redistribution typically include duration of flow, time between successive flows, subsurface layering, sediment properties, and patterns and rates of water loss to evapotranspiration. Redistribution of water following prolonged infiltration through a virtually homogeneous medium is generally assumed to be gravity dominated and to occur at a near constant vertical rate throughout the subsurface. Measurements made at shallow depths beneath the bed of Rillito Creek, however, show an atypical drainage pattern (Figure 1) in that the rate varies with depth at any given time (Blasch et al., 2000, Hoffman et al, 2003). The rate of advance of this drainage front determined from subsurface water-content data is about 0.005 mm/s, which compares well with the rate of infiltration during streamflow of about 0.004 mm/s determined using heat and fluid transport modeling (Blasch et al., 2000, Hoffman et al, 2003).

Flow paths of redistributing water are influenced primarily by the subsurface distribution of sediment hydrologic properties and determine the rate and direction of travel of percolating water (Renard et al., 1964). Bostick (1978) used stable-isotope data from

wells near channels in the Tucson Basin to determine the distance recharged water travels away from the channel. He was able to distinguish recharged water up to 3.2 km from the source and determined that percolating waters from the channel formed a mound at the water table that caused the water to travel a longer horizontal distance than vertical distance.

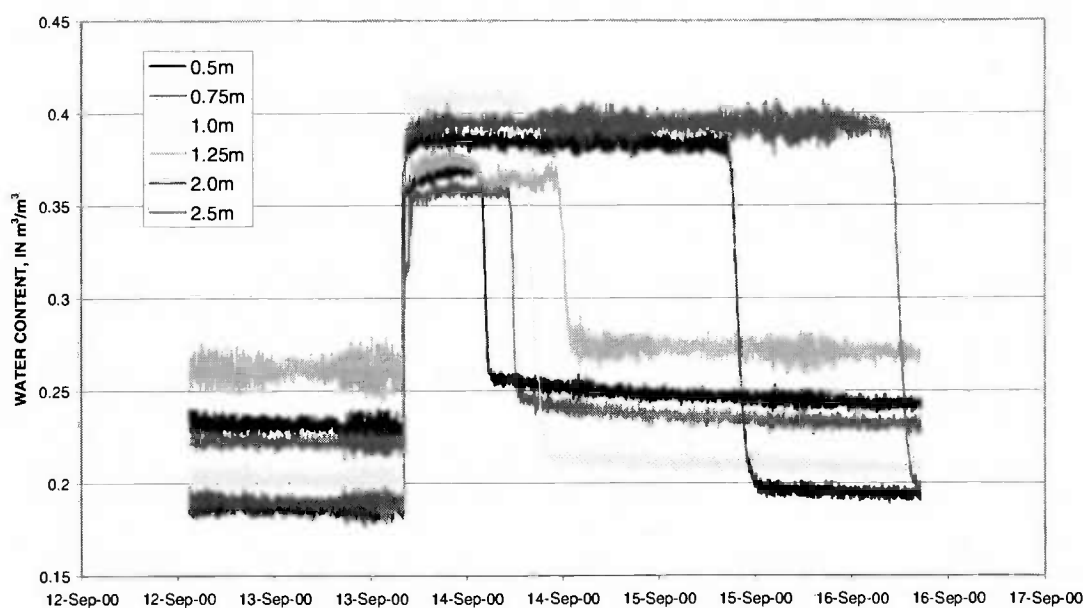


Figure 1. Water content data showing rapid increases at the onset of streamflow; a stabilization of water content during the event; and subsequent dewatering after streamflow is over.

Deep temperature monitoring has provided improved measurements to constrain models of infiltration at depth. The transport of thermal energy through the thick unsaturated zone has been recorded in deep wells in the Tucson Basin and has been used to infer both recharge from ephemeral channels and direction of ground water flow (Smith, 1910; Supko, 1970). Migration of water through the subsurface has been shown to cause

variations in the Earth's thermal gradients (Rousseau et al., 1998). The magnitude of the variations is proportional to the vertical flux of water. Coupled heat and fluid transport models are being used to infer the flux of water required to cause the deviations in the thermal gradient (Rousseau et al., 1998). Current development of multidimensional modeling studies (e.g., Reid and Dreiss, 1990; Niswonger and Prudic, 2003) coupled with water-content and pressure measurements made throughout the subsurface beneath ephemeral streams may provide greater insight into these redistribution patterns as water percolates through a deep unsaturated zone to an underlying saturated zone.

Temporal Recharge Considerations

Estimating current and future recharge rates or rebuilding historical records of channel recharge for use within ground-water flow models requires that fluctuations in infiltration and recharge be represented properly. Within the context of the Tucson Basin, a network of precipitation gages, streamflow-gaging stations, and piezometers, operational for more than half a century has enabled reasonable estimates of runoff and infiltration. These records have been used to identify changes in stream discharge and recharge rates owing to seasonal, annual and decadal fluctuations in climate and in riparian corridors. Trends in these data are likely representative of data trends for basins across the Southwest.

Long-Term Climate Variations

Improved understanding of periodic climate variations at annual, decadal, and longer time scales raises questions about the validity of annual recharge estimates for ephemeral

channels. Extreme variations in precipitation in basins of the Southwest have a significant effect on recharge from ephemeral channels. Estimates of recharge based on average precipitation may not be accurate because precipitation is a non stationary process, especially in the analysis of the effects of short-duration events. Decades of observation are needed to begin assembling a representative range of values, but even this length of record may not be long enough for many systems.

Fundamental to this notion of estimating future channel recharge contributions is that long-term climate phenomena cannot be accurately forecasted; because of this, the use of annually averaged channel recharge rates may not be adequate for water-resource planning. For example, Burkham (1970) developed a nonlinear regression equation relating streamflow loss to discharge for Rillito Creek, Arizona. Coefficients in the regression equations were developed using event data from all seasons. Comparison of streamflow losses between two streamflow-gaging stations during a 67-year period (1933 – 1999), however, indicate that Burkham's relation underestimates measured streamflow losses (Figure 2). Streamflow measurements show that annual streamflow losses appear to be growing during the 70-year period. This increase emphasizes the point that recharge within dynamic systems cannot be considered stationary, whether the increase in recharge is owing to longer time-scale climate oscillations, changes in basin runoff characteristics, or changes in stream-channel recharge efficiency.

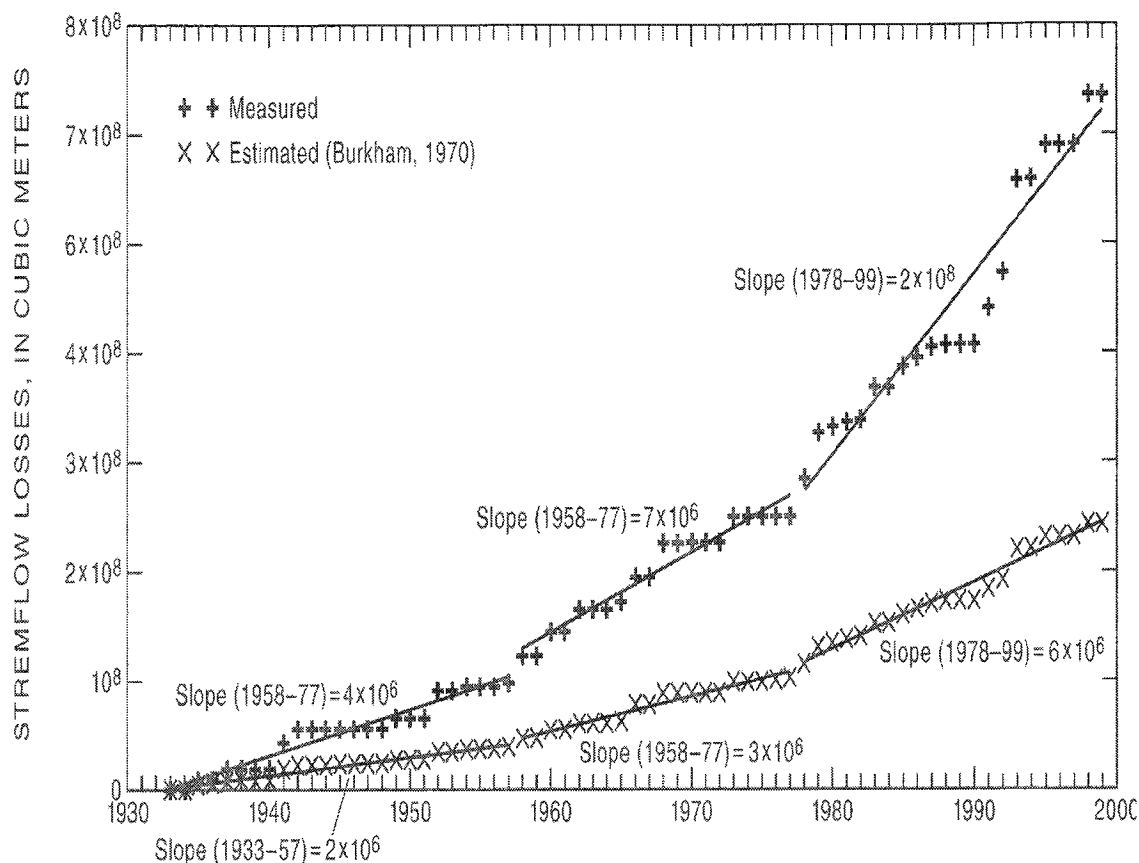


Figure 2. Comparison of measured streamflow losses within Rillito Creek, Tucson, Arizona, from 1933 through 1999 to computed streamflow losses using the Burkham (1970) relation with annual recharge coefficients.

Seasonal Variations

The North American Monsoon affects southern Arizona and the Tucson Basin during the months of July, August, and September. Deep, localized, convective cells produce short bursts of intense rain, which can account for much of the precipitation during the late summer and early fall. Surface runoff in response to monsoon storms is immediate and short lived. Conversely, winter precipitation within the Tucson Basin is typically produced by frontal storms of broad expanse that produce low-intensity rainfall and

snowfall. Flows in response to these precipitation events are longer lived and are less flashy than those derived from monsoon storms. Large events such as the flood of record for Rillito Creek that occurred in 1983 are caused by the presence of El Niño Southern Oscillation or other climate anomalies. Precipitation during these months is not typical of monsoon and winter seasons and results in extreme volumes of annual recharge.

Patterns of precipitation affect the growth and life cycle of vegetation within the riparian corridor. Moderate streamflow may enhance the growth of riparian vegetation. Conversely, vegetation commonly is removed during large-magnitude flows. High discharges of tremendous energy have uprooted mature trees and other stream-channel vegetation within Rillito Creek, leaving open, bare channels. Extensive changes in vegetation can change both channel evaporation and transpiration rates, and may also have a considerable effect on the downward rate of percolation along preferential flow paths (Solomon, 2003).

Seasonal growth and senescence of vegetation outside the riparian corridor can influence the magnitude of channel recharge rates. Reaches along the San Pedro River in southern Arizona fluctuate between gaining and losing depending on the senescence of vegetation (Lawler, 2002). During winter months, agricultural ground-water withdrawals cease and evapotranspiration demand of riparian vegetation is reduced; consequently, the water table rises (Lawler, 2002). Theis (1940) described a similar circumstance as “rejected recharge,” or the rejection of infiltrating water as a result of rising water levels in the

underlying aquifer. In areas where this occurs, the estimation of annual recharge rates for these reaches will depend upon the seasonal condition of the ground-water flow system, location of the reach, and hydrologic properties of the channel sediments.

Seasonal and long-term temperature fluctuations in the subsurface sediment profile will influence the rate of infiltration primarily through its influence on hydraulic conductivity (Constantz, 1998; Ronan et al., 1998). Increases in sediment and fluid temperatures translate into an increased kinetic energy of the fluid resulting in a decrease in fluid density and dynamic viscosity. Hydraulic conductivity, which is inversely proportional to viscosity and directly proportional to density, is consequently also dependent upon temperature

$$K = \frac{\rho(T)gk}{\mu(T)} \quad (4)$$

where, $\rho(T)$ is the density [$M L^{-3}$], g is gravity [$L T^{-2}$], k is the intrinsic permeability [L^2], and $\mu(T)$ is the dynamic viscosity [$M T^{-1} L^{-1}$]. Thermally induced changes in density are much smaller than changes in dynamic viscosity resulting in an overall increase in hydraulic conductivity with increased temperature. Observations within Rillito Creek show an increase in drainage rates of as much as 50 percent coinciding with a doubling in temperature from 14°C to 28°C (Blasch et al., 2000). Thus, temperature can be an important consideration for determining seasonal recharge rates.

Summary

Recent investigations of channel recharge have improved our understanding of hydrological factors controlling infiltration and recharge to include permeability of the channel surface, connection to the water table, and composition of the underlying unsaturated zone. Investigators have also demonstrated the utility of new monitoring techniques, such as the use of temperature, and stable isotopes to monitor temporally induced variations in recharge rates and to explore the pathways of infiltrating water. Because of periodic climate oscillations, development of representative recharge values for ephemeral channels will require collection and analysis of long-term hydrologic data. Finally, future deliberations on recharge will be most effective when each aspect of the process is considered from infiltration at the channel surface through percolation across the water table.

Acknowledgements. This work was supported by the U.S. Geological Survey Southwest Ground-Water Resources project.

References

- Anderson, T. W., G. W. Freethey, and P. Tucci, *Geohydrology and Water Resources of Alluvial Basins in South-Central Arizona and Parts of Adjacent States*. U.S. Geological Survey Professional Paper 1406-B, 67 pp., 1992.
- Bailey, M. A., *Analysis Of One-Dimensional Vertical Infiltration Using Heat As A Tracer In Rillito Creek*, Tucson, The University of Arizona, master's thesis, 152 pp., 2002.

- Bakry, M. F. and A. A. E. Awad, Practical Estimation of Seepage Losses Along Earthen Canals in Egypt, *Water Resources Management*, 11, 197-206, 1997.
- Blasch, K. W., J. B. Fleming, P. A. Ferré, and J. P. Hoffmann, One- and two-dimensional temperature and moisture-content profiling of an ephemeral stream channel in a semiarid watershed: *EOS, Trans Amer. Geophys. Union*, 81(48), F502, 2000.
- Bostick, K. A., *A Stable Isotope Investigation of Recharge to the Tucson Basin Aquifer From the Santa Cruz River*, Tucson, University of Arizona, master's thesis, 51 pp., 1978.
- Burkham, D. E., *Depletion of streamflow by infiltration in the main channels of the Tucson Basin, southeastern Arizona*, U.S. Geological Survey Water Supply-Paper 1939-B, 36 pp., 1970.
- Constantz, J., C. L. Thomas, and G. Zellweger, Influence of diurnal variations in stream temperature on streamflow loss and groundwater recharge, *Water Resources Research*, 30(12), 3253-3264, 1994.
- Constantz, J., Interaction between stream temperature, streamflow, and groundwater exchanges in alpine streams, *Water Resources Research*, 34(7), 1609-1615, 1998.
- Constantz, J., A. E. Stewart, R. Niswonger, and L. Sarma, Analysis of temperature profiles for investigating stream losses beneath ephemeral channels, *Water Resources Research*, 38(12), 1316, doi:10.1029/2001WR001221, 2002.
- Davidson, E. S., *Geohydrology and Water Resources of the Tucson Basin, Arizona*, U.S. Geological Survey Water-Supply Paper 1939-E, pp. E1-E78, 1973.

- Freeze, R. A., The Mechanisms of natural groundwater recharge and discharge 1. One-dimensional, vertical, unsteady, unsaturated flow above a recharging or discharging groundwater flow system, *Water Resources Research*, 5(1), 153-171, 1969.
- Freeze, R. A. and J. Banner, The mechanism of natural groundwater recharge and discharge 2. Laboratory column experiments and field measurements, *Water Resources Research*, 6(1), 138-155, 1970.
- Freyberg, D. L., J. W. Reeder, J. B. Franzini, and I. Remson, Application of the Green-Ampt Model to Infiltration Under Time-Dependent Surface Water Depths, *Water Resources Research*, 16(3), 517-528, 1980.
- Galyean, K., Infiltration of Wastewater Effluent in the Santa Cruz River Channel, Pima County, Arizona, U.S. Geological Survey Water-Resources Investigations Report 96-4021, 82 pp., 1996.
- Gee, G. W., P. J. Wierenga, B. J. Andraski, M. H. Young, M. J. Fayer, and M. L. Rockhold, Variations in Water Balance and Recharge Potential at Three Western Desert Sites, *Soil Sci. Soc. Am. J.*, 58, 63-72, 1994.
- Green, W. H. and G. A. Ampt, Studies on soil physics: I. Flow of air and water through soils, *J. Agr. Sci.* 4, 1-24. 1911.
- Guzman, A. G., L. G. Wilson, S. P. Neuman, and M. D. Osborn, Simulating effect of channel changes on stream infiltration, *Journal of Hydraulic Engineering*, 115(12), 1631-1645, 1989.

- Hanson, R. T. and J. T. Benedict, *Simulation of ground-water flow and potential land subsidence, Upper Santa Cruz Basin, Arizona*, U.S. Geological Survey Water-Resources Investigations Report, 93-4196, 47 pp., 1994.
- Hoffman, J. P., M. A. Ripich and K. E. Ellett, *Characteristics of shallow deposits beneath Rillito Creek, Pima County, Arizona*, U.S. Geological Survey Water-Resources Investigations Report 01-4257, 51 pp., 2002.
- Hoffman, J. P., K. W. Blasch, and T. P. Ferre, *Combined Use of heat and soil-water content to determine stream/ground-water exchanges, Rillito Creek, Tucson, Arizona*, U.S. Geological Survey Circular, pp., 2003.
- Knighton, D. A. and G. C. Nanson, Flow transmission along an arid zone anastomosing river, Cooper Creek, Australia, *Hydrological Processes*, 8, 137-154, 1994.
- Katz, L. T., *Steady State Infiltration Processes Along the Santa Cruz and Rillito Rivers*, Tucson, The University of Arizona, master's thesis, 119 pp., 1987.
- Lacher, L. J., *Recharge Characteristics of an Effluent Dominated Stream Near Tucson*, Arizona: Tucson, The University of Arizona, Ph.D. dissertation, 219 pp., 1996.
- Lawler, D., *Using Streambed Temperature Sensors to Monitor Flow Events in the San Pedro River, Southeast Arizona and North-Central Mexico*, Tucson, The University of Arizona, master's thesis, 68 pp., 2002.
- Lerner, D. N., A. S. Issar, and I. Simmers, *Groundwater Recharge: A Guide to Understanding and Estimating Natural Recharge*, International Contributions to Hydrogeology, 8, 345 pp., 1990.

- Maurer, D. K. and J. M. Fischer, *Recharge to the Eagle Valley Ground-Water Basin by Streamflow in Vicee Canyon, West-Central Nevada*. U.S. Geological Survey Water-Resources Investigations Report 88-4158, 66 pp., 1988.
- Niswonger, R. G. and D. E. Prudic, Modeling Variably Saturated Flow Using Kinematic Waves in MODFLOW, in F. M. Phillips, J. Hogan, and B. R. Scanlon, editors. Recharge and Vadose Zone Processes in Alluvial Basins in the Southwestern United States. AGU. 2003.
- Renard, K. G., R. V. Keppel, J. J. Hickey, and D. E. Wallace, Performance of local aquifers as influenced by stream transmission losses and riparian vegetation, *Transactions of the American Society of Agricultural Engineers*, 7(4), 471-474, 1964.
- Reid, M. E. and S. J. Dreiss, Modeling the effects of unsaturated, stratified sediments on groundwater recharge from intermittent streams, *Journal of Hydrology*, 114, 149-174, 1990.
- Rohwer, C. and O. Van Pelt Stout, Seepage losses from Irrigation Channels, Technical Bulletin 38, Colorado Agricultural Experiment Station, Colorado A&M College, Fort Collins, CO, 100 pp., 1948.
- Ronan, A. D., D. E. Prudic, C. E. Thodal, and J. Constantz, Field study and simulation of diurnal temperature effects on infiltration and variably saturated flow beneath an ephemeral stream, *Water Resources Research*, 34(9), 2137-2153, 1998.

- Rousseau, J. P., E. M. Kwicklis, and D. C. Gillies, Hydrogeology of the unsaturated zone, northramp area of the exploratory studies facility, Yucca Mountain, Nevada, U.S. Geological Survey Water-Resources Investigations Report 98-4050, 244 pp., 1998.
- Scott, R. L., W. J. Shuttleworth, T. O. Keefer, and A. W. Warrick, Modeling multiyear observations of soil moisture recharge in the semiarid American Southwest, *Water Resources Research*, 36(8), 2233-2247, 2000.
- Smith, G. E. P., Groundwater supply and irrigation in the Rillito Valley: Tucson, AZ, Bulletin No. 64, University of Arizona Agricultural Experiment Station, 81-243, 1910.
- Heilweil, V. M. and D. K. Solomon, Millimeter- to Kilometer-Scale Variations in Vadose-Zone Bedrock Solutes: Implications for Estimating Recharge in Arid Settings, in F. M. Phillips, J. Hogan, and B. R. Scanlon, editors. Recharge and Vadose Zone Processes in Alluvial Basins in the Southwestern United States. AGU. 2003.
- Supko, D. J., *Subsurface Heat Flow as a Means for Determining Aquifer Characteristics in the Tucson Basin, Pima County, Arizona*, Tucson, University of Arizona, Ph.D. dissertation, 184 pp., 1970.
- Theis, C. V., The source of water derived from wells—essential factors controlling the response of an aquifer to development, *Civil Engineering Magazine*, 277-280, 1940.
- Trout, T. J., Factors Affecting Losses from Indus Basin Irrigation Channels. *Water Management Technical Report*, No. 50, pp. 201, Colorado State University, Fort Collins, CO, 1979.

- Walvoord, M. A. and B. R. Scanlon, Hydrologic Processes in Deep Vadose Zones in Interdrainage Arid Environments , in F. M. Phillips, J. Hogan, and B. R. Scanlon, editors. Recharge and Vadose Zone Processes in Alluvial Basins in the Southwestern United States. AGU. 2003.
- Webb, R. H. and J. L. Betancourt, *Climatic Variability and Flood Frequency of the Santa Cruz River, Pima County, Arizona*, U.S. Geological Survey Water-Supply Paper 2379, 40 pp., 1992.
- Wilson, L. G. and K. J. DeCook, Field observations on changes in the subsurface water regime during influent seepage in the Santa Cruz River, *Water Resources Research*, 4(6), 1219-1234, 1968.
- Wilson, L. G., K. J. DeCook, and S. P. Neuman, *Regional Recharge Research for Southwest Alluvial Basins*, U.S. Geological Survey SWAB/RASA Project, The University of Arizona, Tucson, Arizona, 1980.